The use of color as alternative to size measurements in *Fusarium graminearum* growth studies and prediction of deoxynivalenol synthesis

[*Fusarium graminearum* の生長評価における形態測定の代替としての色調変化の利用とデオキシニバレノール産生量の予測]

Hokkaido University

Graduate School of Agriculture

Division of Bio-systems Sustainability

Doctoral Course

Edgar Manuel Cambaza

Acknowledgements

I would like to thank the Japanese Ministry of Education, Culture, Sports, Science and Technology (MEXT), for providing me with this unique opportunity to be part of the academic community of this fantastic country, to learn about Japanese culture and to make friends from all over the world.

I would also like to thank Professors Koseki and Kawamura for accepting me into the Laboratory of Agricultural and Food Process Engineering, for their patient guidance and for providing me with global views in scientific enquiry which I may not have otherwise been able to acquire. I will remain forever grateful to them, and I do promise to make your effort worthwhile, in the future.

I would also like to thank Chen, Edenio, Umi Ogawa, Abe Kun, Shoda, Kento, Murashita, Kuroda, Harada, Morita and all other lab mates for their indispensable contribution to my work. No matter where you are or what you need, please never forget that I will be only a message away from you.

List of acronyms

ANCOVA	Analysis of covariance
CSA	Competitive saprophytic ability
CAS	Chemical Abstracts Service
DNA	Deoxyribonucleic acid
DON	Deoxynivalenol
ELISA	Enzyme-linked immunosorbent essay
EU	European Union
FAO	Food and Agriculture Organization of the United Nations
FHB	*Fusarium* head blight
GC	Gas chromatography
HPLC	High-performance liquid chromatography
NIV	Nivalenol
PTX	Cytotoxicity of paclitaxel
RGB	Red-green-blue color space
RIA	Radioimmunoassay
TLC	Thin-layer chromatography
YEA	Yeast extract agar
ZEA	Zearalenone
JCM	Japanese Collection of Microorganisms
IPEC-J2	Intestinal porcine epithelial cells
CAO	Carotenoid oxygenase
USA (US)	The United States of America
UV	Ultraviolet
PKS	Polyketide synthase

List of tables

List of figures

Table of contents

Chapter 1 Introduction

1.1 Background

The past two decades have witnessed a rapid global re-emergence of *Fusarium*, a genus of fungal parasites in cereals and other plants [1-3], due to climate change [4], edaphic and agro-technical factors [5-7]. These molds have garnered considerable attention from researchers, scholars and legislators because of their deleterious impact on agriculture, trade, health and animal sciences. The most commonly found *Fusarium* in temperate areas are *F. graminearum* and *F. moniliforme*, with *F. culmorum*, *F. proliferatum*, *F. equiseti* and *F. poae* being found sometimes as well [8-10]. *F. graminearum* is perhaps the most responsible for *Fusarium* head blight (FHB), which is a rapidly spreading plant disease in crops such as oats (*Avena sativa*), rice (*Oryza sativa*) and other cereals [5] , causing yield losses and reduced nutritive, physical and chemical quality of seed, leading to difficulties in marketing, export and processing of infected grains [1, 10-12]. Furthermore, *F. graminearum* produces several mycotoxins including deoxynivalenol (DON) [13, 14].

DON (also called vomitoxin or 3,7,15-trihydroxy-12,13-epoxytrichothec-9-en-8-one) is a trichothecene, a group of compounds which are one of the most potent inhibitors of protein synthesis [2, 15-17]. Vomitoxin was discovered for the first time in Japanese barley, then characterized by Morooka*, et al.* [18]. Consumption of DON causes disease in animal with numerous records of human intoxication also being available [19]. It is well known for causing nausea, vomiting, diarrhea, immunosuppression, toxicity to the nervous system, embryo and teratogenic effects, feed refusal, reduction in weight and sometimes death [10, 14, 15, 17, 20-22] in pigs from all age groups, and other non-ruminants [14]. There have been cases of human

intoxication in India, China and at least 8 outbreaks in Japan during the 20th century [15, 23], with people affected being manifested with gastrointestinal troubles, dizziness, vomiting and headache among other symptoms [21]. Therefore, it is necessary to prevent DON from entering the food chain and a key strategy in achieving this is through control of *F. graminearum* [1, 24].

The symptoms of *F. graminearum* infection in grains are fairly well-known. The infected grains become smaller and shriveled, with the surface becoming pale as if it were covered with white chalk, and frequent appearance of pink coloration [6, 13, 25]. These characteristics can generally be identified by experienced personnel. According to Goswami and Kistler [11] , the fungus overwinters as a saprobe (white mycelium) in dead leaves, growing in decaying leaves and producing conidia (orange and pink) and perithecia (purple) just before invading a living host. All these processes produce specific colors, the knowledge of which could be used by researchers and farmers as a digital imaging tool to analyze the quality of the grains and possibly estimate the quantity released by the parasite into food or feed matrix. In fact, Dammer*, et al.* [19] were able to detect FHB-infected grains using RGB imaging analysis combined with statistical approaches. Jirsa and Polišenská [25] went a step further in being able to identify samples containing DON, although they had only compared samples heavily damaged by FHB with healthy ones, without accounting for any intermediate stages or the impact of environmental or nutritional factors.

The current study was designed to verify if the colors developed by *F. graminearum* throughout its lifecycle can be used as a tool to analyze its growth pattern and also to estimate the quantity of DON released into the food matrix. It is an attempt to overcome some limitations of size-based models, particularly (1) the lack of information pertaining to the metabolic condition of the mold, especially during

stages at which there is no size expansion, such as the lag and stationary phases and (2) the inaccuracy of the most common size-based variables (radius, diameter) in representing growth when the mold presents irregular forms [26]. This thesis dedicates one chapter to a literature review, followed by a chapter describing the use of colors in the analysis of *F. graminearum* growth and DON production in yeast extract agar (YEA) under distinct temperatures and a_w settings. Subsequently, there is a chapter in which the experiment has been repeated in oats and rice, followed by a final chapter devoted to synthesis and conclusions.

1.2 Problem

In order to improve *status quo,* it is important to understand the challenges associated with the two issues regarding *F. graminearum* infection, which are FHB and DON. In several parts of the world, FHB-infected kernels are still separated by buyers or trained inspectors through visual inspection [13] , and although this process is fast, it is labor intensive, subjective, has low reproducibility and is hence inconsistent and unsuitable for large amount of samples [1, 13, 25]. In the case of DON, the standard analytical methods are destructive, expensive, time consuming and inappropriate for screening [1, 13, 27]. For these reasons, there is a need for a simple, inexpensive and reliable method to assess the quality of the grains and measure the amount of DON, in order to predict and therefore prevent the release of DON into the food matrix. A suitable approach in achieving this is the development of models based on the variables likely to be associated with *F. graminearum* infection and DON contamination [19].

In 2009, Garcia*, et al.* [28] reviewed the major analytical approaches used to predict the level of mycotoxins in food. The first part of the article is focused on predictive models for mold germination growth and inactivation. According to them,

the major growth methods used for molds were derived from bacterial studies: linear, Gompertz and Baranyi (Figure 1).

Gompertz model	Baranyi model
$y = y_{max} * \exp\left\{ -\exp\left[\left(\frac{\mu_{max} * \exp(1)}{y_{max}} \right)(\lambda - t) + 1 \right] \right\}$	$y = y_0 + \mu_{max} A - \ln\left\{ 1 + \frac{[\exp(\mu_{max} A) - 1]}{\exp(y_{max} - y_0)} \right\}$ $A = t + \left(\frac{1}{\mu_{max}} \right) \ln[\exp(-\mu_{max} t) + \exp(-\mu_{max} \lambda) - \exp(-\mu_{max} t - \mu_{max} \lambda)]$

Figure 1. Gompertz and Baranyi growth models. Notes: y - size; y_{max} - maximum size; y_0 initial size; λ - lag time; μ_{max} – maximum growth rate; t – time.

Although these models are easy to use and practical in some situations, they require spatial variables such as the radius or diameter. However, fungal growth is more complex than mere spatial expansion. For instance, when *F. graminearum* grows on solid agar in a Petri dish and attains its full size, it can no longer expand, although the fungus is still alive, with the ability to grow further, produce spores and propagate. In these cases, size is not a useful variable. It is also impractical to use size as a measurable when the mold grows in an irregular fashion. Garcia*, et al.* [28] have also highlighted the use of quantification of ergosterol in the medium to estimate fungal growth. Although this is a good idea as it would provide information regarding the mold's metabolic state, it would be preferable to use less destructive or invasive methods.

Garcia*, et al.* [28] have also described models for toxin quantification, although the challenge persists in doing so reliably, through an easy applicable method. Most of these methods use variables such as time, temperature and a_w to predict toxin concentration but the limitation of this method, similar to the size-based approach, is the lack of information regarding the mold's metabolic state. Time and environmental variables are not inherent characteristics of an organism, although they

usually play a significant role in its behavior. Homeostatic forces need to be disrupted in order to effectively impact the organism. Growth indicators within the organism are perhaps the best approach towards understanding them.

Fungal pigmentation might be a more rational approach in analyzing the developmental and metabolic state of molds [26]. Also, pigmentation does not necessarily have to be directly related to toxin production although the variations must be statistical significant. Indeed, there is a body of evidence demonstrating the feasibility of image-based approaches in obtaining reliable information regarding growth of *F. graminearum* and DON synthesis, some of which have been described in detail by Saccon*, et al.* [1].

1.3 Rationale

Cereals are arguably the most important food constituent and as reported by the Food and Agriculture Organization of the United Nations (FAO), rice (*Oryza sativa*) is the predominant staple food for 17 countries in Asia Pacific, 9 countries in the Americas and 8 countries in Africa [21], and Olivares Diaz [29] described this commodity as the main source of calories for half of the human race. A cereal pathogen with the potential to destroy high-yielding crops within few weeks of harvesting, considerably reducing the quality of kernels and spreading toxins through the grains [11] , is a major threat to food security, safety and quality. This is why the European Union fixed the maximal residual limits (1.25 μg/g) for DON in 2006, and Japan has also set the provisional limits at 1.1 μg/g.

Although remarkable progress has been made in the development of imaging analysis strategies to better understand FHB and DON, plenty of work remains to be done to improve these methods. Apart from the insightful review by Saccon*, et al.* [1], the RGB analyses by Jirsa and Polišenská [25] and Dammer*, et al.* [19], there are

many articles available which are closely related to the focus of this thesis. For instance, Ruan*, et al.* [30] combined RGB imaging with a neural network to distinguish infected kernels and Wiwart*, et al.* [13] used digital image analysis to detect FHB in triticale. Yet, none of these authors have analyzed the entire process of infection in a gradual or longitudinal fashion, through observing the pattern of color variation as the mold expands to mycelium, subsequently maturing and producing different types of spores. Correlation of color with DON contamination has not been studied in meticulous detail. Hence, it is necessary to perform a detailed analysis across different nutrient sources, temperatures and a_w.

This study explores the novel perspective that the color of *F. graminearum* can be treated the same way as mycelial radius or diameter has been conventionally treated as a measure of growth. All approaches, however, have their advantages and disadvantages. The use of spatial variables such as height, length, depth, etc. is commonly used as a measure of growth in most organisms including plants, mammals, fish or even other organisms. This is a good juncture to explore more innovative ideas, and I believe this work will promote a better understanding of the biology and ecology of *F. graminearum* and plant pathogens in general, and would be useful for scholars, researchers, farmers, the industry, policymakers and society in general.

1.4 Objectives

1.4.1 General

The general objective of this thesis is to demonstrate the potential of RGB imaging analysis as a reliable tool to analyze *F. graminearum* growth and predict the quantity of DON produced by the mold when grown on agar, oats or rice.

1.4.2 Specific

The specific objectives of this thesis have been listed below:

- Verify the predictability of *F. graminearum* superficial color change as it grows on yeast extract agar (YEA), oats or rice;
- Analyze the relationship between color change and the concentration of DON released by the mold in the medium under different temperatures and water activity (a_w).

1.5 Hypotheses

Mold surface coloration results from a combination of several pigments produced throughout its lifetime and are related to a particular state of its maturity. For instance, some melanins are associated with the formation of perithecia [31] while other pigments are associated with spore development [32]. Furthermore, mycelium of *F. graminearum* is predominantly white, not exhibiting abundance of any pigment. On the other hand, the mold produces different pigments, each with its own peculiar chemical properties [33], which might lead to a chaotic color change pattern. Thus, the following hypotheses arise:

- H_0: Periodic digital photos of *F. graminearum* throughout its lifecycle will not present predictable variation of the RGB components;
- H_A: Periodic digital photos of *F. graminearum* throughout its lifecycle will present predictable variation of RGB.

Furthermore, the abundance of DON can intuitively be associated with the mold's latter stages since the toxin is a product of secondary metabolism and is known to be released in higher quantity when the organism stops expanding and senescence starts [32]. Indeed, several studies show a predictable trend of DON accumulation [34, 35]. Thus, if colors and DON present predictable changes over time, the colors

might be a reliable tool to predict the quantity of DON accumulated with growth of *F. graminearum*. Indirect support for this hypothesis comes from Jirsa and Polišenská [25] who have shown significant differences in RGB and DON between healthy and damaged wheat grains. Yet, very little attention has been paid to establish a consistent relationship between color changes caused by *F. graminearum* and DON accumulation. Therefore, the following hypotheses have been considered:

- H_0: RGB measurements of digital photos of *F. graminearum* throughout its lifecycle will not present any consistent relationship with the amount of DON accumulated in the medium;
- H_A: RGB measurements of digital photos of *F. graminearum* throughout its lifecycle will present a consistent relationship with the amount of DON accumulated in the medium.

Chapter 2 Literature review

2.1 RGB imaging and plant pathology

Optical techniques are among the most favored tools to assess large numbers of samples in a fast and non-destructive way [1]. According to Gupta*, et al.* [36], the main types of imaging techniques are photometric feature-based (also called RGB), fluorescence, hyperspectral, and thermal. Padmavathi and Thangadurai [37] have described an RGB image as represented by three color component intensities (red, green and blue). RGB-based methods have been broadening their applications in several areas of agronomic sciences because of their suitability in analyzing color discrepancies between distinct biological samples [13, 36, 37].

RGB imaging is progressively replacing human vision in the evaluation of food quality [36] because it provides the investigator with newer tools of higher quality, reliability, ability to analyze the commodity's shape and color intensity of several plant structures including seeds [13]. Furthermore, these methods are relatively easy and inexpensive [19, 38], particularly when combined with statistics [39]. According to Wiwart*, et al.* [13], this technique can be used to effectively evaluate grains and also assess DON content through the frequency of *Fusarium* damaged kernels. Yet, they detected the RGB values and then converted them to HSI (hue, saturation, intensity), perhaps because their study was more concerned with these variables.

ImageJ (National Institutes of Health, Bethesda, Maryland, US) is an open-source Java-based imaging program [40] worth mentioning, as it has been contributed significantly to imaging analysis for over 25 years [41]. It had been originally developed for medical research but its tools can be applied to virtually any field

requiring imaging analysis. The software has a very intuitive interface and very effective embedded plugins embedded with the website allowing the download of more plugins created by independent developers. One of the plugins, *Color Histogram* [42], is suitable for imaging analysis in agriculture and can be used to determine average RGB values of grains, fungi or any other sort of images.

2.2 *F. graminearum*

F. graminearum Schwabe (Figure 2) is the most common agent of *Fusarium* head blight (also known as scab) [11].

Figure 2. Macroconidia of *Fusarium graminearum sensu stricto*. Retrieved from Wikimedia Commons [43]. This file is licensed under the Creative Commons Attribution-Share Alike.

The earliest known descriptions of *Fusarium* head blight (FHB) date back to 1884 in England, where it was regarded as a major wheat (*Triticum*) and barley (*Hordeum*) disease in the subsequent years [11]. Nowadays, this mold is found virtually all over the world and it is known to cause FHB in other commodities such as oats (*Avena*), rice (*Oryza*), and *Gibberella* stalk and ear rot disease in maize (*Zea*) [11, 17]. The mold also parasites sorghum (*Secale cereale*) and triticale (× *Triticosecale*) [21]. There have been outbreaks in Asia, including Japan [44], South America, Canada, United States and Europe [11].

According to Goswami and Kistler [11], the teleomorphic state of *F. graminearum*, named *Gibberella zeae* (Schwen.) Petch, is classified as follows: superkingdom Eukaryota, kingdom Fungi, phylum Ascomycota, subphylum Pezizomycotina, class Sordariomycetidae, subclass Hypocreomucetidae, order Hipocreales, family Necriaceae and genus *Gibberella*.

F. graminearum has high competitive saprophytic ability (CSA), sometimes surviving for several years in the soil, and it can adapt to a wide range of environmental variations [5]. The anamorphic form is frequently observed in winter as a saprophytic mycelium in plant debris spread throughout the soil, but producing conidia and perithecia with ascospores during spring (cool and wet) [2, 5, 11]. Once released, the sticky ascospores colonize flowering hosts with the aid of insects, wind or water [11]. The primary sites of infection are anthers and ovaries and transmission is usually through contaminated pollen, and once the mold sets in the reproductive structures it can easily spread through the plant [45].

2.3 Meta-analytic review on the impact of temperature and a_w in DON synthesis by *F. graminearum*

2.3.1 Introduction

Deoxynivalenol (DON or vomitoxin) is a mycotoxin belonging to the group of sesquiterpenoid epoxytrichothecenes, capable of inhibiting protein synthesis and causing gastrointestinal disorder such as vomit and probable growth impairment in animals and humans [15, 46]. It has been associated with *Fusarium* head blight (FHB), a common wheat, barley and maize disease caused by *F. graminearum*, *F. moniliforme* and less frequently by *F. culmorum*, *F. proliferatum* and *F. equiseti*.

The most commonly reported detection methods of FHB are mass spectrometry, radioimmunoassay (RIA), enzyme-linked immunosorbent essay

(ELISA), and several forms of chromatography including thin-layer chromatography (TLC), gas chromatography (GC), and high-performance liquid chromatography (HPLC) [47, 48]. They have been improving over time with all these techniques having their advantages and disadvantages [48]. Thus, the best choice might depend on the objective and conditions of the particular experiment. HPLC is perhaps the most commonly reported method in *Fusarium* toxin studies [49].

In a review by Yoshizawa [23] based on research of over three decades on DON and nivalenol (NIV), at least eight FHB outbreaks in Japan between 1890 and 1970 have been reported, resulting in considerable loss in yield of wheat and barley, and several cases of human and animal intoxication. The review also reports two human intoxications in Hokkaido, in 1956. Weidenbörner [50] has described a simultaneous intoxication with NIV in Japan, 1972. Kubo, *et al.* [51] have described more recent cases (2002 to 2006) where DON was found in more than half of 7746 wheat samples with 3.3% of them being above the provisional limit in Japan (1.1 μg/g).

2.3.2 Sources

The studies analyzed were performed by Martins and Martins [15] in Portugal, and Marin, *et al.* [34] in Argentina. Data for the following variables were collected from all authors: growing medium (substrate), *F. graminearum* strain, incubation time, temperature, water activity and DON levels. The data were then subjected to statistical analyses, consisting of tests of hypotheses ($p = 0.05$) and descriptive parameters.

2.3.3 DON overall levels

Natural sources of the nutrient were used in these studies, different from the yeast extract agar. The latter was designed to specifically feed the fungi in a balanced manner. Such an appropriate form of nourishment will reduce the toxin concentration

while increasing the incubation time, temperature and a_w at which the fungus will produce DON. It might reduce DON content since stress promotes the production of secondary metabolites. The actual range of the variables may probably be higher because a more nutritious medium also favors the fungus' resistance to harsh environments. Moreover, it is important to bear in mind that some media could pose challenges in HPLC purification, compared to others. Figure 3 supports the idea that different substrates exhibit different mycotoxin synthesis levels (p = 0.003), though there may be other factors to consider, such as strain.

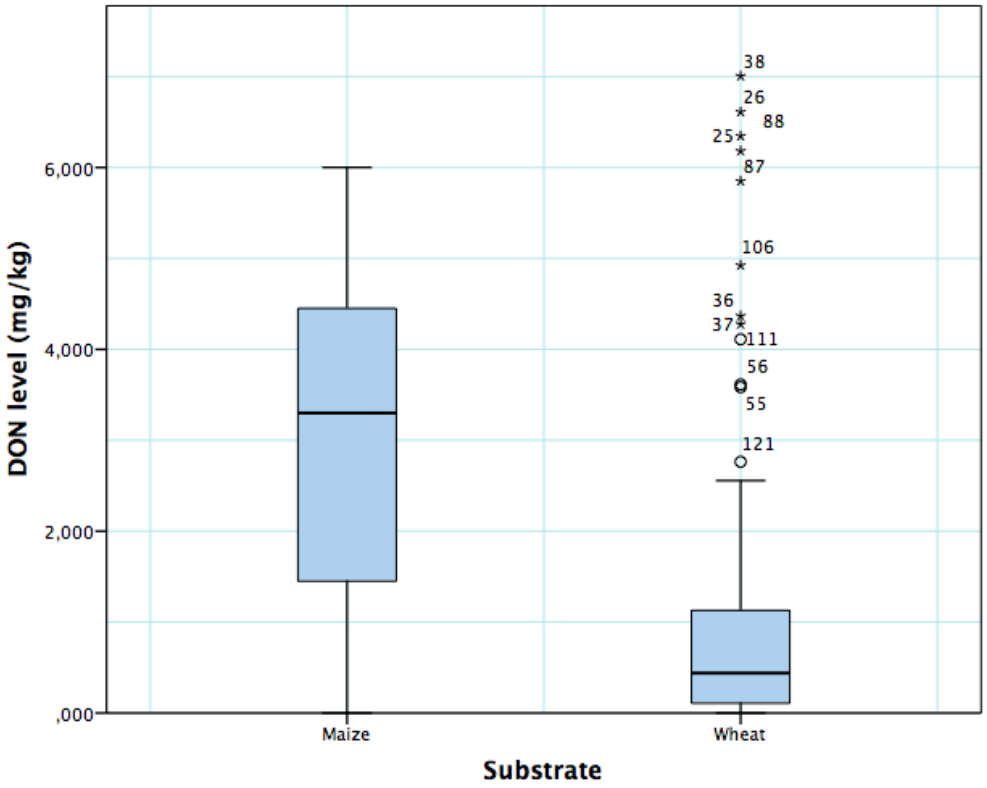

Figure 3. Differences in DON level between *F. graminearum* grown in maize and wheat. The data above the right box are values out of the confidence interval. The numbers represent the samples according to the order they were arranged in the spreadsheet used to make this chart. The circles and asterisks above the boxes represent values out of the confidence interval, and their numbers represent the position in the order of samples as they were registerend in the database.

The genetic differences might lead a fungus to produce more or less of a secondary metabolite, including mycotoxins. The wild Portuguese strain used by

Martins and Martins [15] and the RC17-2 and RC 22-2 used by the Argentinean authors certainly differ from the *Gibberella zeae* (Schwabe) Petch of the JCM database. Indeed, the meta-comparison of median DON levels shows significant differences between the strains (Figure 4) with the wild strain showing the highest value.

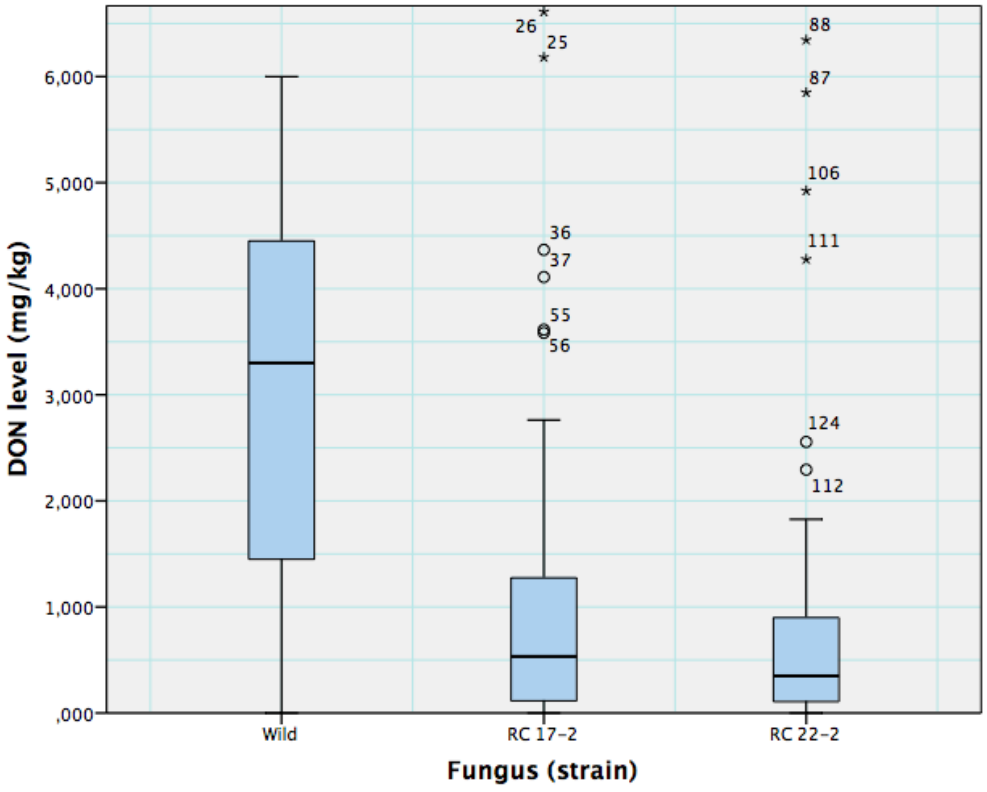

Figure 4. Median values of DON levels between the different *F. graminearum* strains (p = 0.008). The data above the boxes are values outside the confidence interval. The numbers represent the samples according to the order they were arranged in the spreadsheet used to make this chart. The circles and asterisks above the boxes represent values out of the confidence interval, and their numbers represent the position in the order of samples as they were registerend in the database.

Yet, irrespective of the differences arising due to different media and strains, the incubation time, temperature and a_w are expected to have an impact on DON production. Overall, the average level of DON in these studies, within a 95% confidence interval of 0.7-1.3 µg/g, is 1.05 µg/g. A Kolmogorov-Smirnov test

revealed a significant difference in the DON levels ($p < 0.001$). Hence, the overall variation resulted in distinct profiles.

As Figure 5 below shows, the incubation time has a correlation with DON synthesis ($p = 0.001$). This observation is intuitive since the fungus germinates and accumulates the toxin in the medium, especially when it reaches the stationary phase and starts senescence. However, regression analyses do not show significant correlation with either any polynomial function below the 6th degree, nor with any major algebraic non-parametric function, as R^2 was consistently lower than 0.5. Thus, the model to best fit this behavior is yet to be found. Similar regressions were also performed for temperature and a_w, showing a similar result ($R^2 < 0.5$).

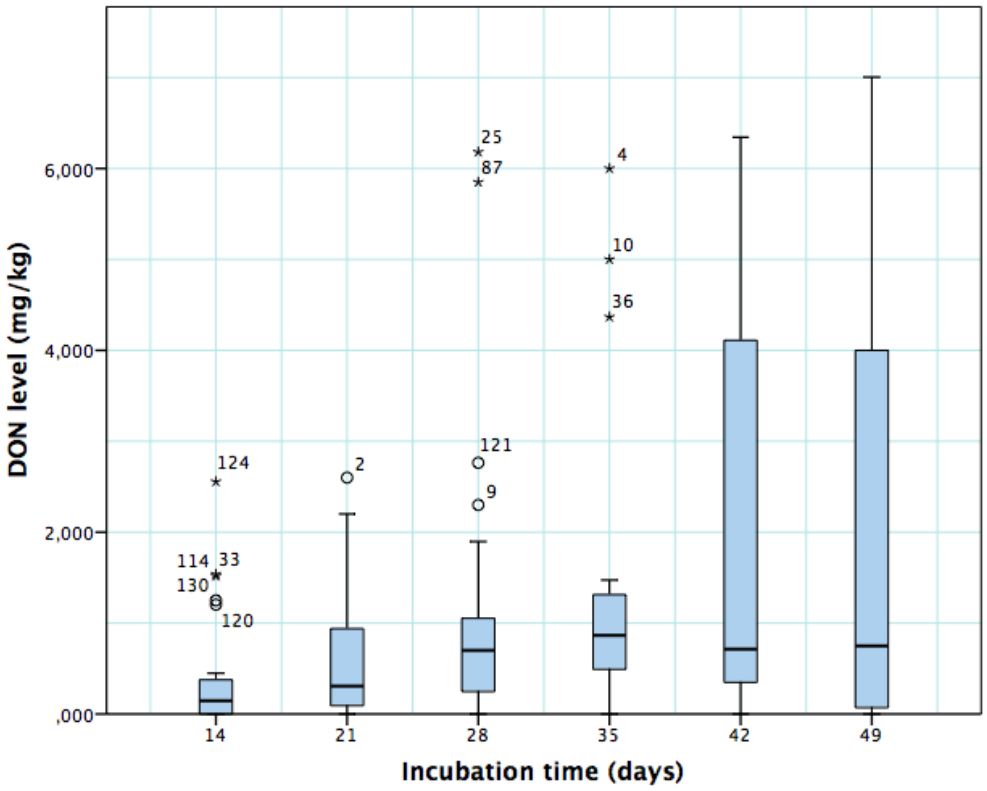

Figure 5. DON levels as a function of incubation time. The data above the boxes are values out of the confidence interval. The numbers represent the samples according to the order they were arranged in the spreadsheet used to make this chart. The circles and asterisks above the boxes represent values out of the confidence interval, and their numbers represent the position in the order of samples as they were registerend in the database.

Assuming DON synthesis is a function of growth itself, including possible direct proportionality, the logistic regression maybe expected to be an applicable fit for both phenomena, when in a batch system. However, toxin accumulation may also influence the measurement, probably resulting in accumulative values. However, a decrease in the observed levels from the 35th day onwards suggests that it may not have a significant impact on measurement. Another factor affecting the measurement could arise from the possibility that the oldest parts of the colonies, which usually contain the highest toxin concentrations, were picked to conduct these measurements.

2.3.4 DON and temperature

A Kruskal-Wallis test suggests that temperature also influenced toxin production (Figure 6, $p < 0.001$). However, the relationship between temperature and toxin production seems complex as the DON levels at room temperature (25 °C) are unexpectedly lower than at the experimental temperatures immediately above or below.

Various explanations can be provided for the above observation for example discrepancies arising from different strains. In addition, a wider dispersion is observed as the temperature nears 25 °C, probably because it is the optimal temperature for fungal growth. This dispersion might explain the differences in the adaptation of different strains to the medium and in toxin production.

Another possible cause of contamination could be natural adversarial microorganisms, which could have the same optimal growth temperature and could compete with the fungus and affect its growth. However, they might not be as competitive to *F. graminearum* in less favorable environments. The current experiment will allow a better understanding of this scenario.

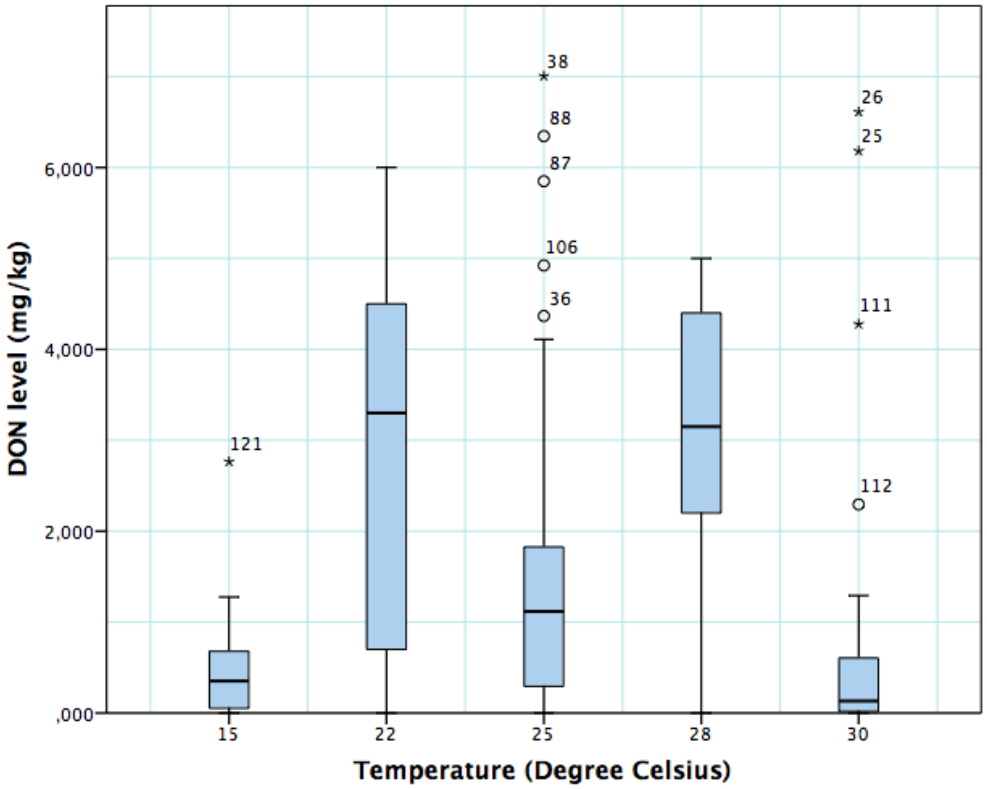

Figure 6. The relationship between temperature and DON level. The data above the boxes are values out of the confidence interval. The numbers represent the samples according to the order they were arranged in the spreadsheet used to make this chart. The circles and asterisks above the boxes represent values out of the confidence interval, and their numbers represent the position in the order of samples as they were registerend in the database.

2.3.5 DON and water activity

Finally, analysis of water activity (p = 0.026) showed that the highest DON levels were at a_w = 0.97 and 0.995 (Figure 7). Marin, *et al.* [34] identified 0.98-0.944 as the most favorable range for growth and 0.92 as a harsh environment for *F. moliniforme and F. proliferatum*. These results are fairly consistent with the hypothesis that growth is direct proportional to mycotoxin production. However, it must be borne in mind that Marin, *et al.* [34] used different species, although from the same genera.

2.3.6 Remarks

The meta-analysis provided us with some ideas regarding the results to be expected from the current experiment although technical differences must be borne in mind. From the above results, it can be concluded that temperature and water activity affect DON levels. Extreme temperatures and the optimal growth temperature seem to be associated with low toxin synthesis, although for different reasons. The extreme temperatures do not allow sufficient maturation of the *Fusarium* to produce the toxin while the optimal temperature does not stimulate secondary metabolism. Water activity is probably directly proportional to DON synthesis but beyond a certain extent, it is obscured by nutritional and genetic factors.

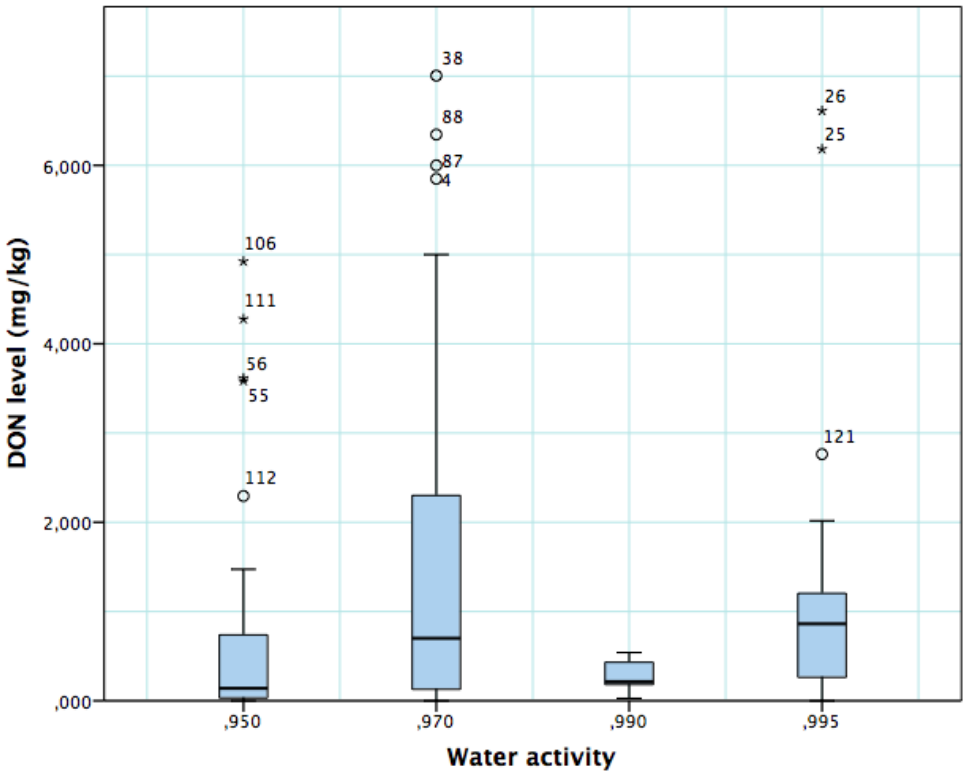

Figure 7. The relationship between water activity and DON level. The data above the boxes are values out of the confidence interval. The numbers represent the samples according to the order they were arranged in the spreadsheet used to make this chart. The circles and asterisks above the boxes represent values out of the confidence interval, and their numbers represent the position in the order of samples as they were registerend in the database.

Future researchers are recommended to begin by using a minimal medium such as YEA as it can prevent any influence of the host organism. Furthermore, these studies should include a few standard strains as controls for proper comparison.

2.4 *F. graminearum* pigments and related compounds

Fusarium graminearum (teleomorph: *Gibberella zeae*) is a pathogen infecting maize, wheat, rice and barley and is responsible for *Fusarium* head blight (FHB) and mycotoxin contamination [52, 53]. FHB destroys the grain starch and protein and was responsible for losses of over $2.7 billion in the United States between 1998 and 2000 [53]. The mold's most common mycotoxins are nivalenol (NIV) and deoxynivalenol (DON) [54], usually occurring together and are frequently associated with gastrointestinal disorders, among other health impairments [50] . However, there are other relevant toxins, such as zearalenone (ZEA) [23], an estrogenic compound capable of causing abortion and other reproductive complications [55, 56].

There are very few comprehensive studies related to *F. graminearum* surface colors and its pigments, their properties, and their biosynthetic or genetic origin, though some of them were isolated during the 1930s–1960s [57-61]. There was also a detailed chemical analysis of *Fusarium* pigmentation in the late 1970s and early 1980s, but this was never correlated with the mold's observable biological phenomena [62]. Recent sequencing of the *F. graminearum* genome and development of gene editing tools have allowed major progress in genetic and biochemical studies [62]. Now, it is known that the red pigmentation of *F. graminearum* is due to the deposition of aurofusarin in the walls [53, 63], although it is likely to be the result of a combination of several pigments [64, 65].

Pigmentation is part of the mold growth process and it can be used as a tool for studying growth, as an alternative to size expansion [26]. This approach can help

overcome spatial constraints in fungal studies or applications, such as the limited size or particular shape of a Petri dish or bioreactor, or even predict toxin production through sole analysis of the mold surface color. For instance, mutants lacking in aurofusarin seem to produce an increased amount of ZEA [53] , and histone H3 lysine 4 methylation (H3K4me) is important for the transcription of genes required for the biosynthesis of both DON and aurofusarin [66]. Thus, there is some correlation between the production of major *Fusarium* mycotoxins and pigments.

This review aims to identify the major *F. graminearum* pigments described in the literature and summarize the current knowledge in this field to enable future researchers to comprehensively relate the growth dynamics of the mold with its color change.

2.4.1 *F. graminearum* colors throughout its lifecycle

It is important to acknowledge that a single set of colors cannot be used to describe *F. graminearum* throughout its lifecycle. The surface colors change depending on several variables such as strain, maturity, nutrients, temperature, pH, water activity, light exposure and aeration [26, 57, 59, 65]. Ashley*, et al.* [57] mention early studies identifying pH as the main determinant of *Fusarium* colors, observing the same culture turning from orange or yellow colored in an acidic solution to red or blue in an alkaline one. Medentsev*, et al.* [67] propose that the biosynthesis of naphthoquinones (major secondary metabolites, including pigments) is the mold's main response to stress. *F. graminearum* produces different types of pigments with distinct properties [57, 64, 68-70] , numerous combinations of which result in distinct chromatic attributes. For instance, the teleomorph was found to have violet pigmentation in its perithecia [71]. Since it would be tedious to summarize all possible combinations, this chapter will only focus on the combinations arising in

mold grown on yeast extract agar (YEA) at 25 °C as a prototypical example (Figure 8).

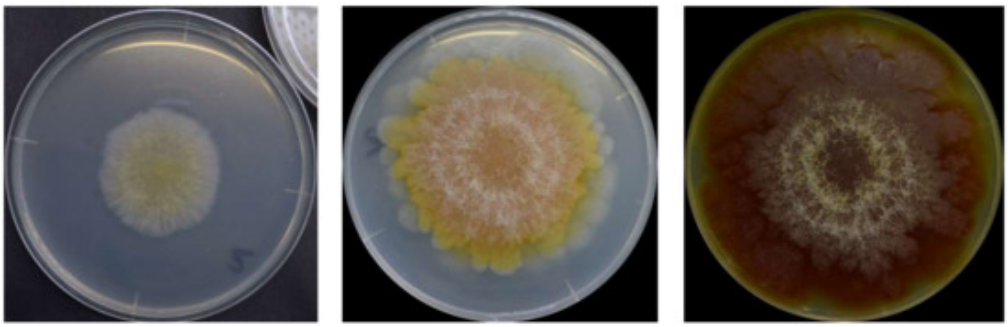

Figure 8. *F. graminearum* colors on its (a) 3rd day, (b) 6th day, and (c) 16th day.

The isolate was obtained from the Catalogue of the Japan Collection of Microorganisms (JCM), where it is registered as the teleomorph *Gibberella zeae* (Schwabe) Petch, and it was isolated by Sugiura [72] from rice stubble in Hirosaki, Aomori Prefecture, Japan.

YEA is a highly nutritive medium containing agar as a solidifier, peptic digest of animal tissue, and yeast extract, and is thus rich in nitrogenous compounds, vitamin B, and other nutrients [73]. Furthermore, yeast extracts do not seem to affect the quality or level of aurofusarin, which is a major pigment, in any *Fusarium* species [74]. This is important because it is desirable to use the mold's original coloration in the studies, without much change, because of the available nutrients.

F. graminearum colors change in a very consistent and predictable pattern [26]. At a glance, the mold germinates as a pale mycelium and starts to acquire a yellowish coloration between the third and fourth day. It attains its full orange tone on the sixth day and then shifts to dark wine red by the 16th day. The color distribution is heterogeneous forming a radial gradient with the center more intensely colored and increasingly pale surroundings. Kim*, et al.* [52] described the *F. graminearum* as a

yellow to tan mycelia with white to carmine red margins, depending on the growth condition. A dominant red color tends to become more evenly distributed as the fungus ages, with alternate concentric layers of white and red rings close to the center becoming increasingly evident. The white rings are hairy and seem to be formed of colorless hyphae. The medium's color change (Figure 8c) from pale to yellow is due to the accumulation of aurofusarin [63].

Recent analysis based on red, green and blue (RGB) channels taken for *F. graminearum* photographs shows that the three color components are positively correlated and all exhibit a third-degree polynomial trend when measured throughout the first 20 days of its lifecycle. This makes the measurement of colors a potential tool to replace size-based measurements for growth studies and prediction of toxin production [26].

2.4.2 Major *F. graminearum* pigments

Most of what is known about the pigmentation of *F. graminearum* is derived from studies on *F. culmorum*, *F. aquaeductuum*, *F. fujikuroi*, and *F. oxysporum*, and the eventual confirmation that these pigments are conserved across species [64]. Such studies are aimed primarily at enhancing pigment production for the dye industry as an alternative to synthetic counterparts [33]. A pioneering study by Ashley*, et al.* [57] identified aurofusarin, rubrofusarin, culmorin, and their derivatives among other pigments. Since then, other pigments have been discovered including perithecial melanin [31] and carotenoids [64]. The most relevant carotenoids from *F. graminearum* are perhaps neurosporaxanthin and torulene [63, 64, 69].

F. graminearum pigmentation is highly complex, with most pigments having similar colors, ranging from yellow and orange to red. Thus, it is difficult to estimate the contribution of each pigment to its color. However, from literature it can be

concluded that aurofusarin and neurosporaxanthin, and possibly rubrofusarin as well, impact *F. graminearum* surface color to the greatest extent. Non-carotenoid and carotenoid pigments have never been simultaneously compared and articles describing each of these classes tend to state the respective compounds as the main source of coloration, probably because the pigments have similar colors. It would be useful to determine the contribution of each pigment to the coloration, perhaps through experiments based on their distinctive properties. For instance, carotenoids are expected to react to light, but so far from literature, it is known that polyketides such as aurofusarin and rubrofusarin do not differ considerably in the presence or absence of illumination. By simple observation, aurofusarin appears to be predominant because *F. graminearum* specimens grown in the dark and illuminated settings do not differ in coloration when maintained at the same temperature.

In any case, the color change has previously been demonstrated to follow a predictable trend, irrespective of the pigments involved. Thus, irrespective of the dominant pigments, a consistent pattern over time is observed. It is difficult to determine if the changes are due to variations in the proportion of different pigments or chemical reactions leading to changes of the same compound into its derivatives, like in the case of aurofusarin at different pH. It could also be due to the breakdown of aurofusarin into rubrofusarin molecules.

There are two more aspects to consider before listing *F. graminearum* pigments or related compounds. Culmorin is colorless, but it has been included in this review because it was isolated together with other pigments for the first time, during the studies on *Fusarium* pigmentation. Bikaverin and fusorubin are *Fusarium* pigments [67, 75, 76] , but they have not been included in the following list because

there is very little evidence about their occurrence and impact on the coloration of *F. graminearum*.

A. Aurofusarin

Aurofusarin was obtained chemically and isolated from *F. culmorum* before Baker and Roberts [59] extracted and purified it from a strain of *F. graminearum* Schwabe. It is a dimeric metabolite belonging to the naphthoquinone group of polyketides [62, 77] and is described as a golden yellow-orange or red micro-crystalline pigment in the form of a prism [57, 62, 68, 78] . Its chemical formula is $C_{30}H_{18}O_{12}$ with a molecular formula (Figure 9) of 570.5 g/mol and a melting point above 360 °C [57, 79] . It is currently assigned as 13191-64-5 under the Chemical Abstracts Service (CAS) [79]. Aurofusarin is the only *F. graminearum* pigment produced under a deficiency of nitrogen, phosphorus, oxidative stress, and inhibition of respiration [67].

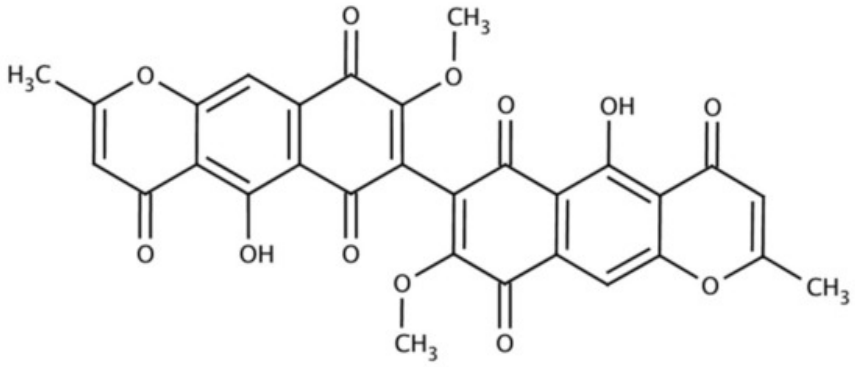

Figure 9. Structure of aurofusarin. Source: Glentham Life Sciences [79].

The species *F. acuminatum*, *F. avenaceum*, *F. crookwellens*, *F. culmorum*, *F. graminearum*, *F. poae*, *F. pseudograminearum*, *F. sambucinum*, *F. sporotrichioides*, and *F. tricinctum* all produce aurofusarin [62]. Different strains of *F. graminearum* produce different quantities even under similar conditions [80]. Besides *Fusarium* species, aurofusarin can also be isolated from *Hypomyces rosellus* and *Dactylium*

dendroides [81]. It is negatively correlated with vegetative growth [52], thus the pigment is expected to be more abundant in differentiated structures. Aurofusarin definitely increases the organism's competitive saprophytic ability due to its antibiotic properties, but it does not help the fungus in colonizing the host crops or protecting it against radiation [53]. The pigment can be extracted using benzene-acetone (4:1) and purified by chromatography on silica gel saturated with oxalic acid [61, 68].

The aurofusarin biosynthetic pathway involves several genes clusters and at least five enzymatic steps, with rubrofusarin being an intermediate [82]. For instance, its synthesis requires the intervention of polyketide synthase genes [83] within a 30 kb cluster (Figure 10), including *pks12*, *aurR1*, *aurJ*, *aurF*, *gip1*, and *gip2* [82, 84] in 11 reading frames (FG02320.1–FG02330.1) along with a facilitator transporter gene (FG02331.1) [85].

Figure 10. Biosynthetic gene cluster for aurofusarin in *F. graminearum*. Based on Hoffmeister and Keller [85].

Among these genes, *aurR1* and *gip2* are believed to be the transcription factors of the cluster [52, 62], and the putative laccase Gip1 has been described as potentially responsible for the dimerization of rubrofusarin into aurofusarin [82, 86]. More recently, two more genes, *gip3* and *gip8* were also shown to be important for the dimerization [84]. Frandsen*, et al.* [82] have shown that two more orphan genes *aurZ* and *aurS*, along with AurT, an aurofusarin pump, are responsible for transporting aurofusarin and rubrofusarin across the plasma membrane.

Though aurofusarin had been described before 1937 [57], it has only been regarded as a food and feed contaminant since the beginning of the 21st century [87] , as evident from available literature [77, 87]. It is frequently found in several

commodities almost across all climatic regions of the world, sometimes at concentrations as high as 2046 μg/kg to 10,200 μg/kg [77]. Beccari*, et al.* [80] detected 10,400–140,000 μg/kg in Italian samples of durum wheat, Ezekiel*, et al.* [88] detected concentrations above 800 μg/kg in chicken feed, and Nichea*, et al.* [89] detected median concentrations of 71.4 μg/kg (2011) and 80.7 μg/kg (2014) in native grass of Argentina, intended for grazing cattle. The latter was found to occur along with zearalenone.

Aurofusarin is bioactive and considered to be a neglected mycotoxin [77, 90]. According to Medentsev*, et al.* [78], it inhibits the growth of some molds and yeasts. Tola*, et al.* [91] also found it to impair the growth of red tilapia (*Oreochromis niloticus* × *O. mossambicus*). Moreover, it was found to be cytotoxic for colon adenocarcinoma cell line HT29 and the non-tumorigenic colon cells HCEC-1CT at concentrations above 1 μM [77]. It has also shown toxicity towards differentiated intestinal porcine epithelial cells (IPEC-J2) when combined with DON [46]. Dvorska, Surai and their colleagues [87, 92-94] performed a series of studies demonstrating the detrimental effects of aurofusarin in Japanese quail eggs. They found aurofusarin to cause a significant decline in vitamins E and A, total carotenoid, lutein and zeaxanthin, and stimulated lipid peroxidation in the egg yolk. However, the mechanistic details of how aurofusarin causes these effects remain unknown. Regarding the correlation of aurofusarin with fats, Dvorska*, et al.* [94] stated that aurofusarin exhibited an association with decreased docosahexaenoic acid proportion in phospholipid, and cholesteryl ester and free fatty acid proportions in egg yolk. A simultaneous increase in the proportion of linoleic acid in phospholipid, and free fatty acid and triacylglycerol fractions was observed. Dvorska*, et al.* [87] also proposed

that aurofusarin reduces the quality of chicken meat, although the mechanism through which this happens remains unclear.

Limited but convincing literature is available regarding the relationship between pigmentation and mycotoxins. For instance, the genetic and biosynthetic origins of aurofusarin and both DON and ZEA have been previously described [53, 66]. As mentioned earlier, Malz*, et al.* [53] demonstrated that mutants for the gene *pks12*, unable to produce aurofusarin, produced an increased quantity of ZEA. It suggests that some inhibitory factor in ZEA is related to aurofusarin synthesis, although the mechanism is yet to be elucidated. Furthermore, combined results from two studies suggest a quantitative relationship between these three compounds [54, 80], although this theory requires further investigation. These studies are still in the preliminary stages, but they demonstrate that some genetic factors are common between aurofusarin and these mycotoxins. If such factors have a similar influence on aurofusarin and the toxins, variations in the quantity of aurofusarins might theoretically be used to predict the quantity of DON or ZEA. Thus, there is a possibility that *F. graminearum* surface color can be a good predictor of toxicity. Furthermore, aurofusarin is a toxin itself and may be quantifiable by using the mold's surface color.

B. Rubrofusarin

Rubrofusarin (CAS: 3567-00-8) is a crystalline polyketide red-orange pigment [57, 68] usually found in the form of needle-like structures [59, 95]. Demicheli*, et al.* [96] have described it as a powder. Rubrofusarin belongs to a class of naphthopyrones and resembles the aurofusarin monomer [62], consisting of a mono methyl ether [57] (Figure 11). Indeed, the biosynthesis of both pigments seem related because different levels of aeration produce distinct proportions of rubrofusarin and aurofusarin [70].

Thus, the hypothesis that aurofusarin could be a predictor of *F. graminearum* toxicity could also be applicable to rubrofusarin.

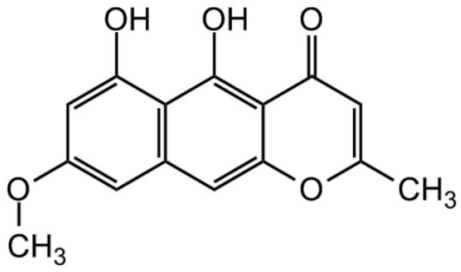

Figure 11. Structure of rubrofusarin. Source: BioViotica [95].

Stout and Jensen [58] and Tanaka and Tamura [97] were the first investigators to present its structure in 1962. According to them, rubrofusarin's molecular formula is $C_{15}H_{12}O_5$ with a molecular weight of 272.3 g/mol [95] and a melting point of 210–211 °C. Rubrofusarin is insoluble in water, but is soluble in ethanol and dimethyl sulfoxide (DMSO) [98]. Unlike aurofusarin, its color does not respond to pH [57]. Furthermore, it has chelating properties, forming complexes with Mg^{2+}, Al^{3+}, Fe^{3+}, Ni^{2+}, and Cu^{2+} in solid state and aqueous medium [96, 99, 100].

Several studies cite the isolation of rubrofusarin or its derivatives from different sources, usually fungi [101], plant roots or seed [99], for pharmacological purposes. Ashley*, et al.* [57] published a pioneering report on the isolation of rubrofusarin from *F. culmorum* and *F. graminearum*. From the fungus *Guanomyces polytrix*, Mata*, et al.* [102] isolated rubrofusarin B, a variation of the compound in which methyl ether is replaced by a hydroxy group at position 6 [103]. Another rubrofusarin producing mold is *Aspergillus niger*, also known for producing ochratoxins and consequently causing the Balkan nephropathy [104]. With respect to rubrofusarin in plants, Rangaswami [105] isolated the compound from *Senna tora* in India, and Oliveira*, et al.* [106] obtained rubrofusarin glycoside from the softwood of *S. macranthera* in Brazil. *Senna* comprises of diverse genera of native leguminous

plants across the tropics [98]. *Berchemia polyphylla var. leioclada*, a woody deciduous plant abundant in China, produces at least three different rubrofusarin glycosides [107]. Other rubrofusarin producing species are *Paepalanthus bromelioides* [108] and *Flavoparmelia euplecta* [109]. Moreover, it is reasonable to hypothesize that all aurofusarin producing organisms also have the potential to produce rubrofusarin since the latter is an intermediate in the aurofusarin biosynthetic pathway [82].

F. graminearum synthesizes rubrofusarin through a polyketide chain intermediate by condensing seven acetate units [110]. Deletion mutants of *aurR1* and *pks12* cannot synthesize rubrofusarin, similar to aurofusarin [62]. Furthermore, the FG12040 protein is also responsible for rubrofusarin synthesis, and the process is inhibited in mutants of *cch1*, which encodes for a calcium ion channel [111]. Rugbjerg*, et al.* [112] confirmed the intervention of the genes mentioned and the metabolic pathway by reconstructing it using *Saccharomyces cerevisiae*. They "paved the way" for industrial production of the pigment.

There is plenty of pharmaceutical potential of rubrofusarin and derivatives to be unlocked, and some of it has already been demonstrated. Rubrofusarin has antimycobacterial, antiallergic, and phytotoxic properties to herbs *Amaranthus hypochondriacus* and *Echinochloa crus-galli* [52, 84, 86, 104]. Alqahtani*, et al.* [113] have shown that rubrofusarin can enhance the cytotoxicity of paclitaxel (PTX) against the adriamycin-resistant breast cancer cell line MCF-7 and rubrofusarin B was found to be cytotoxic to the colon cancer cell line SW1116 [104]. It also completely inhibited human DNA topoisomerase II-α, demonstrating its potential as an anticancer and antiviral drug [101]. Jing*, et al.* [107] found that rubrofusarin glycosides have antioxidant properties, with the effect of one of these glycosides being even stronger

than vitamin C. The pigment was also found to exhibit estrogenic activity [114]. Rubrofusarin bioactivity led Moreira*, et al.* [99] to effectively demonstrate its applicability as a fluorescent probe.

C. Culmorin

Culmorin (CAS: 18374-83-9) is a natural colorless metabolite found in various *Fusarium* species [57, 68, 115, 116], with a molecular formula of $C_{15}H_{26}O_2$ (Figure 12). It was first isolated by Ashley*, et al.* [57] and later described by Barton and Werstiuk [60].

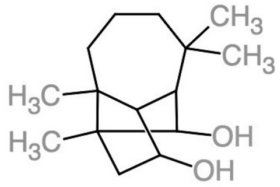

Figure 12. Structure of culmorin. The representative structure was sketched using ChemDoodle [117], based on the structure by Nara Institute of Science and Technology [118].

Culmorin is a longifolene sesquiterpene diol with a tricyclo-[6.3.0.0] undecane skeleton [119], with a molecular weight of 238.3 g/mol [120]. It is biosynthesized from *trans*-farnesyl pyrophosphate [115] and compounds closely related to it include hydroxyculmorins, culmorone, and hydroxyculmorone [121-123]. As previously mentioned, it is colorless and hence technically not a pigment, but it was initially isolated during pigment studies along with aurofusarin and rubrofusarin [61], possibly owing to some shared chemical properties.

So far, the culmorin producing *Fusarium* species mentioned in literature include *F. graminearum*, *F. culmorum*, *F. crookwellense* (*F. cerealis*), *F. venenatum* [124], and more recently, *F. praegraminearum*, which is a basal species of the *F. graminearum* complex [125]. Laraba*, et al.* [126] stated that 77% of *F. culmorum* genotypes in Algeria were capable of producing culmorin, and most of them were

around the subtropical areas. Besides *Fusarium*, the marine fungi *Leptosphaeria oreamaris* [127] and *Kallichroma tethys* also synthesize culmorin [124].

The biosynthesis of culmorin requires the gene *CLM1* (GenBank: GU123140.1), which is responsible for encoding a longiborneol synthase for the compound's pathway [128, 129]. The gene *CLM2* encodes cytochrome P450 and this is responsible for the subsequent hydroxylation of longiborneol. Culmorin was also synthesized in vitro using tetrahydroeucarvone [127]. Citric and lactic acids (5 %) seem to attenuate the culmorin synthesis in feed, which also happens to other *Fusarium* metabolites, including DON [130].

F. graminearum grown in durum wheat in central Italy was found to produce culmorin at exceedingly high concentrations (2.5–14 g/kg), with considerable variations between strains [80]. It was also detected in Norway at median concentrations of 100 µg/kg (wheat), 292 µg/kg (barley), and 2000 µg/kg (oats) [131]. Similar results were found in an ensemble study from Austria, Denmark, and Hungary [90]. In Cameroon, Abia*, et al.* [132] detected culmorin in cereals, nuts, and derivatives at a median concentration of 100 µg/kg. Generotti*, et al.* [133] have demonstrated that culmorin from contaminated wheat flour can endure an entire biscuit baking process, with final levels up to 92 µg/kg in baked biscuits, corresponding to a 25-80 % heat degradation at 180 °C. Their final products also exhibited 15-hydroxy-culmorin. Culmorin and its derivatives also seem to resist the brewing process, even after treatment of the substrates with the fungicide Prosaro® 250 [134].

Culmorin shows mild [124] antifungal activity against several molds, particularly wheat and corn parasites [127]. It is also phytotoxic [119]. With regards to the fungal-plant interaction, the amount of culmorin correlated with the amount of

lutein in durum wheat contaminated with *Fusarium* [135], and this could be a way to empirically estimate the extent of contamination. Furthermore, it is frequently detected along with DON [115, 123, 133], typically at three-fold higher concentrations, although some variables can influence this ratio [119]. However, since culmorin is colorless, it cannot be directly measured through *F. graminearum* surface color. Culmorin and other *F. graminearum* secondary metabolites seem to enhance DON toxicity in caterpillars [136] and pigs [123, 137]. However, culmorin itself is weakly toxic and it tests negative in the Ames test for mutagenicity [124].

D. Black perithecial pigment

Fusarium is among the deuteromycota class which are now known for including a teleomorphic Ascomycota called *Gibberella*, and develops a reproductive fruiting body called perithecium. The black perithecial pigment, sometimes described as dark blue, violet, or purple [31, 138], is almost restricted to the fruiting body [139], although the producing gene is present even in *Fusarium* species with an unknown teleomorph [71]. The nature of the pigment is still under study and recently it has been related to fusorubins [140] and described as a 5-deoxybostrycoidin-based melanin [31], with a molecular formula of $C_{15}H_{11}NO_4$ [141] (Figure 6).

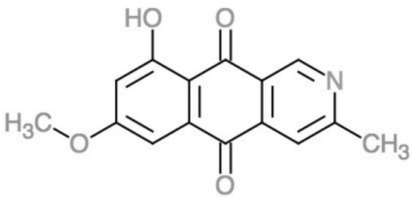

Figure 13. Structure of 5-deoxybostrycoidin. The representative structure was sketched using ChemDoodle [77], based on the structure by Frandsen et al. [28].

Several *Fusarium* species, including *F. graminearum*, *F. verticillioides*, and *F. fujikuroi* [31, 140], produce the blackish perithecial pigments, and appear to be related to an ancestral highly conserved gene cluster [142]. The fungus *Nectria*

haematococca also showed the ability to produce 5-deoxybostrycoidin [141]. In *F. graminearum*, the six-gene *pgl* cluster, particularly the genes *pgl1* or *pks3*, seem to be associated with the production of the polyketide synthase responsible for biosynthesis of the black perithecial pigment [83, 143]. The gene *pgl1* is related to a transcription-associated protein (TAP) cluster called *tc*3 [139]. Studt*, et al.* [140] demonstrated an association between the dark pigments and fusarubin under the intervention of the *fsr* gene cluster.

Evidence suggests that this pigment is important for UV or desiccation protection during the differentiation of perithecia and ascospores [83], and this role is a function of its chemical composition, free radical quenching ability, and its distribution throughout the perithecial surface [144].

E. Carotenoids

Natural carotenoids comprise of a family of more than 750 natural lipophilic terpenoids, several of which are produced by fungi, although they are not essential for these organisms [64]. Carotenoids are common in molds and they contribute to the yellow, orange and reddish coloration [145]. They have been produced industrially and are widely used as food and feed additives [146].

An important characteristic of carotenoids worth mentioning is their sensitivity to light. As Avalos*, et al.* [64] have stated, illumination induces the synthesis of carotenoids through the transcriptional induction of structural genes in *Fusarium*. Jin*, et al.* [69] identified neurosporaxanthin and torulene as the most relevant carotenoids, but others carotenoids likely to play a minor role in *F. graminearum* color pattern are torularhodin, β-carotene, γ-carotene, ζ-carotene, and β-zeacarotene [147-149].

Torulene

Torulene (CAS: 547-23-9) is a natural carotenoid of great industrial importance [150, 151], with a molecular formula of $C_{40}H_{54}$ and a molecular weight of 534.9 g/mol [151]. As Figure 14 shows, it has 13 double bonds, a β-ionone, and a long polyene chain [150]. In petroleum ether solution, torulene has a pinkish-red color, depending on the concentration [150].

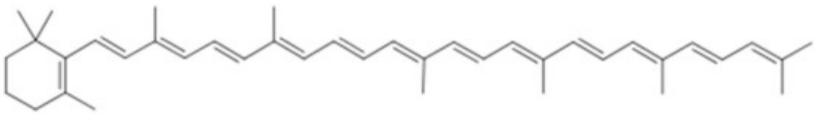

Figure 14. Structure of torulene. Source: Royal Society of Chemistry [152].

Neurospora crassa is the most well-known producer of torulene, but it is also synthesized by *F. fujikuroi* [153], *F. graminearum* [69], the red yeasts *Sporidiobolus pararoseus* and *Rhodotorula glutinis* [154], and related organisms as also organisms belonging to genera *Cystofilobasidium*, *Dioszegia*, *Rhodosporium*, and *Sporobolomyces* [149]. These organisms probably produce it as protection against photo-oxidation and free radicals [155].

Geranyl-geranyl diphosphate is the precursor of torulene, and it is transformed by the intervention of two enzymes AL-2 and AL-1, produced by eponymous genes [153]. The biosynthesis is mostly influenced by nutrients, especially the sources of carbon and nitrogen, but it also responds to other factors such as aeration, temperature, acidity, exposure to radiation, and the presence of chemicals such as alcohols [149].

There is very little information on torulene's bioactivity and nutritional value, perhaps because it is rarely found in food [156], but its nature, structure and limited evidence provide some hints. Animal studies have demonstrated its safe usage as a food additive [150], and Kot*, et al.* [149] have shown that it can also be used as

feedstock and cosmetic additive. The presence of a non-substituted β-ionone ring makes torulene pro-vitamin A, which is likely to have higher antioxidant or free radical scavenging activity than β-carotene. It also has higher reactivity in aqueous solutions, and more efficient electron transfer-reactions than lycopene [154], along with evidence of anti-prostate cancer activity [150].

Neurosporaxanthin

Neurosporaxanthin (CAS: 2468-88-4), or β-apo-4′-carotenoic acid, is a carboxylic apocarotenoid xanthophyll [145, 157], with a molecular formula of $C_{35}H_{46}O_2$ (Figure 15) and a molecular weight of 498.8 g/mol [153, 158].

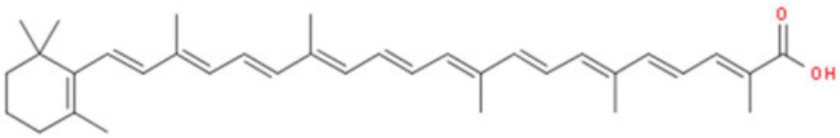

Figure 15. Structure of neurosporaxanthin. Source: National Center for Biotechnology Information [158].

Neurosporaxanthin carries the name of *Neurospora crassa*, from where it was originally isolated, but *Fusarium, Verticillium*, and *Podospora* species also synthesize it [145, 157].

Prado-Cabrero*, et al.* [159] have described neurosporaxanthin as a cleavage product of torulene. The biosynthesis is initiates by the condensation of two geranylgeranyl pyrophosphates into phytoene followed by desaturations [145, 146]. The cleavage of torulene into neurosporaxanthin requires the carotenoid oxygenase CAO-2, first resulting in β-apo-4'-carotenal, which is the aldehyde of neurosporaxanthin [153]. The major genes involved in this process are *carRA*, *carB*, *carT*, and *carD* [145], with the latter gene being in a different cluster.

2.4.3 Remarks

In summary, it is reasonable to assume the possibility of using *F. graminearum* surface color to estimate the amount of toxin produced by the mold and possibly estimate its potential bioactivity. However, a lot remains to be investigated in relation to *F. graminearum* and several other molds. It is necessary to catalog the pigments produced by each species and clarify their biosynthetic relationships to prevent information gaps. For instance, a trichothecene-producing mold is perhaps likely to also produce culmorin, and similar parallels can be drawn between aurofusarin and rubrofusarin or torulene and neurosporaxanthin. It is true that commercial demand is frequently a major driving force in research and sometimes it is not merely choice or curiosity that drives investigators, but it is always important to build a comprehensive body of knowledge from which other researchers can draw information and make their own contributions.

Chapter 3 *F. graminearum* surface color as predictor of DON production in yeast extract agar (YEA)

3.1 Standard curve for DON quantification

In the experiments presented in this chapter and the next, DON was quantified using high performance liquid chromatography using a Jasco HPLC system (JASCO Applied Sciences, Victoria, British Columbia Canada). The standard curve (Figure 17) was obtained using Biopure (Romer Labs, Singapore) reference deoxynivalenol in acetonitrile, certified by Streicher [160]. The material was used to prepare 10 dilutions, ranging from 10 to 100 µg/ml and the standard curve prepared.

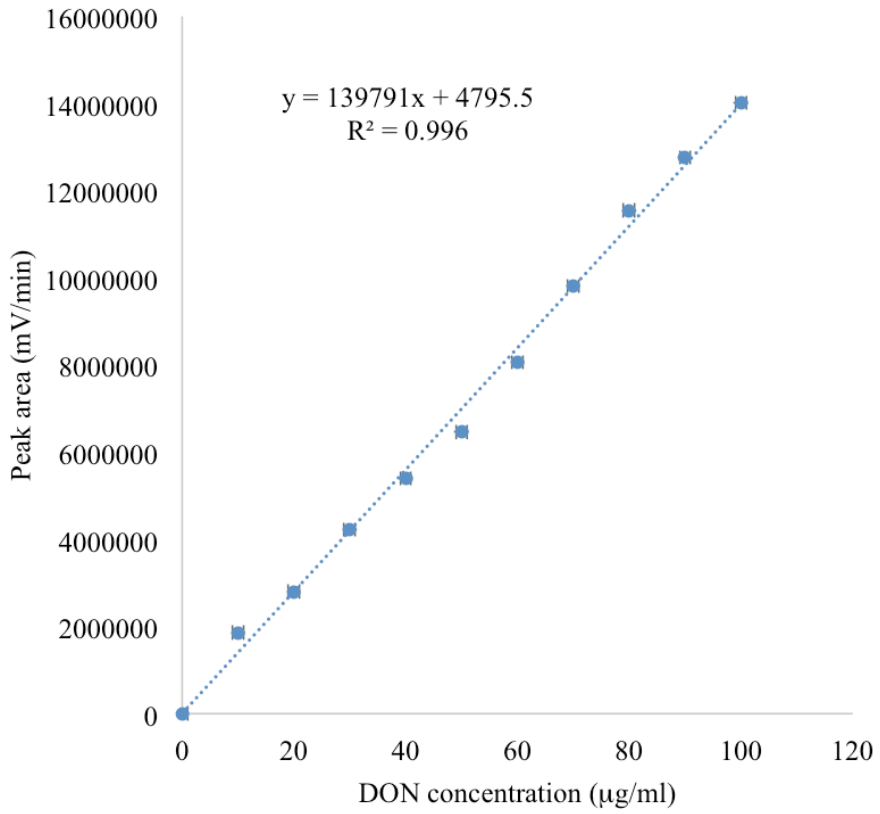

Figure 16. Standard curve used in this study to quantify DON levels, using HPLC.

3.2 *F. graminearum* growth and its fitness to the commonly used size-based models

3.2.1 Introduction

Fusarium graminearum is a fungal plant parasite responsible for the disease known as FHB (*Fusarium* head blight) in crops such as wheat and corn, and mycotoxin contamination in humans [23, 50]. The toxins include deoxynivalenol, nivalenol and zearalenone [72, 161, 162]. The former two are emetic and the latter has estrogenic properties.

Substantial studies have been conducted on fungal growth [28, 163-165], most of which were done for practical applications such as brewing or drug production rather than mere scientific curiosity. Thus, the knowledge is either focused on substrate or environmental conditions, and is superficial or speculative regarding bacterial studies. Hence, there is a need to properly describe fungal growth, especially molds.

Three major models have been used to describe fungal growth, one lineal and two sigmoidal (Gompertz and Baranyi) [28], although there is considerable debate about which is the best model for practical purposes. While some prefer the simplicity of the lineal model, others claim that the sigmoidal models are more accurate and representative of the irregular nature of the biological phenomenon [166]. The choice of an appropriate growth model for *F. graminearum* will allow scientists to more accurately predict the propagation of FHB and prevent outbreaks. This study was aimed at determining the model which better explains *F. graminearum* growth in a system with limited nutrient supply, in minimal medium and at room temperature.

3.2.2 Material and methods

A. Isolate

This study used *F. graminearum* from the JCM Catalogue which is registered as the teleomorph *Giberella zeae* (Schwabe) Petch isolated by Sugiura [72] from rice stubble in Hirosaki, Aomori Prefecture, Japan. It is a known producer of deoxynivalenol, 15-acetyldeoxinivalenol and zearalenone [167].

B. Incubation and growth analysis

Three *F. graminearum* replicates were grown in yeast extract agar (YEA) in a black box inside a chamber, at room temperature during for days. Daily images were taken using Nikon D3200. The shots were performed vertically at 25 cm above the specimens after opening the Petri dishes.

The radii were measured using ImageJ software. After setting the scale, using 90 mm of the plate's diameter as reference, the fungal area was isolated using RGB color threshold. The Feret's diameter was then determined and converted to radius. The growth models were determined using reference values such as the duration of the lag phase (λ), end of exponential growth (t_{max}), maximum growth rate (μ_{max}) and the maximum radius (y_{max}). The different models were compared with the actual growth using Wilcoxon's paired test at $\alpha = 0.05$.

3.2.3 Results and discussion

A. Observed growth

The mold growth followed a logarithmic pattern with a typical sigmoidal curve (Figure 17a). The lag phase continued for 1 day followed by 10 days of exponential growth. The maximum growth rate was 33 mm/d and the maximum radius was 45 mm. Figure 17b shows the mold's growth rate during the exponential phase,

consistent with a 4th degree polynomial. The growth was at its peak on the 2nd day, between the 4th and 5th days, and also around the 9th and 10th days. There is a notable valley between the 6th and 7th days.

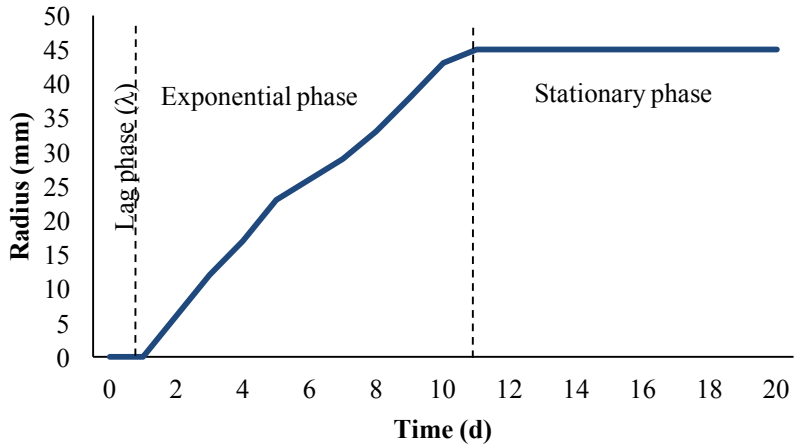

(a)

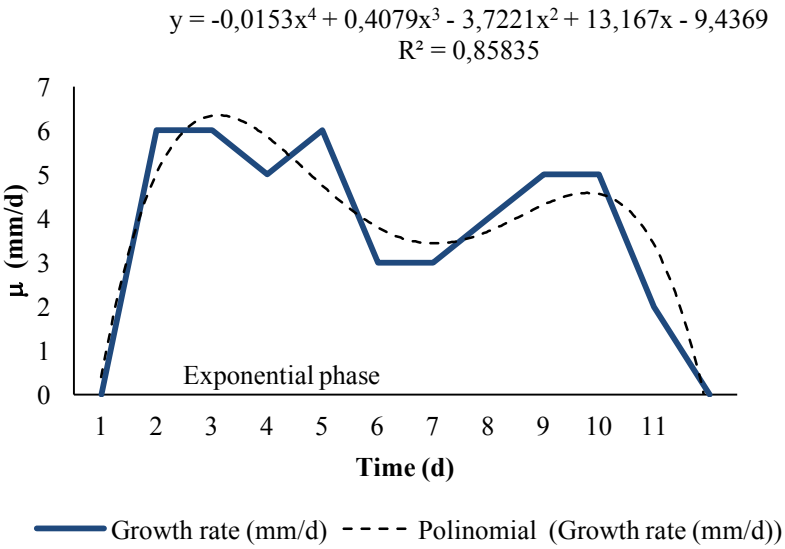

(b)

Figure 17. *F. graminearum* (a) growth during 20 days and (b) growth rate from the first day up to the end of the exponential phase.

B. Comparisons with the models

The lineal model was first compared to the actual growth. A paired t-test suggests significant differences between the expected and observed growth trends ($p = 0.002$). Figure 18a below shows the growth trend of *F. graminearum* expected from the lineal model over a period of 20 days. The differences were notable, especially during the log phase. The lag phase also showed some discrepancy, with the actual growth started at least one day before what would be expected from the lineal model. On the other hand, the curves seemed to converge as time progresses and finally meet at the beginning of the stationary phase. According to these observations, the lineal model was not fit to represent *F. graminearum* growth.

The Gompertz model was then analyzed (Figure 18b) and a paired t-test showed considerable differences between the model and the actual growth trend ($p < 0.001$). It seemed less representative when compared with the lineal model. The Gompertz model seemed very smooth, almost lacking a lag phase and showing very harmonious transitions between the phases. The stationary phase's onset also took some days longer than expected. Thus, this model was not the most accurate in representing *F. graminearum* growth.

Barany's was the last to be compared (Figure 18c). This model did not show sufficient statistical difference according to a paired t-test, to be regarded as substantially distinct from the observed values ($p = 0.280$). There were noticeable discrepancies between the two growth trends, especially in the slope variations in the log phase. Barany's model also seemed smooth but not as much as Gompertz. Its shape was somewhere between the two previously analyzed models. Nevertheless, apart from the considerably irregular shape of the actual growth curve during the log phase, Barany's model seemed most suitable to represent *F. graminearum* growth.

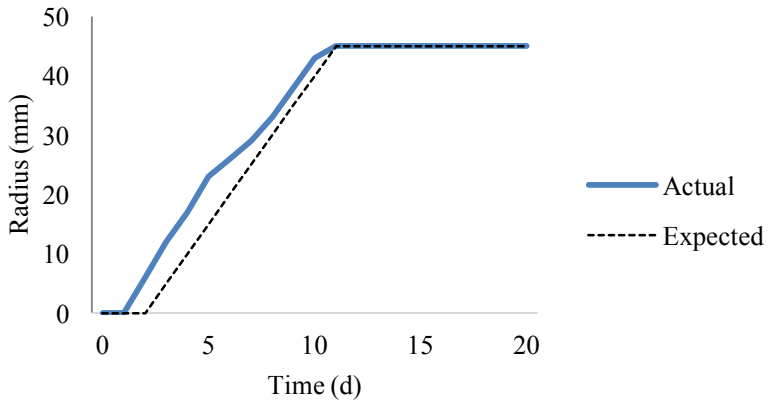

(a)

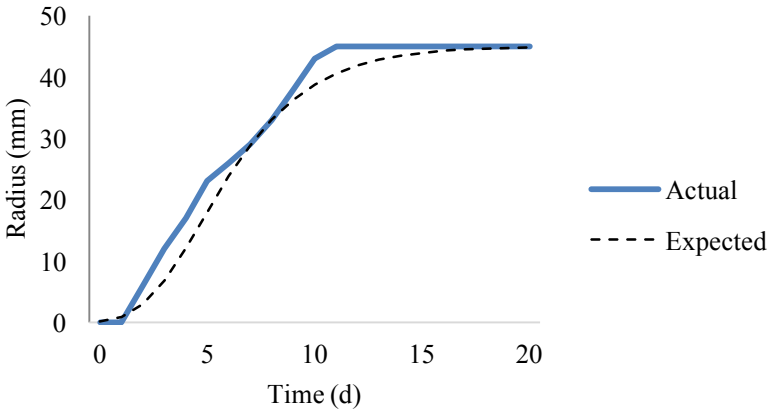

(b)

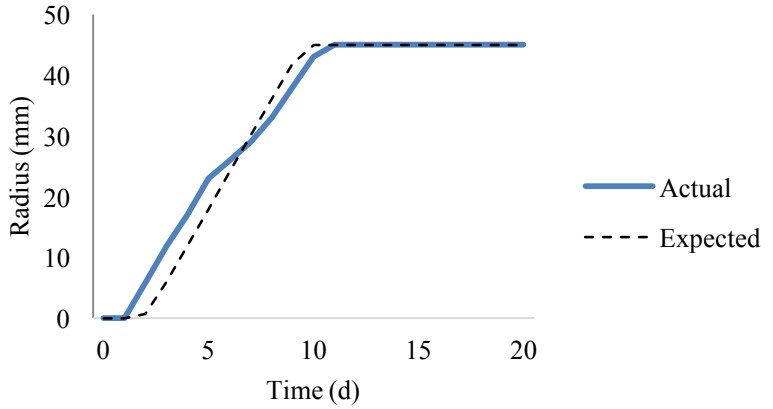

(c)

Figure 18. Comparison between the actual growth and estimations through the (a) lineal, (b) Gompertz and (c) Baranyi models.

3.2.4 Discussion

The logarithmic growth pattern was expected, as it is common in biological systems, especially when subjected to confined spaces rich in nutrients [32]. In this case, the mold stopped growing in size due to limited availability of surface area rather than nutrient shortage. Color change is noticeable once growth stops and it is probably a result of nutrient shortage [26].

Neagu and Borda [168] also studied *F. graminearum* growth and they observed a higher maximum growth rate (13.5 mm/d) with the fungus attaining its full size on the 8^{th} day. The difference might have been due to the media used by them which was enriched with barley and wheat extract, while the medium used by us was minimal, containing only yeast extract. Different yeast extracts can induce different behavior even in the same mold [74]. The difference in the strain might have been another reason for the difference in growth rate, particularly since *F. graminearum* comprises of a polyphyletic group with distinction between strains and species which are still under scrutiny [11]. Unfortunately, Neagu and Borda [168] did not use the models described above and ignored details such as phase distinction, probably because the focus of their study was to determine the time taken for the mold to occupy the entire surface area of the plate.

The growth rate might be explained by some biological interactions [32, 169]. The lag phase involves adaptation followed by rapid growth. The following reduction is probably due to signal from the first hyphae reaching the plate boundary and encountering nutrient exhaustion. However, it is not a major problem because there are more nutrients underneath the surface. After re-adaptation to the new situation, they grew for a few more millimeters and finally stopped growing as most fungi reached the boundary.

The lineal model is certainly the most convenient model to apply and hence is the most widely used [28], but it cannot be applied to *F. graminearum*, even for screening purposes. The Gompertz model also cannot be used for the same reason. The Baranyi model seems to be the only representative model that can be applied to *F. graminearum* growth. This result concurs with Garcia's opinion on fungal growth [28] based on Buchanan's meta-analysis of bacterial growth [166].

3.2.5 Conclusion

F. graminearum growth follows a sigmoidal curve with its growth rate predicted by a 4^{th} degree polynomial regression. Further studies may provide more insights into the growth trend of *F. graminearum*. However, from current observations it is evident that among the size-based models originally developed for bacteria, the Baranyi model is the best suited to represent the growth of *F. graminearum* and other related fungi.

3.3 Colors as an alternative to size in *F. graminearum* growth studies

3.3.1 Introduction

Mycelial size is widely regarded as the gold standard in measuring mold growth [28] , regardless of the parameter being measured, which include radius, diameter, perimeter or area. However, this approach has the following drawbacks: (1) molds do not stop growing if the conditions allow; (2) the size does not provide any information about metabolism, especially in this field; (3) in closed systems, the growth in size is limited by the container and the mold takes its shape; (4) it is vulnerable to biotic or abiotic factors without much explanation with respect to metabolic variations; (5) it is not adequate to describe non-circular or irregular shape of the growth curve and (6) usually volume is not part of the measurement.

A constraint is present when the mold is grown in Petri dishes. Radius and diameter are very effective growth predictors during the lag and exponential phases. This explains why Marin*, et al.* [170] and many other authors have used size in their studies for many years. However, expansion slows down as the fungus reaches the plate's boundary, and its thickness is increased. Although, it does not necessarily stop growing, but it can lead be misleading and lead to some inaccurate interpretations. In fact, according to Deacon [32], most of the secondary metabolism processes happen during this period. Hence, there is a need for viable alternative measurement tools.

Color could be a good predictor of both physical and chemical changes for any organism. Although not much is known about the use of color as a predictor of biological processes, but it would be useful in *F. graminearum* growth studies because it is a response to its metabolic and maturation processes [171, 172]. Color changes reflect the state of the fungus in both closed systems and in the field, under antagonistic or any other condition [173], and can now be measured using accessible electronic tools.

If colors are validated as a tool to measure mold growth, they might enhance the overall quality of research on mycotoxins and other metabolites such as antibiotics or enzymes. In the current context, if the color change is effectively demonstrated as being related to growth, it has the potential to be used by researchers or farmers to know if *F. graminearum* is producing deoxynivalenol (DON) and zearalenone (ZEA) merely by observing its color.

3.3.2 Material and methods

A. Mold isolate

This study used a *F. graminearum* isolate from the JCM Catalogue which is registered as the teleomorph *Giberella zeae* (Schwabe) Petch isolated by Sugiura [72]

from rice stubble in Hirosaki, Aomori Prefecture, Japan. It is a known producer of deoxynivalenol, 15-acetyldeoxinivalenol and zearalenone [167].

B. Experimental procedure

Three replicates were grown inside a chamber at room temperature on yeast extract agar (YEA) in Petri dishes. The plates were inside a black box to minimize light interference and maximize the contrast between the objects and the background. The only source of light was the light-emitting diode (LED) lamp in the chamber.

Daily photos were taken from upper view at a height of approximately 25 cm, using a Nikon D3200 camera. The photos were taken for 20 days and used for color determination using ImageJ software (FIJI edition), developed by the National Institutes of Health [41]. The images of fungi were separated from the background using the color threshold. There were three basic measurements taken: gray quantification, RGB (red, green and blue) analysis and area determination. The gray scale consists of pixels representing only the monochromatic intensity of light in the image, shown as shades of gray. ImageJ FIJI bears a native plugin to analyze the gray scale. As a predictor, the gray scale would be better than RGB because it ignores the variations in hue and it could be suitable for analysis of different mold species, as they often differ in colors. The Color Histogram plugin available on the website of ImageJ (https://imagej.nih.gov/ij/index.html) is designed to measure RGB from pixels of an image.

The gray scale measurements include mean, mode, minimum, maximum, skewness and kurtosis. The RGB components were analyzed through mean and mode for each color. The mycelial area was measured to validate the mean and modal gray values because it is a better-known growth variable for fungi. Mode and mean were chosen as parameters to represent color change as they show a central tendency and

are probably the most simplified representation of the phenomenon. The mean is good because it accounts for all the values, while the mode is focused on only the most abundant value. In the case of *F. graminearum*, it is important to pay attention to the mean because the mold's surface has a heterogeneous color distribution (Figure 19).

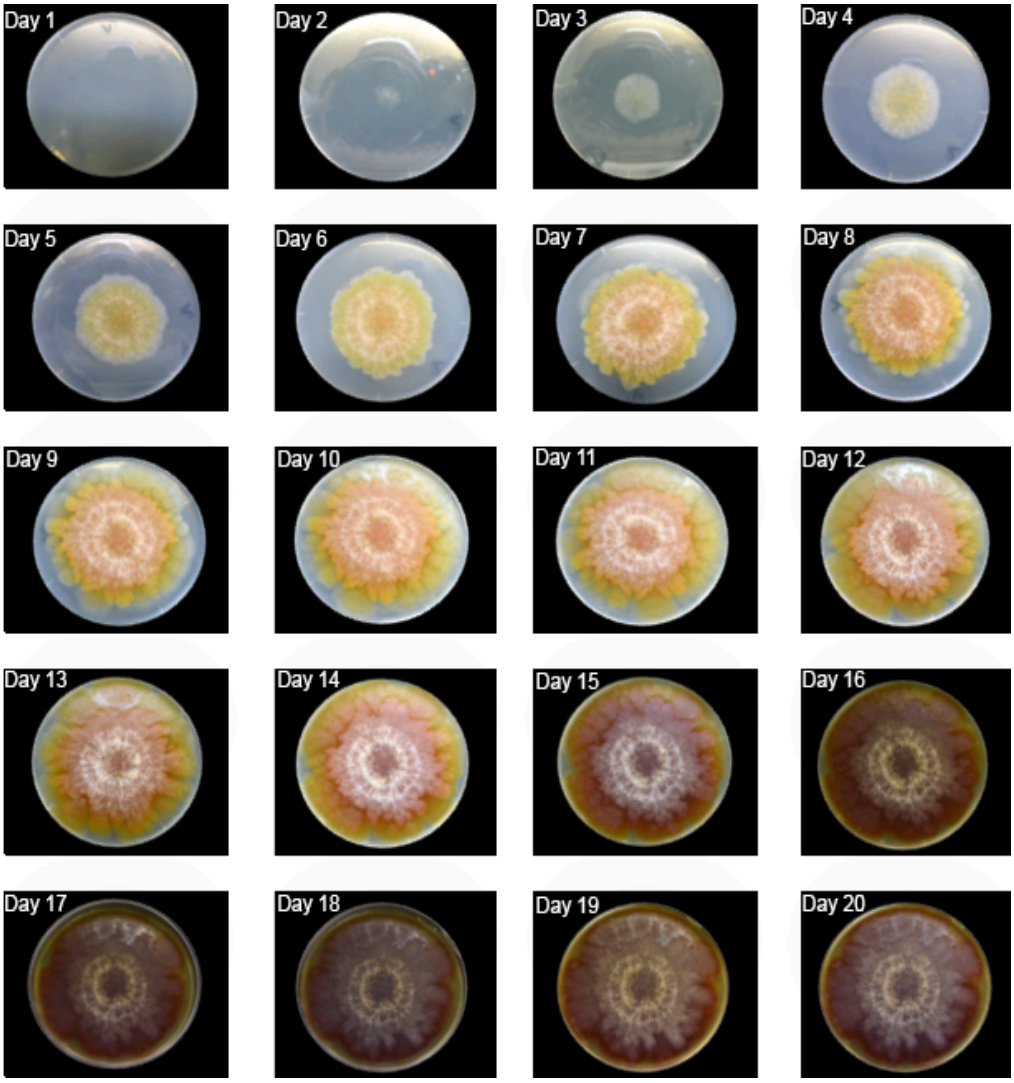

Figure 19. Daily growth of *F. graminearum.*

However, the mean might not be the best approach to analyze secondary metabolites such as mycotoxins because it includes areas with different colors, which possibly differ in metabolic contents and activity. Thus, mode can be a good alternative as it captures the essential colors and will be particularly significant if the most pigmented areas are also the ones producing more toxins.

Nevertheless, the most important aspects of the measurement are consistency of the parameter and its ease of use in mathematical and statistical processing. Due to this reason, levels of dispersion of the gray scale mean and mode values were compared. Additionally, the raw version of the 6-day photo was given to a panel of 21 university students with basic instructions regarding image isolation from the background, to determine the mean and mode.

This procedure was repeated by a number of people because the isolation of the photo from the background is based on visual impression and is therefore subjective. The most consistent parameter would be the one which shows closest proximity between the central tendency measurements and less dispersion.

C. Statistical analysis

The data was analyzed in StataMP, IBM SPSS Statistics 20 and Microsoft Excel. All hypotheses were tested at $\alpha = 0.05$. For the gray value, the mean and mode were compared using Wilcoxon signed rank test to see if there were significant differences. It was performed to select the best measure of central tendency for the study. After analyzing the variation in the gray value, its skewness and kurtosis were also plotted to better analyze its distribution. The gray value was then correlated with the mycelium's area.

The RGB components (mean values) were plotted and compared with trend lines through coefficients of determination (R^2). The correlation between the different colors was also determined to see if they were interchangeable in *F. graminearum* growth studies. The RGB channels were correlated with the gray scale for the same reason.

3.3.3 Results

A. Qualitative description

At the peak of the maximum growth rate, *F. graminearum* formed a yellowish mycelium forming a gradient densely pigmented at its center. The lag phase took 2 days, followed by a 9-day exponential growth. It finally covered the entire surface of the Petri dish on the 11th day. At this point, it became compact and a central reddish color expanded towards the boundaries.

From day 15, there was a reduction in brightness, perhaps reflecting a low metabolic rate. A white layer of mycelium increased as most of the surface changes color to slightly brown.

B. Mean versus mode

Figure 20 illustrates the differences between the mean and modal gray values, following measurements based on the 6th day photo.

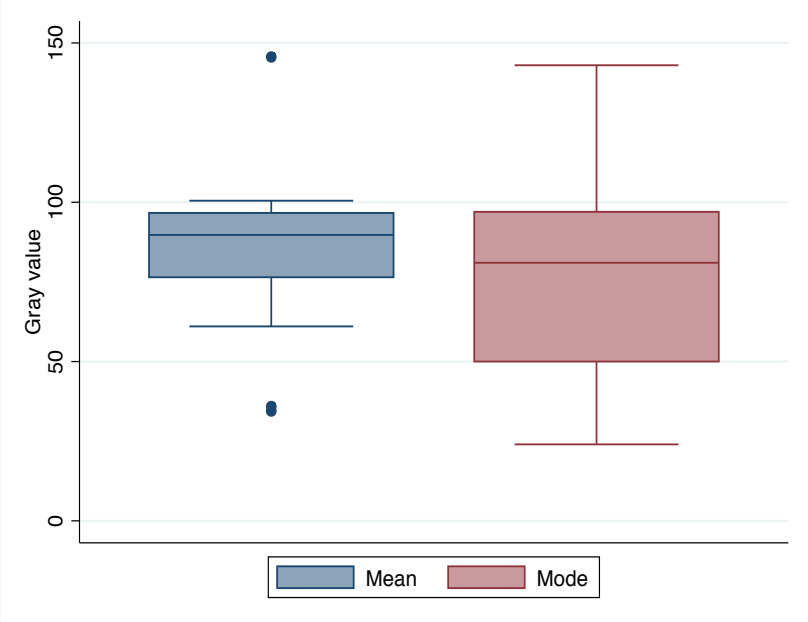

Figure 20. Comparison between the mean and modal gray values from the experimental data.

The mean gray value shows a narrower range of values within the confidence interval. Indeed, the mode value showed a higher standard error (7.29 against 5.56) than other measures of dispersion such as standard deviation, variance, range, and interquartile intervals.

The distance between the average values and median values is 5 units for both, but the mean had higher kurtosis (2.36 against −0.019) and a narrower interquartile range (20) compared to the mode (47). These observations suggest that the mean gray value is the best parameter to analyze *F. graminearum* brightness. As $p = 0.014$ (Wilcoxon signed rank test), it would be unadvisable to use both mean and mode for growth analysis.

Similar results were observed for the RGB mean and mode values obtained from the panel of 21 students (Table 1), though it might be acceptable to interchange both parameters, considering a Wilcoxon signed rank test value of $p = 0.333$.

Table 1. Comparison between the mean and modal colors (RGB) from the 6th day photo of *F. graminearum* measured by 21 different people.

Statistics	**Mean**	**Mode**
Average	147.9	146.7
Standard error	3.1	3.6
Median	157	160
Mode	157	173
Standard-deviation	24.6	28.7
Variance	605.8	826
Kurtosis	−1.52	−1.52
Skewness	−0.53	−0.61
Range	63	66
Minimum	111	107
Maximum	174	173
Sum	9317	9243
Count	63	63

Mode still shows higher standard error and dispersion in general, although the kurtosis is similar for both. The distance between the central tendency measurements

is smaller for the mean value and it also shows equal median and mode values (157). The observations above suggest that mean is a more consistent central tendency measurement than mode, therefore being a more reliable variable to analyze the growth of *F. graminearum* in yeast extract agar, based on colors.

C. Mycelial area and color measurement

The mycelial area increase will be briefly described (Figure 21), as it is an important parameter to validate the color parameters as growth descriptors. The fungus grew according to the typical "s" pattern with the median lag phase lasting for 2 days. Before that, the specimens were not observable without the aid of a microscope. Thus, the major measurements were started on the second day and continued up to the 20th day. The exponential growth increased until the 10th day and it was possible to observe a considerable change to a darker tone in the overall color.

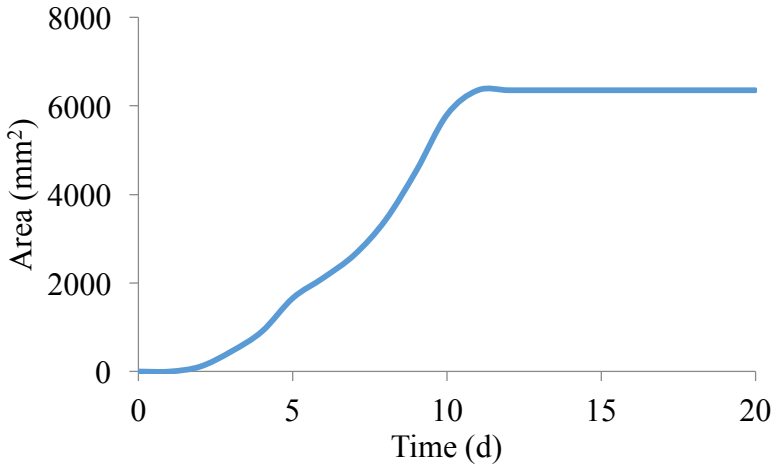

Figure 21. Mycelial area of *F. graminearum* for 20 days.

D. Gray value analysis

The colors observed covered the entire range of gray scale (0 to 255) (Figure 22). The darkest tone was consistently black (0) but the maximum gray value in general increased from 117 to 255 and remained there from the 18th day. Yet, there

are notable variations, such as peaks on days 6, 10 and others, or the valley from the 16th to the 17th day.

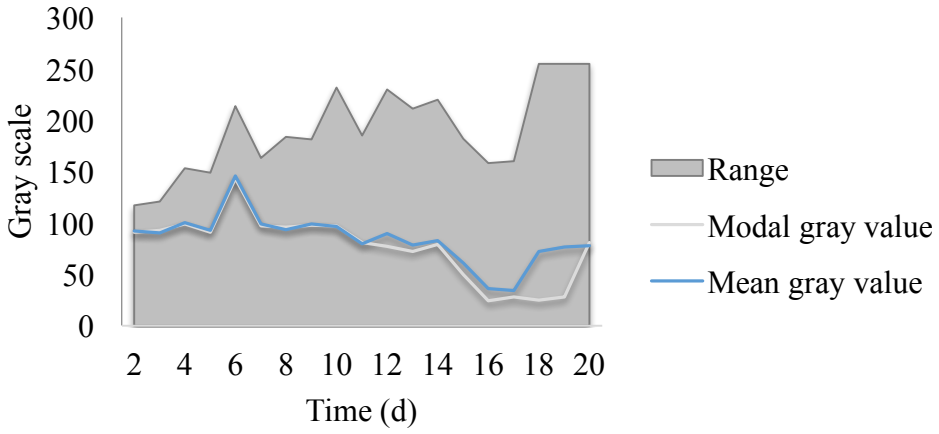

Figure 22. Gray value variation over the course of the measurements. The equation represents the trend line for the mean gray value.

A peculiar phenomenon observed is the daily change in the slope. The brightness first increased and then decreased, with only two exceptions in the final days. Unlike the maximum gray value, the central tendency measures tend to globally decrease, though the mean and mode are, as shown before, significantly different. From the shape of the curve it is evident that they have similar trends until the 11th day (beginning of the stationary phase), when the darker tones become more dominant. The mean is considerably consistent with a cubic function (R^2 = 0.65). Thus, it can be used to analyze the growth of *F. graminearum* and perhaps mycotoxin production, especially with increase in degree of the polynomial.

The skewness and kurtosis of the gray scale were also analyzed (Figure 5). The skewness increased logarithmically from negative values and becomes positive after the 9th day. This suggests that until this day, there was a dominance of lighter colors with a subsequent shift to darker colors. Such a shift might be considered a milestone for the start of metabolism of the stationary phase.

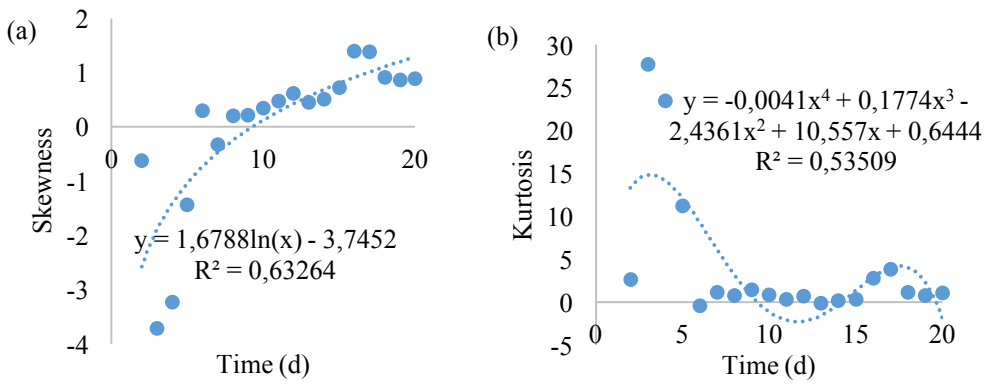

Figure 23. Skewness (a) and kurtosis (b) of *F. graminearum* gray scale.

Kurtosis is a good measure of how narrow the distribution of color tones is and the simplest acceptable fit for the kurtosis trend was a 4th-degree equation. It is evident from the results that there are relatively fewer colors during the first few days, particularly until the 6th day when there is a peak in gray values. The number of colors increases drastically thereafter and remains as such until the end.

Together, skewness and kurtosis point to a variation from few bright colors to a wide-range of darker colors. It is equally important to know the applicability of the gray scale if there is a need to discuss results from previous research, considering size as the major growth predictor. Area might be a more relevant predictor of size than radius or diameter, especially if the mycelium is not regularly formed.

Table 2 correlates the mean and modal gray values with the area. As can be seen from the table, both variables have significant correlation with size at $p = 0.01$, especially the mode values. This suggests that mode is the best parameter to correlate colors with fungal area, even though the mean is easier to measure and develop studies, based on colors.

Table 2. Correlation between the gray central tendency measures and mycelial area of *F. graminearum*.

Variable	Parameter	Area (mm^2)
Mean gray value	Pearson Correlation	−0.533 *
	Sig. (2-tailed)	0.019
	N	19
Modal gray value	Pearson Correlation	−0.577 **
	Sig. (2-tailed)	0.010
	N	19

* Correlation is significant at the 0.05 level (2-tailed)
** Correlation is significant at the 0.01 level (2-tailed)

E. RGB analysis

All RGB channels (Figure 24) showed trends similar to the gray value. Likewise, they presented a peak on the 6th day having an acceptable fit to cubic functions, with an overall decline in value.

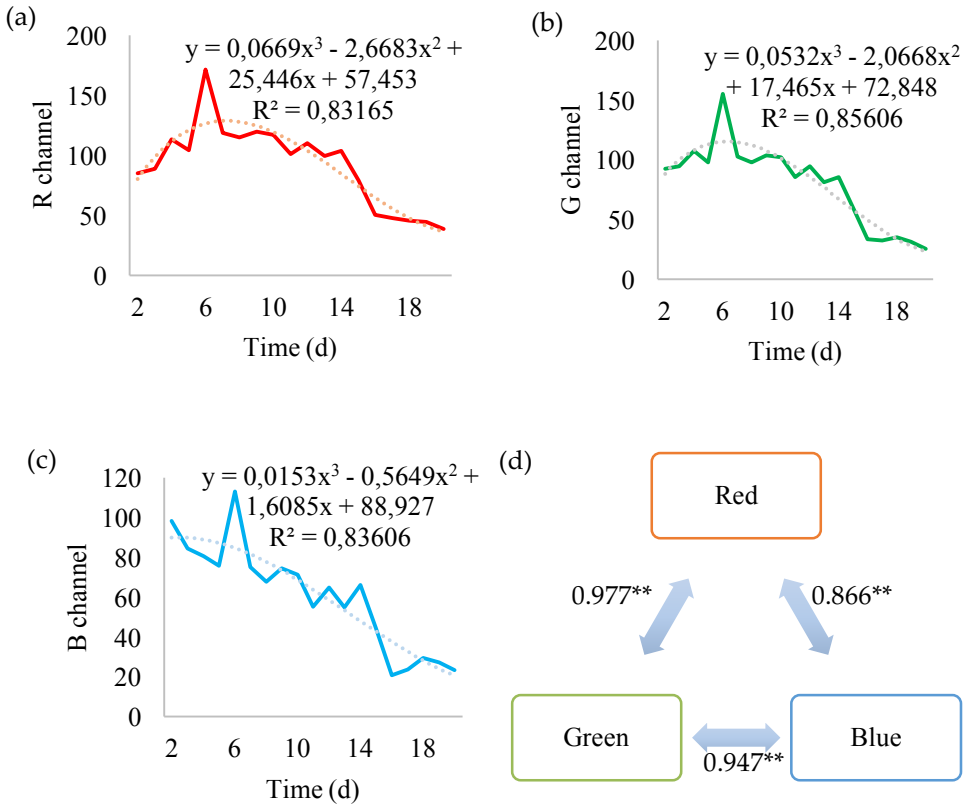

Figure 24. The mean values of the red (a), green (b), and blue (c) channels, and the correlations between their means (d). ** Correlation is significant at $p = 0.01$ (2-tailed).

The cubic regressions resulted in an $R^2 > 0.8$ which allows them to be combined into a single equation with approximately 59.5 % probability of effectively representing simultaneous behavior in the RGB channels. Indeed, the colors seem to be highly correlated, implying that some factor is causing them to change in a similar fashion.

As is evident, each color can be individually used to analyze the growth of *F. graminearum*, although the green component shows the best performance. However, they cannot replace each other, as shown by Friedman's two-way analysis showed ($p < 0.001$). Until more advanced analyses strategies are developed wherein each color can be used to study a particular chemical or metabolic phenomenon, it is advisable to study all as well as separately.

F. How related are the gray and RGB measurements?

As Table 3 shows, all colors are correlated with gray parameters with green showing the strongest relationship yet again. The choice of gray scale to analyze color is convenient as it consists of only one parameter. However, it neglects the hue and saturation, which might be related to some phenomena contributing to pigmentation.

Table 3. Correlations between RGB colors and the central tendency gray measures.

	Correlations	Mean Gray Value	Modal Gray Value
Red	Pearson Correlation	0.825 *	0.865 *
	Sig. (2-tailed)	<0.001	<0.001
	N	19	19
Green	Pearson Correlation	0.858 *	0.902 *
	Sig. (2-tailed)	<0.001	<.001
	N	19	19
Blue	Pearson Correlation	0.846 *	0.881 *
	Sig. (2-tailed)	<0.001	<0.001
	N	19	19

* Correlation is significant at the 0.01 level (2-tailed).

Furthermore, gray scale might be more convenient in comparing observations between species as fungi from even the same genera might substantially differ in color, especially hue. On the other hand, colors, especially green, seem to be more consistent.

Unlike most results shown above (except for the correlation with area), the modal gray value shows more affinity with the mean RGB values. This observation might require more attention in future, as some property of colors was more evident through its abundance, even in the absence of hue and saturation. If the modal gray value showed higher correlation with mean RGB values and area, it is probably more accurate than the mean, although being less precise.

3.3.4 Conclusion

It is possible to use color to analyze and predict *F. graminearum* growth during the first 20 days in yeast extract agar. The color parameters have shown algebraically predictable behaviors either when observed throughout *F. graminearum* growth or when in relation to radius, a well-known growth variable. Even a simple observation shows gradual change, prevalent in several biological phenomena. This approach can be extended to other species or groups of molds in future, with respect to their own color variations. It would be useful to develop a detailed catalog of color variations of different fungi containing their mathematical description throughout their lifecycle.

However, the colors do not necessarily behave like size, although it is possible to correlate the color change with fungal area. Thus, it is necessary to develop new models rather than use the models already established for radius or diameter. In future, it will also be important to standardize this method to ensure reproducibility. For instance, it is important to standardize the type of camera or lens used to

photograph the mold, the growth medium, the exact light settings, temperature, angle and height at which the photos are taken, among other factors potentially affecting the results.

Color analysis is a very promising strategy for growth measurement as it keeps changing even in the stationary phase. Indeed, the number of colors in the fungus increases during this stage, although it also becomes very dark. This method of verifying color change will certainly provide a better understanding of fungal metabolism, than simple size measurements.

3.4 *Fusarium graminearum* colors and deoxynivalenol synthesis at different temperatures

3.4.1 Introduction

Deoxynivalenol (DON) is a toxin produced by *Fusarium graminearum*, and it is responsible for gastrointestinal disorders [50]. It belongs to the family of trichothecenes and its occurrence in food is widespread and is increasing [174]. There have been 8 major outbreaks of contamination in Japan throughout the last century, two of which were in the Hokkaido area [23]. The Japanese Ministry of Health, Labor and Welfare has established a provisional limit of DON in food at 1.1 μg/g for wheat and its derivatives [175, 176], 4000 μg/g for cow feed at least 3 months after birth and 1000 μg/g for cow feed for less than 3 months after birth [176].

There are several in vitro methods to detect DON in food samples [174, 177, 178], which are usually destructive. Development of non-destructive methods would perhaps be more advantageous and cost-effective, particularly if applicable in the field. Color could be an alternative, as a previous study has shown that *F. graminearum* surface color intensity is fit for algebraic analysis through incubation time [26]. Factors such as incubation time and temperature have been frequently

associated with mycotoxin production, including deoxynivalenol [15, 28, 34]. Color has also been associated with toxicity. For example, according to Dufossé, *et al.* [179] a colorant produced by *Monascus* is not allowed for use in Europe and the United States because of its adverse health effects. Also, the major aflatoxins are classified based on their UV fluorescence [180]. Relevant to the current study, Kim*, et al.* [65] have shown that the same set of genes (*fgwc-1* and *fgwc-2*), have the ability to control the biosynthesis of aurofusarin and trichothecenes.

There are some studies with regards to the pigmentation in *F. graminearum*. Typically, the genes or metabolic pathways producing the pigments, and other related factors are the most studied [64]. An early study describes the isolation of rubrofusarin, aurofusarin and culmorin [57]. There were two more pioneering studies (in early 1960s) on the chemical structure of rubrofusarin, a pigment synthesized by *F. graminearum* [97, 181]. More recently, Jin*, et al.* [69] have published a research letter about the two carotenoids neurosporaxanthin and torulene. These knowledge contributions towards *Fusarium* pigmentation are invaluable to the dye industry but do not provide information regarding the relationship of color to the mold's toxicity.

This study was aimed to examine the relationship between mycelial surface colors of *F. graminearum* grown on yeast extract agar (YEA) and the quantity of deoxynivalenol produced by the mold at different temperatures.

3.4.2 Material and methods

A. Mold isolate

A *F. graminearum* isolate from the Catalogue of the Japan Collection of Microorganisms (JCM) was used in this study. It is registered as the teleomorph *Giberella zeae* (Schwabe) Petch, isolated by Sugiura [72] from rice stubble in

Hirosaki, Aomori Prefecture, Japan. It is a known producer of deoxynivalenol, 15-acetyldeoxinivalenol and zearalenone [167].

B. Experimental procedure

F. graminearum specimens (144) were grown on yeast extract agar (YEA) at four temperatures: 15 °C, 25 °C, 30 °C and 36 °C. From the 4th incubation day, 12 replicates per temperature were used for DON quantification. Before extraction, the fungi were photographed in a black bucket, from a vertically height of 30 cm. The camera model used was Nikon D3200 with a lens DX SWM VR. The only source of light was a round LED attached to the bucket's lid. The photos were then processed on the ImageJ software (*FIJI* edition), developed by the National Institutes of Health [41] using the method described by Cambaza*, et al.* [26] (Figure 25).

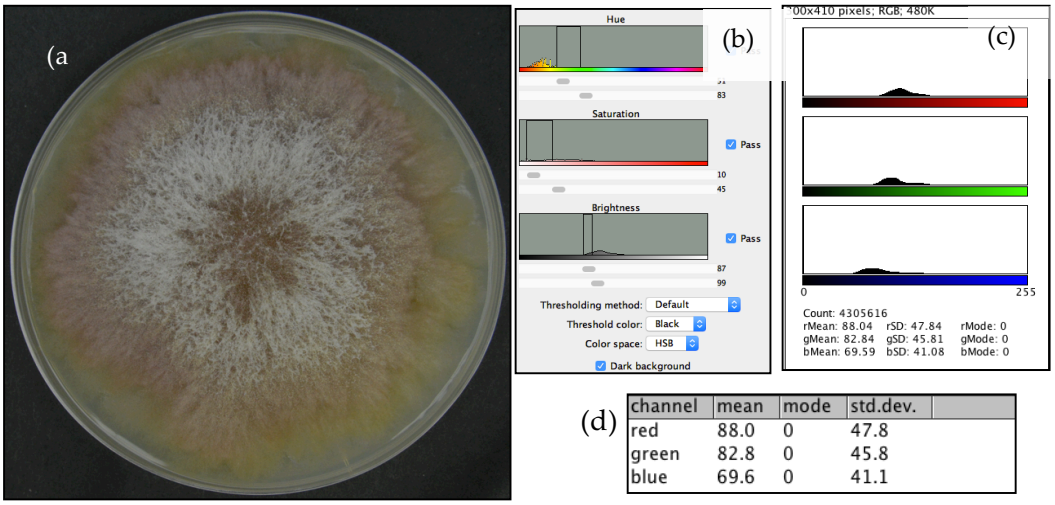

Figure 25. Process of *F. graminearum* color analysis using ImageJ: (a) photo of the mold (8th day, 25 °C); (b) ImageJ panel used to remove the background by filtering colors; (c) color measurement panel; (d) color measurement table.

ImageJ allowed the determination of average intensities of the RGB components from the photos. At the end, the variables used for the analysis were incubation time (in days), temperature (^{o}C) and the RGB parameters, converted from the 8-bit notation (0 – 255) to arithmetic index (0.0 – 1.0).

C. Statistical analysis

Statistical analysis was focused on each color. For each color, a Kruskal-Wallis test determined if the distribution of color intensity between the samples grown at distinct temperatures, presented significant differences. Subsequently, descriptive data were also compared (mean, standard deviation, minimum, maximum, skewness and kurtosis).

In the final step, the impact of both incubation time and temperature on pigmentation was analyzed. A Kruskal-Wallis test was used to assess if the color changed considerably throughout the incubation time, regardless of temperature. The final analysis shows the relationship between color change and DON concentration at different temperatures.

3.4.3 Results

A. Temperature and colors

No sample grew at 36 °C and almost all but one of the remaining specimens grew at 25 °C. Therefore, from this point onwards, the terms “all specimens” or “all temperatures” excludes cases where there was no growth. Red pigmentation was the most abundant, followed by green and then blue (ANOVA: $p < 0.001$). Tukey’s post-hoc tests indicate that no RGB component presented values similar to any of the others throughout the duration of the experiment ($p < 0.001$ for all comparisons), although red and green values presented considerable similarity on day 4. All the colors seemed correlated, exhibiting direct lineal proportionality (Figure 26).

The green component showed the strongest correlation with the others, especially red. However, multiple regression shows that the RGB components cannot be fit as covariates in determining DON concentration ($R^2 = 0.27$). These observations suggest that some common factor influences RGB color components of

F. graminearum, but it is not sufficient to combine them into a single model to predict DON concentration.

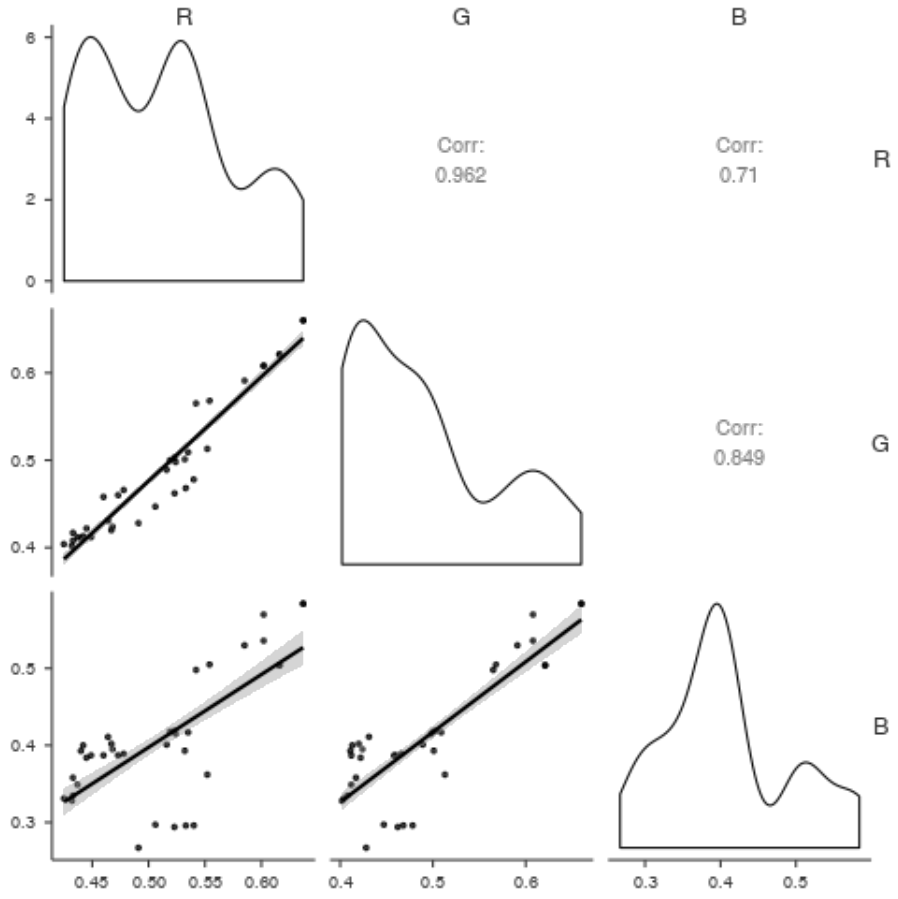

Figure 26. Correlation between the RGB components exhibited, their distributions of shades and lineal relationships.

According to the Friedman test, the red component presented significantly different intensity over time when the molds were incubated at different temperatures (Table 4). The blue component also presented different intensities, but the distinction was less pronounced. The evidence was not sufficiently strong for the green component to assume that the intensities were similar throughout the time analyzed although the *p*-value was close to 0.05. This result points to red being the most susceptible to temperature variation, followed by blue, with green seemingly resistant to any substantial change when *F. graminearum* is grown under different temperatures.

Table 4. Comparison between color intensities between specimens incubated at different temperatures.

Color	p_{ANOVA}*	Post Hoc Comparisons**				
		T (°C)		MD	t	p_{Tukey}
R	0.003	15	25	0.04	3.48	0.002
			30	0.02	1.79	0.175
		25	30	-0.02	-1.69	0.211
G	0.059	15	25	0.04	2.3	0.06
			30	0.01	0.51	0.865
		25	30	-0.03	-1.78	0.179
B	0.033	15	25	-0.04	-2.25	0.066
			30	-0.04	-2.32	0.056
		25	30	0	-0.06	0.998

*For each color considering the different temperatures (Friedman);
**Degrees of freedom: 140; MD - mean difference; SE - standard error

According to Tukey's tests, the differences in the intensity of the red component were significant only between 15 °C and 25 °C, concurrent with DON concentration. For the blue component, the differences were not significant when two temperatures were considered at a time, implying that the discrepancies were significant when three temperatures were combined rather than two. Regardless, the difference in intensity was only far from $p = 0.05$ when specimens incubated at 25 °C and 30 °C were compared. The green component also did not show significant differences in the post hoc test but the discrepancies between the colors were not far from the significance when the molds incubated at 15 °C and 25 °C were compared. From these observations, it appears that green is the only color which shows no significant changes when all temperatures are compared simultaneously or two at a time.

Despite the temperature differences, all colors exhibited similar trends over time (Figure 27). They all showed an initial decrease until day 8, followed by an

increase up to day 12 and subsequently remaining constant until the end of the experiment.

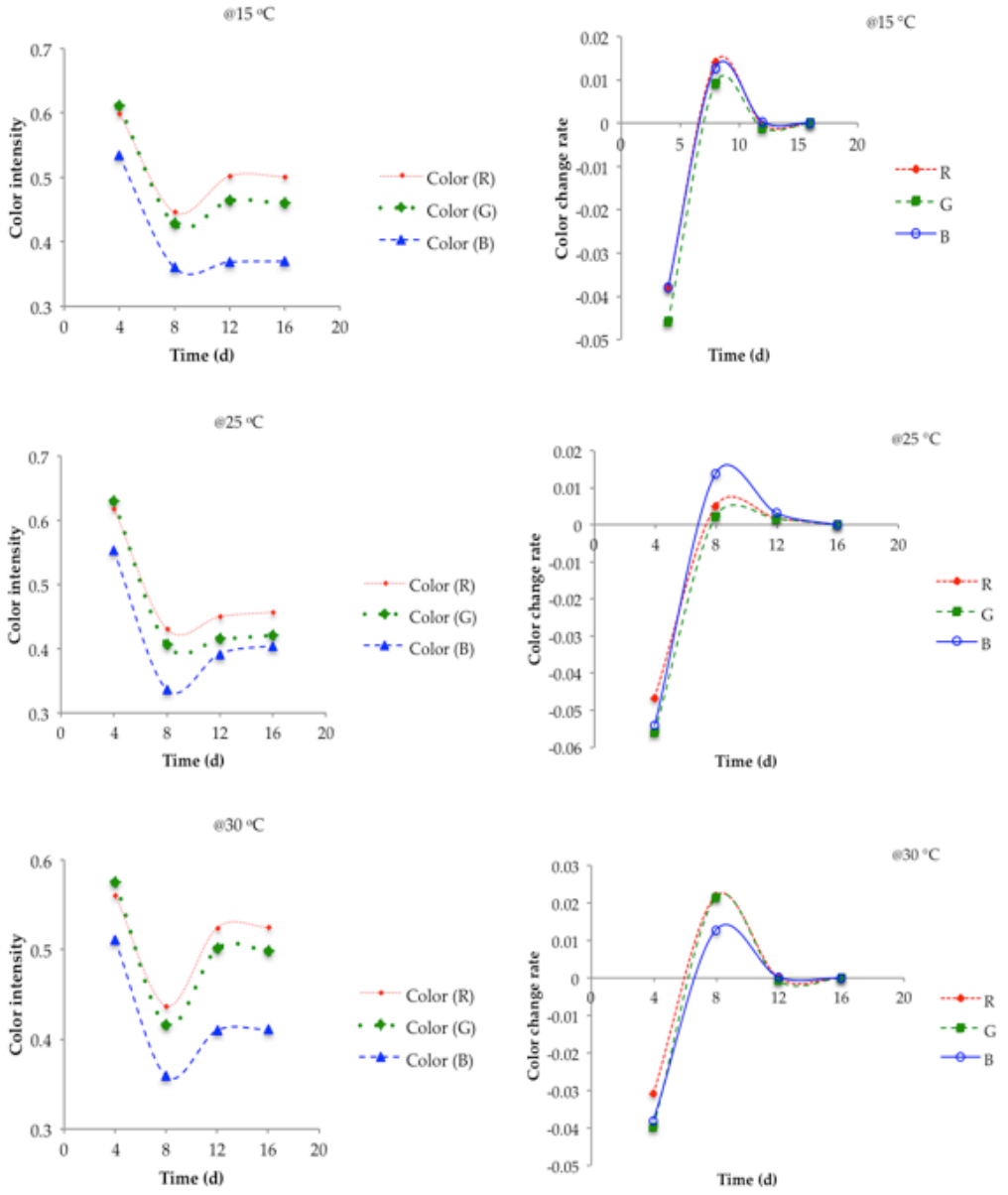

Figure 27. Analysis of *F. graminearum* color change. The left panel of curves show color variations at different temperatures and the right panel shows the rate of color change.

Red color was consistently the most abundant, although it begins with the same intensity as green. Indeed, the red and green components were in general similar over time than blue and either red or green. This is consistent with the correlations observed in Figure 26 where blue was consistently the least intense RGB component.

There were some peculiarities related to the incubation temperatures. The discrepancies between the blue and the other RGB components were notably higher when the samples were incubated at 15 °C and 30 °C. Another noticeable aspect was the graph concavity between day 4 and 12. It was more accentuated at 30 °C, followed by 15 °C and finally 25 °C. There is an exception at 25 °C, where the blue component presented a deeper concavity when compared to its counterpart at 15 °C.

More accentuated concavities indicate higher recovery of the mold's initial intense colors. These observations suggest that all molds were initially very bright, becoming progressively darker and developing a moderate pigmentation in the end. The final pigmentation was more intense at 30 °C, followed by 15 °C and 25 °C. Thus, suboptimal temperatures perhaps stimulate the development of pigmentation in *F. graminearum*.

Regarding the rate of color change, the trends were also similar for all RGB components. They started as negative values, implying that the mold was darkening until sometime between day 4 and 8 when the trend reversed. After attaining a peak near day 8, the value decreased to 0 in day 12 and did not change much until the end of the experiment. In summary, all colors followed the same pattern of variation wherein the molds seem to darken considerably up to a lower threshold at which they become slightly lighter and maintain this color indefinitely.

The peculiarities for each temperature were also visible through variations in the rate of color change. Though red values still seemed to be closer to green and not as close to blue in all cases, but at 15 °C, the latter color showed a higher peak compared to when the molds were incubated at 25 °C and lower at the other temperatures. Blue showed almost entirely the same curve as red at 15 °C, but its initial rate was the same as green's for the remaining temperatures. The final rates

seem to be descending at 25 °C and ascending at 15 °C and 30 °C. The observations suggest smoother transitions in rate at 25 °C, especially for red and green.

To summarize, the above observations suggest that temperature has an impact on the intensity of each RGB component of *F. graminearum* and the rate of color change. The changes are smoother at 25 °C, especially for the green color which is the most resistant to temperature variations.

B. Color and DON concentration

Variations in DON concentrations between the samples incubated at different temperatures were in general significantly dissimilar (Table 5). However, a Tukey's test showed that such differences were only between the samples incubated at 15 °C and 25 °C (p = 0.041). These observations suggest that samples incubated at 30 °C presented DON levels in between the ones observed at the other temperatures.

Table 5. Comparisons between the variation of DON concentration at different temperatures.

p_{ANOVA}*	Post Hoc Comparisons**				
	Temperature (°C)		MD	t	p_{Tukey}
0.038	15	25	376.9	2.451	0.041
		30	74.4	0.486	0.878
	25	30	-302.5	-1.967	0.124

*DON concentration considering the different temperatures (Friedman)
** Degrees of freedom: 140; MD - mean difference

The DON concentration increased over time except at 30 °C between the 8th and 12th days (Figure 28). However, more DON was accumulated in samples incubated at 30 °C in the beginning and end of the measurements, in comparison to other temperatures. This was followed by 15 °C and then 25 °C. Thus, suboptimal temperatures not only stimulated strong pigmentation but also led to the highest DON concentrations.

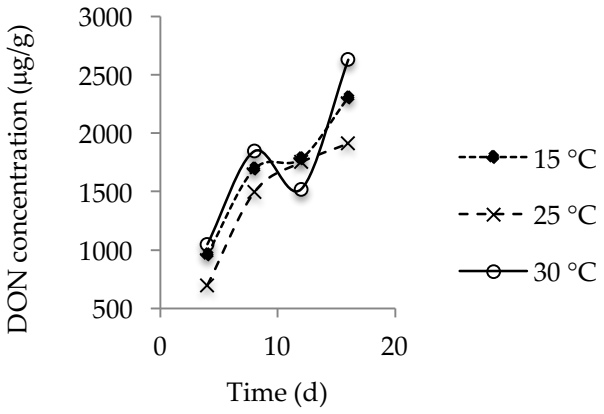

Figure 28. DON concentration at different temperatures and its relationship with *F. graminearum* RGB channels. Each marker corresponds to an average value obtained from 12 samples.

The variation of DON concentration in relation to pigmentation seemed consistent with quadratic functions, at all temperatures (Table 6). The relationship was stronger at 25 °C, followed by 15 °C and then 30 °C. At the latter temperature, R^2 values were moderate (close to 0.5) but these values were acceptable in considering any of the colors as a predictor of DON concentration. All RGB components seemed to present very similar degrees of association with DON concentration with R^2 values of 0.99 for all of them. All colors showed very close differences regarding their association with DON concentration at particular temperatures, including the moderate association at 30 °C. At 15 °C, the highest coefficient of determination was found to be for the blue component with green being the highest at 30 °C although the differences were small and likely insignificant.

Negative quadratic relationships indicate the existence of a range of pigments related to high toxin production, all with a vertex within a vertical axis of symmetry. The vertices occupy different positions depending on temperatures and the color. Thus, even though the colors showed similar trends at different temperatures, DON concentration did not exhibit the same relationship with particular intensities of

different colors when the temperatures were different. For instance, the color range at which DON is more abundant at 30 °C is different for red and green.

Table 6. Quadratic curve fitting of DON concentration, in relation to surface colors of *F. graminearum*.

Color	Temperature (°C)	Function	R^2	SE
R	15	$y = -113224x^2 + 113533x - 26418$	0.85	761.7
	25	$y = -119148x^2 + 120852x - 28474$	0.99	761.7
	30	$y = -254734x^2 + 247618x - 57718$	0.53	761.7
G	15	$y = -87091x^2 + 86337x - 19269$	0.83	664.2
	25	$y = -147715x^2 + 149411x - 34815$	0.99	664.2
	30	$y = -104187x^2 + 98045x - 20900$	0.55	664.2
B	15	y = -288876x2 + 254764x - 52651	0.87	899.8
	25	y = -60308x2 + 49966x - 8494.8	0.99	899.8
	30	y = -97943x2 + 80019x - 14266	0.54	899.8

y – DON concentration (μg/g); x – color intensity; SE – standard error

All colors produced different results, possible due to the range of RGB components being a function of temperature differences. The observation that all concentrations in relation to color at different temperatures showed a strong relationship with quadratic functions is supportive of the idea that quadratic relationships are representative of this phenomenon. It is perhaps better to consider the cases where DON concentration covered the same range at the same temperatures as in the DON concentration × time graph. The average concentration range at 15 °C was ~ 1,000-2,000 μg/g, suggesting that the red and green components presented the best results. At 25 °C, the same rationale would imply that the blue component corresponds to the most accurate range of DON concentration. For specimens at 30 °C, the red component seemed more accurate. In general, the red component showed the most moderate interpolations, although it did not show the best results at 25 °C. Thus, red is perhaps the most appropriate RGB component to predict DON concentration through *F. graminearum* surface color, using a quadratic function.

3.4.4 Discussion

In summary, all RGB components seemed correlated as they presented the same pattern of variation over time, although red was consistently the most intense, followed by green. The high correlation between the RGB channels suggests a common causative factor, possibly accumulation of the same pigment [171, 172]. Suboptimal temperatures stimulated both pigmentation and DON synthesis. Incubation at 25 °C resulted in smoother transitions in rate of color change. Only the green color was significantly resistant to temperature differences. All RGB channels presented the same potential as predictors of DON concentration but red showed the best correspondence with actual ranges of toxin concentration at the temperatures analyzed, although blue presented the best result at 25 °C.

There are very few studies regarding the nature of their color of *F. graminearum* pigments. Ashley*, et al.* [57], in a pioneering study, described rubrofusarin (red), aurofusarin (golden yellow to wine red and dark blue, depending on the acidity of the medium), and culmorin (colorless) as the major pigments in several *Fusarium* species including *F. graminearum*. According to this study, aurofusarin is likely to be a major cause for the mold's color change if there is considerable change in pH during the course of the experiment. Later, Tanaka*, et al.* [181] have described the chemical properties of rubrofusarin, and Jin*, et al.* [69] have described two carotenoids neurosporaxanthin and torulene. Neurosporaxanthin is the major carotenoid responsible for the orange pigmentation in *Fusarium* [182] and torulene confers red pigmentation [155]. This could explain the predominance of red color and the relative scarcity of blue. Orange is a complementary color to some shades of blue (around R-0.0, G-0.5 and B-1.0) in the RGB model [183, 184]. If all RGB components are related to the same pigments, then their similar abundance

pattern is likely to result from the variation in the quantity of the pigments. The slight discrepancies might be due to the difference in color between the distinct pigments. The mold is initially pale [26], because the pigmentation is still developing. It then becomes yellow or orange, possibly due to the accumulation of Neurosporaxanthin or aurofusarin, with the fungus becoming red or magenta at the final stages. This is possibly due to changes in the proportion of the different pigments. It can also be due to the conversion of aurofusarin to its derivatives since the pigment turns reddish in presence of acid [57].

Relationship between suboptimal temperatures and DON synthesis has been verified in some studies including a mini-review by Cambaza*, et al.* [8]. In the present study, specimens incubated at 25 °C had milder coloration and softer color transitions. According to some sources that temperature affects production of carotenoids and other pigments in molds [185, 186]. However, the current findings are not consistent with studies by Avalos*, et al.* [64] on *F. aquaeductuum*, where the formation of carotenoids decreased at lower temperatures. Although a different species was used in that study, it belongs to the same genus with the likelihood of a similar carotenoid metabolic pathway. Yet, the temperatures studied were in the range of 5–25 °C, with the lowest temperature perhaps being inadequate for most metabolic reactions including synthesis of carotenoids. If the temperatures are too high or too low to allow fungal growth, it is reasonable to expect the failure of numerous biological functions.

It is perhaps more useful to focus on aurofusarin because this pigment seems to have a more significant impact on *F. graminearum* surface coloration [63]. Garcia-Cela*, et al.* [54] have quantified aurofusarin in natural wheat samples and others through inoculation of *F. graminearum*. The concentration of aurofusarin was consistently higher at 25 °C in relation to 15 °C. This need not necessarily contradict

with the current results, depending on the form of aurofusarin and derivative predominant in the specimens. Aurofusarin changes colors in response to pH, being predominantly golden yellow in acidic medium and wine red as alkalinity increases [61]. Yellow is brighter that its counterpart [187]. Thus, an increase in the quantity of aurofusarin can turn the mold brighter or darker depending on which shade of the pigment increases in abundance.

The RGB components were expected to exhibit some relationship with DON concentration because a previous study had demonstrated the suitability of color change in measuring growth in *F. graminearum* [26], and several publications have shown that it can be used to predict mycotoxin contamination as well [28]. The relationship between fungal pigmentation and mycotoxin contamination had already been explored by Dufossé*, et al.* [179] who showed that the colorant produced by *Monascus* was banned in Europe and the United States due to its toxicity, although their study did not intend to develop models based on such a relationship. It also seems reasonable that all RGB channels have exactly the same algebraic relationship with DON concentration considering that all colors result from the same combination of pigments. However, it is still a mystery as to why the green color did not show significant dissimilarities across different temperatures, although it might be related to the differences between the pigments. Orange pigments are more intense in green than red pigments [188]. Thus, a change in the latter does not affect the quantity of green as much. Therefore, there is a need for further analysis to find out the actual cause. In any case, this feature is desirable because the green can potentially indicate DON concentration without the need to measure. However, green is a common color in plants, and can complicate the RGB analysis if it is based on photos of *F. graminearum* growing on wheat plant parts.

The red component performs the best with better correlation with the range of DON concentration. One possible explanation is its higher abundance in relation to blue and green, which would also explain why a bigger sample tends to be more representative. Red could also be a result of the toxin's color adding to the color of the pigments although the National Center for Biotechnology Information [189] does not have any record of color being among the properties of DON. But if red is to be chosen as a predictor of DON concentration, it would be important to further analyze its accuracy at 25 °C. Otherwise, it is better to use the blue channel at this temperature.

3.4.5 Conclusion

F. graminearum shows predictable color changes and pattern of DON synthesis throughout its lifecycle. Both trends were combined to verify if the colors could be used to predict the amount of DON produced by the fungus, and the analysis considered at different temperatures. The current results confirmed that the relationship for all RGB components if used separately, results in quadratic curves with high coefficient of determination (R^2) at 15 °C and 25 °C, and moderate coefficient of determination at 30 °C. Red, green and blue exhibited the same pattern of variation and rate of color change, and approximately the same relationship with DON concentration. Green was the only color that did not show any significant changes across temperatures with the most appropriate correspondence between color and DON concentration being observed with red color at 15 °C and 30 °C, and blue at 25 °C. Regardless, red seems to be the best choice if the range of DON concentrations are analyzed in detail.

3.5 *Fusarium graminearum* colors and deoxynivalenol synthesis at different water activity

3.5.1 Introduction

Mycotoxin studies have been gaining prominence since the second half of the 20th century, and deoxynivalenol (DON) or vomitoxin ($H_{15}O_{20}O_6$, Figure 29) is among the most well-known toxins [50]. In its physical form, DON forms colorless fine needles, is soluble in polar organic solvents and water and its melting point is 151–153 °C [190]. DON belongs to the class of trichothecenes and causes nausea, vomiting, diarrhea, abdominal pain, headache, dizziness, and fever [50, 190]. The World Health Organization considers DON as a teratogenic and immunosuppressive neurotoxin [191].

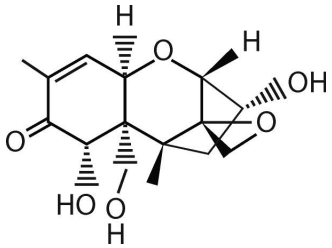

Figure 29. DON structure, according to Sobrova, *et al.* [190].

DON highly affects the cost of commodities as it increases the use of fungicides and the expense to screen them for toxicity [192]. According to Schmale III and Munkvold [193], DON is responsible for losses of approximately $655 million per year in the United States, mostly in wheat. The toxin was also identified as the cause of at least eight outbreaks of intoxication in Japan, including two cases in the Hokkaido prefecture. The toxin is among the natural contaminants described by the country's Ministry of Health, Labor and Welfare as a potential threat for public health [175]. DON is frequently found in corn, wheat, oats, barley, rice, and other grains and derivatives [190].

Water activity (a_w) is among the environmental factors with impact on the quantity of DON produced by *Fusarium graminearum* (teleomorph: *Gibberella zeae*) [194-196]. Although there are still some inconsistencies on how they are related, but a_w seems to favor higher DON production [8]. According to Leplat*, et al.* [5], at 25 °C *F. graminearum* a_w tolerance lies between 0.9 and 0.995 at 25 °C, with 0.95-0.995 being the optimal range (higher a_w values are not mentioned). With regards to DON, the same authors were able to detect deoxynivalenol between a_w of 0.95 and 0.995. Furthermore, a_w is frequently used in models to predict mycotoxin concentration *in vitro*, together with temperature and other variables such as concentration of nutrients or fungicides [28]. However, there remains a need to further explore, expand and propagate the current knowledge on how a_w affects DON synthesis by *F. graminearum*.

The RGB (red, green and blue) components of *F. graminearum* surface color were recently found to exhibit predictable changes over time [26], and this feature is desirable as an alternative to size measurement to estimate the mold's maturity because size is highly dependent on factors such as the borders of a Petri dish, and it does not provide much information about the fungus' metabolism [26]. Since both DON concentration [15, 195] and surface color [26] are predictable for *F. graminearum* over time, it is reasonable to admit the possibility that both can be related to a certain degree. Furthermore, surface color and toxin concentration are manifestations of the mold's state of maturity [26, 197].

This study aims to demonstrate that *F. graminearum* surface color can be used to predict how much DON the fungus produces taking a_w in consideration. These analyses will substantiate the idea that color is a viable alternative to size in *in vitro* mold growth studies.

3.5.2 Material and methods

A. Mold isolate

This study was performed using an *F. graminearum* isolate from the Catalogue of the Japan Collection of Microorganisms (JCM). It is registered as the teleomorph *Giberella zeae* (Schwabe) Petch, strain TH-5, isolated by Sugiura [72] from rice stubble in Hirosaki, Aomori Prefecture, Japan. It is a known producer of deoxynivalenol, 15-acetyldeoxinivalenol and zearalenone [167].

B. Experimental procedure

Incubation and RGB determination

Due to the observation of Leplat, *et al.* [5] of an a_w of 0.94, which was found to be the lowest at which the mold grew on yeast extract agar (YEA), thirty-six specimens of *F. graminearum* were grown at 25 °C on yeast extract agar at three water activity (a_w) conditions 0.94, 0.97 and 0.99, experimentally prepared using glycerol. From the 4^{th} incubation day, 3 replicates per a_w value were taken for DON quantification. Before the extraction, the fungi were photographed in a black bucket, at a vertical distance of 30 cm. The camera model used was Nikon D3200 with a DX SWM VR lens, used without flash or any automation affecting illumination. The only source of light was a round LED attached to the bucket's lid. The photos were then processed on the ImageJ software (FIJI edition), developed by the National Institutes of Health [41] using the method described by Cambaza *et al.* [26]. ImageJ allowed determination of the average intensities of the RGB components from the photos. The analysis considered only the fungal surface, excluding any background contribution from the plate borders or agar. In the end, the variables analyzed were incubation time (in days), a_w and the RGB parameters, converted from the 8-bit notation (0 – 255) to the arithmetic index (0.0 – 1.0).

Extraction and high-performance liquid chromatography (HPLC)

For extraction, each sample was mixed with 100 ml of water:acetonitrile (84:16) and blended in a Seward Stomacher 400 machine. Approximately 15 ml of the filtered extract was transferred to a tube and 2 ml of this filtrate were purified using Supel™ TOX DON cartridges [198]. These cartridges eliminate undesirable fat, pigment and carbohydrate and retain only large molecules. HPLC was run through a Jasco CrestPak C18T-5 affinity column using (a) water:acetonitrile:methanol (92:4:4) and (b) acetonitrile as mobile phase with a flow rate of 0.2 mL/min at 35 °C with detection using ultraviolet light at 220 nm. The DON peak consistently appeared at 8 minutes of elution.

C. Statistical analysis

The statistical analysis was performed on JASP 0.9, Jamovi 0.9 and Microsoft Excel. All the hypotheses were tested out with $\alpha = 0.05$. The distribution of intensities of red, green and blue was compared by analysis of covariance (ANCOVA) to determine if these differences were significant. The relationships between the colors were then analyzed through a scatter plot matrix. Subsequently, the focus was oriented towards each color. For each color, a Kruskal-Wallis test determined that the distribution of color intensity between the samples grown at distinct a_w, presented significant differences. In the final step, the impact of a_w on the pigmentation and DON concentration was analyzed.

3.5.3 Results

All the specimens were grown for 16 days and the measurements were successfully carried out. The specimens grown at distinct a_w presented notable visual differences in color and texture (Figure 30), particularly the molds grown at $a_w = 0.99$. However, all specimens were generally similar until the 4th day, developing a white

mycelium with a diameter of approximately 3 cm with a yellow spot at the center, resembling a fried egg. The central spot was less visible in the specimens grown at a_w = 0.94 and it was increasingly noticeable as the water activity increased.

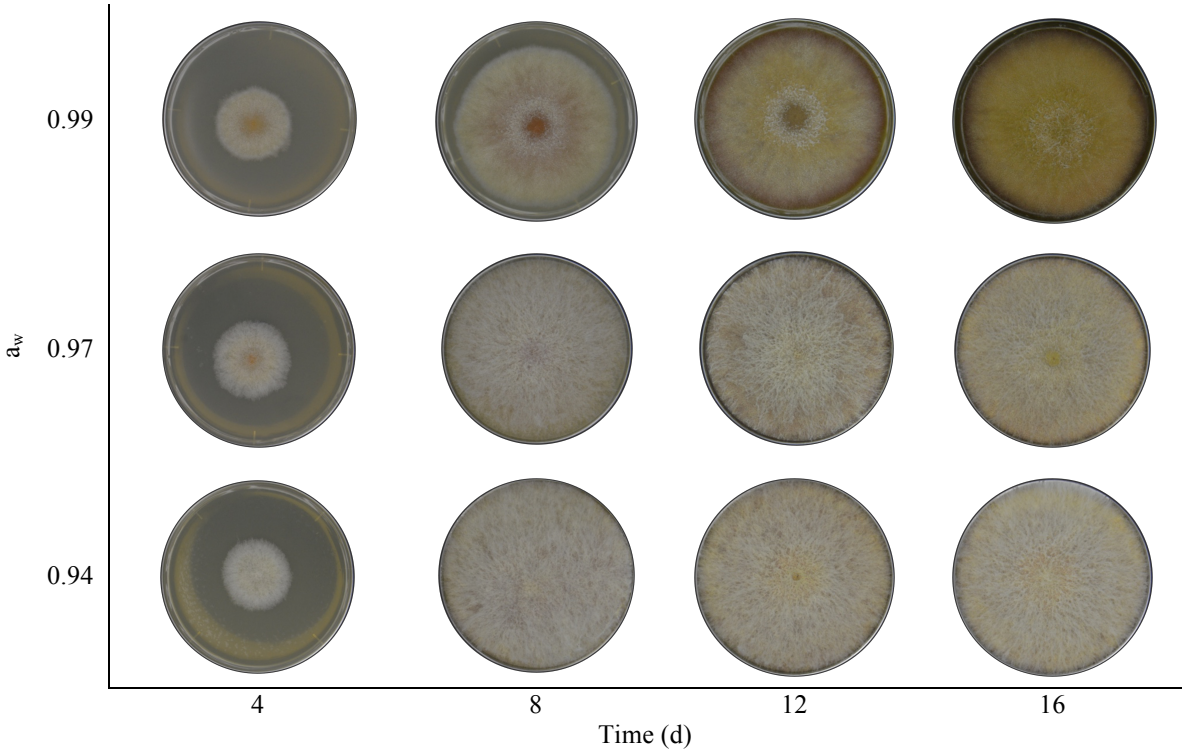

Figure 30. Surface color of *F. graminearum* grown at different a_w for 16 days.

The specimens grown at a_w of 0.94 and 0.97 showed high rate of mycelial growth up to day 8, covering the entire plate with its radially dispersed hairy whitish surface, and seemed to remain unchanged until the end of the experiment. In some cases, the mycelial growth was extensive, touching the Petri dish's lid. However, the molds incubated at a_w of 0.99 did not produce as much mycelial growth and exhibited more clearly visible concentric areas with distinct colors, each with notable changes from one measurement to the next. Its central spot changed to reddish, brown and finally pale, seemingly because of some white mycelial growth on top. Its borders developed a wine-red tone and the surface became increasingly yellow. These observations suggest that *F. graminearum* surface color is highly sensitive to a_w, and a_w reduction promotes mycelial growth, possibly as a stress factor.

Table 7 confirms the impact of a_w on the mold's color, especially on the green and blue components ($p_{ANCOVA} < 0.05$). The red color did not seem to be significantly affected by a_w, even in Tukey's *post hoc* comparisons.

Table 7. Color intensity differences between the specimens grown under different water activity.

RGB channel	p_{ANCOVA}	a_w		*Post hoc* color comparison				
				Mean Difference	SE	df	t	p_{Tukey}
R	0.169	0.94	0.97	0.02	0.03	8	0.63	0.809
			0.99	0.06	0.03	8	2.06	0.159
		0.97	0.99	0.04	0.03	8	1.44	0.369
G	0.007	0.94	0.97	0.02	0.01	6	2.22	0.145
			0.99	0.07	0.01	6	8.06	< .001
		0.97	0.99	0.05	0.01	6	5.84	0.003
B	0.02	0.94	0.97	0.03	0.04	8	0.69	0.778
			0.99	0.13	0.04	8	3.43	0.022
		0.97	0.99	0.1	0.04	8	2.74	0.059

R = red; G = green; B = blue; ANCOVA = analysis of covariance; SE = standard error; df = degrees of freedom; t – student's t statistics.

The green and blue colors showed exactly the same profile of significance in different a_w, although green showed the highest levels of discrepancies in all cases. The overall differences, measured through ANCOVA, were significant. With regards to the *post hoc* comparisons, there were significant differences between the specimens incubated at a_w of 0.99 and the others. These observations are consistent with visual analysis in which a_w reduction drastically affects *F. graminearum* color pattern.

Despite the differences between the colors at distinct a_w, all three RGB components seemed highly correlated (Figure 31), with Pearson's correlation $r > 0.9$. The data suggest direct relationships between the colors, and all colors showed considerably high density of their lighter shades. Red and green were the most strongly correlated, followed by blue and green. Thus, although the red component

seemed consistent at different a_w, unlike the others, its slight variations presented a similar profile to the ones exhibited by the green and blue channels.

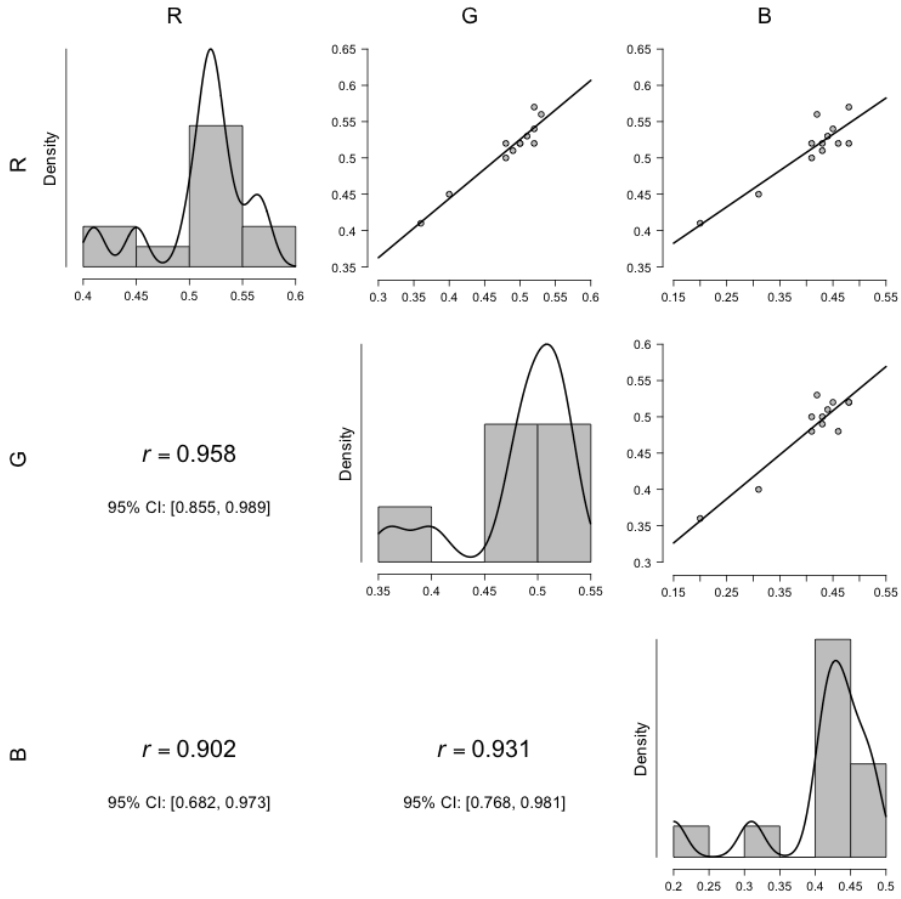

Figure 31. Pearson's correlations between the RGB components. The diagonal charts show the intensity of the colors. CI = confidence interval; r = Pearson's coefficient.

Figure 32 shows the variations in RGB components and DON concentration over time at different a_w conditions. The colors seemed exhibit very similar of variations over time. The specimens grown at a_w = 0.99 decreased in color intensity (all RGB channels) while the others apparently remained constant and considerably high. This is consistent with the photos, where the lowest a_w incubation setting resulted in a predominantly whitish surface for almost the entire experiment.

At a_w = 0.99, the best algebraic representations were $y = 0.0005x^2 - 0.0222x + 0.6416$ for red, $y = 0.0002x^3 - 0.0044x^2 + 0.023x + 0.4992$ for green and $y = 0.0002x^3 - 0.0068x^2 + 0.0588x + 0.2831$ for blue, all with $R^2 = 1$, assuming x as time in days

and y as the RGB component within a scale of 0 to 1. DON concentration seemed to increase in general for all a_w settings, although there are some cases of reduction.

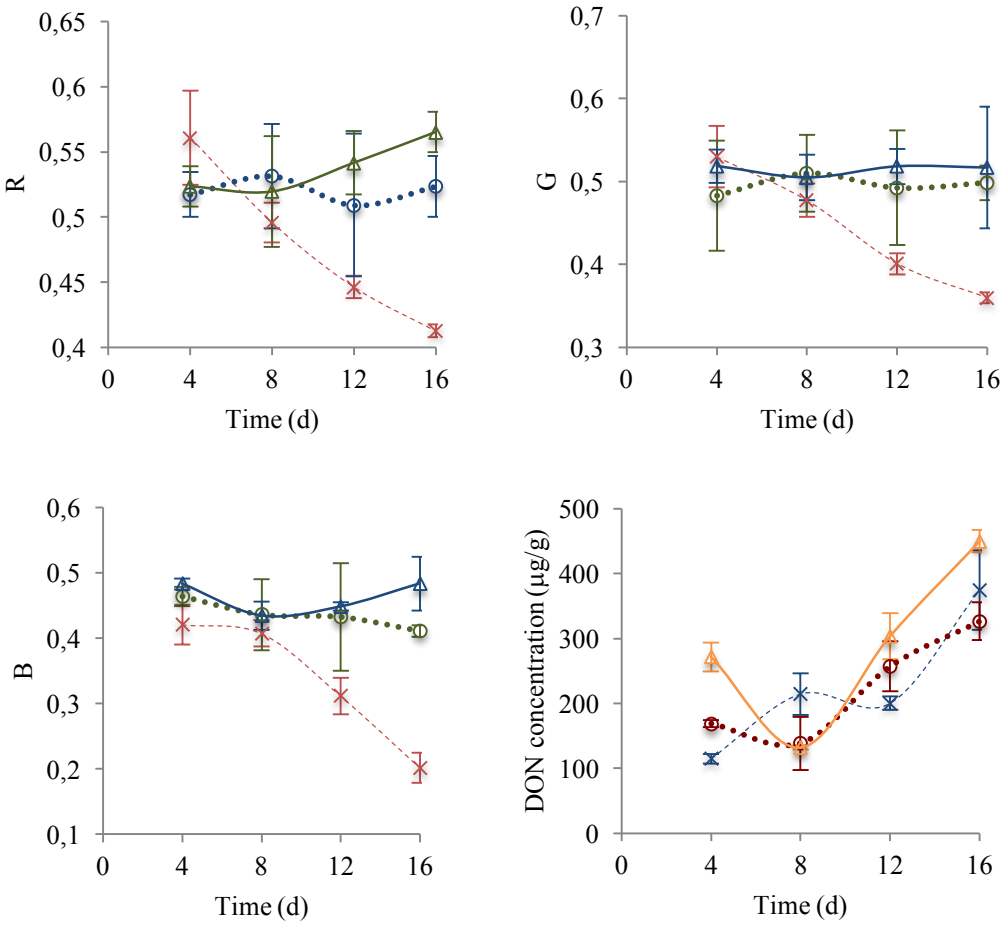

Figure 32. Variation of RGB components and DON concentration over time under different a_w. Note: R = red; G = green; B = blue; a_w = 0.94 (Δ); a_w = 0.97 (O); a_w = 0.99 (✕).

It is difficult to explain why there are reductions because the toxin is expected to accumulate over time but it might have been due to cross-contamination in the column, which was initially cleaned for 10 min after the measurement, which might not have been enough. It was then cleaned for 20 min to ensure proper cleaning.

An analysis of covariance (ANCOVA) shows no significant differences between DON concentrations (p = 0.347) of samples incubated at different a_w. Since the colors change their pattern of variation when the molds are subjected to distinct a_w, although it does not happen to DON concentration, at high superficial mycelial

growth in the specimens at lower a_w, the fungus seems to retain the ability to produce the toxin even when there is higher mycelial growth. It is possible that the layer of whitish hyphae is masking an inferior highly pigmented layer in the specimens grown at lower a_w. This could be due to lowering a_w causing the white mycelium to remain abundant throughout the experiment while DON keeps accumulating.

Only the RGB channels at $a_w = 0.99$ could be used as independent variables to plot against DON concentration (Figure 33) because the colors did not change significantly at lower a_w.

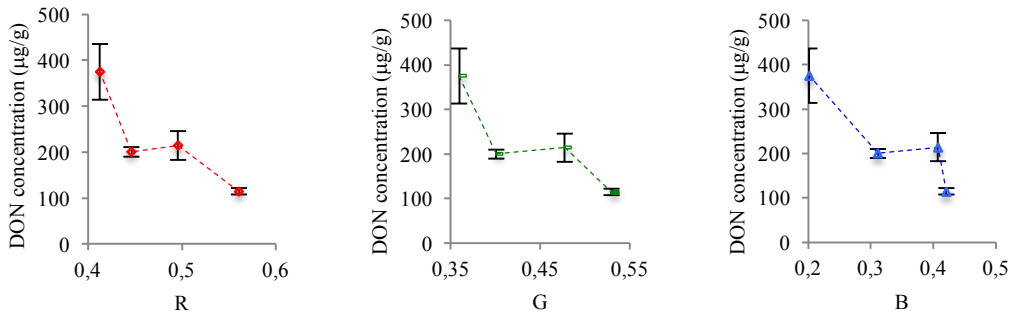

Figure 33. Relationship between color variation and DON concentration at $a_w = 0.99$.

All colors decreased in value with one oscillation. The major differences between the colors seemed to be the wideness and position of their dominium (range of abscissae). Considering x-axis as RGB channel and y-axis as DON concentration, observation of x values from the origin towards 1 shows that blue presented the lowest values but also the widest range, followed by green with intermediate values and range, and finally red. The considerably narrower range of the red component may explain why it did not present significant differences across a_w.

3.5.4 Discussion

In summary, a_w had a major impact on *F. graminearum* surface color. Until day 4, all the specimens were similar in overall appearance, with a yellowish center

surrounded by a whitish mycelium, resembling a fried egg. However, a reduction in a_w seemed to promote *F. graminearum* mycelial growth, masking its conidial pigmentation. Consequently, the specimens grown at a_w = 0.97 and 0.94 remained whitish throughout the entire experimental period, with RGB channels presenting no significant variations, unlike the molds grown at a_w = 0.99. In any case, the RGB components appeared highly correlated, with Pearson's coefficient $r > 0.9$ when the colors were considered two at a time. Yet, only green and blue components exhibited significant variations, even though all colors had the same pattern of variation. The significant differences in green and blue were noticed only between the samples incubated at a_w = 0.99 and the others, and this supports the previous observations from the photos. The highest a_w was marked by a reduction in RGB components, which could all be fit to polynomial functions. The lowest a_w conditions presented notably constant trends. Nevertheless, DON concentration increased under all a_w conditions, independent of the surface color. Thus, only the highest a_w was considered to plot graphs relating DON concentration to color variation. The two variables seemed inversely proportional if colors were represented as the abscissae and DON concentration as the ordinate. As one moved from the origin of abscissae, the blue, green and red ranges overlapped, each narrower than the previous but all having the same shape.

Water activity is among several factors affecting the pigmentation of *F. graminearum* [26, 57, 59, 65], although the manner in which it impacts pigmentation can be very complex because the mold's surface color results from the combination of several different pigments, some with quite different chemical properties [57, 64, 68-70]. For instance, a_w partially attributes its chromatic properties to the polyketide aurofusarin, which is perhaps the most influential pigment, notable for its yellow and

red coloration [54]. Yet, the color differences appeared to be more associated with increased growth of white mycelium on top of the mold, covering the entire dish, rather than with changes in nature or quantity of pigments. The observation that lower a_w stimulated higher mycelial growth might seem counterintuitive and also contradicts previous observations [35, 195], but it is reasonable to assume that the shortage of water leads the fungus to expand its hyphae in search of new sources [32]. The initial similarity between the specimens grown at distinct a_w perhaps occurred because the molds were very small and the shortage of water had not yet impacted the mycelia. As they molds continued to grow, the ones grown at lower pH experienced early exhaustion of water and seemed to react by expanding hyphae in all directions including upwards. Furthermore, during day 4 they were still at exponential growth [26], with minor differentiation.

The fact that all RGB components were highly correlated supports the idea that a small set of pigments with similar colors is producing these colors. Otherwise, one would expect each RGB component to exhibit its own pattern of variation if there were a wide variety of pigments with different colors, especially if the pigments were chemically diverse. From literature, aurofusarin [62], and the carotenoid neurosporaxanthin [145, 157] have already been identified as the major pigments influencing the surface color of *F. graminearum*. These pigments are both yellow, although slightly different. The former is frequently described as “golden yellow”, though its hue varies from orange to wine red with changes in its derivatives [57, 62, 68, 78], and neurosporaxanthin was described as “orange-yellowish” [148], like most carotenoids. There are also the polyketide rubrofusarin [57] and the carotenoid torulene [69], which are both red but not as abundant as aurofusarin and neurosporaxanthin. There are more pigments but they have minor influence on the

overall color [148] or are present only during differentiation [31, 140]. The only pigments influencing the color have similar or closely related hues ranging from golden yellow to wine red. It is worth mentioning that the polyketides (aurofusarin and rubrofusarin) are highly bioactive and potentially an essential part of the competitive saprophytic ability (CSA) of *F. graminearum* [77, 78], The carotenoids are not likely to have CSA and tend to respond mostly to light rather than nutrients [64], except in cases of extreme shortage of nutrients essential for synthesis of such pigments. Thus, the polyketides, especially aurofusarin, appeared to be key pigments contributing to *F. graminearum* surface color variation in the current experiment.

A previous experiment had already shown that all RGB components exhibit a similar pattern of variation, consistent with 3rd degree functions [26]. It is not clear why the red component did not show significant variation ($\alpha = 0.05$) while the other colors did, but it might be related to the nature of the most abundant pigments [197]. Perhaps red pigments such as rubrofusarin and torulene, and especially the latter, do not change their colors throughout the mold's lifecycle, contributing to its resistance to change. However, both pigments probably suffer a considerable reduction because the former is an intermediate of aurofusarin synthesis [82] and the latter is a precursor of neurosporaxanthin [159]. Yet, both pigments have been found in *F. graminearum* matrix, even when the others are present [57, 159], from which one can imply the existence of a chemical equilibrium between them. It this case, it is still possible that rubrofusarin and torulene contribute to the endurance of the red component.

RGB values were expected to decrease throughout the experiment, especially for blue, followed by green and finally red. According to a previous experiment [26], this RGB reduction corresponds to the darkening process as the fungus grows towards the stationary growth phase. It surely does not apply to the cases in which the fungi

were covered with white mycelia and did not allow the pigments to be visible. In the cases where the color changed, the variation of RGB components could be represented by polynomial curves, as observed in the aforementioned experiment.

All samples showed an overall increase in DON concentration over time, regardless of whether there was high surface mycelial growth or not. There is some counterintuitive reduction for the samples grown at a_w = 0.94 and 0.97 between days 4 and 8, but it was likely due to fluctuations in the results. Indeed, the ANCOVA test (p = 0.347) indicated that the differences between the DON concentrations at different a_w were not significant. This result contrasts with available literature which shows significant differences between DON concentrations at distinct a_w [194-196]. Although these contradictory results are difficult to explain, this might have been due to chemical, genetic (distinct strains) or nutritional differences [8]. All other experiments were performed with irradiated wheat, while the current one was carried out in YEA. YEA is highly nutritive [73] which perhaps attenuated the stress caused by a_w differences. Furthermore, Sorensen and Sondergaard [74] demonstrated that even different yeast extracts influence DON concentration differently. Regardless, the studies on wheat showed similar trends irrespective of a_w, and it is reasonable that DON tends to accumulate over time because mycotoxins are very stable and the fungi cannot metabolize them [32, 199].

DON concentration seems to have a similar relationship with all RGB components at a_w = 0.94 and it therefore facilitates the use of colors as an alternative to size, in DON analysis at this a_w. This supports the previous study demonstrating that *F. graminearum* color variation is predictable throughout its life cycle [26]. There is also evidence that biosynthesis of the pigment aurofusarin is related to DON production as histone H3 lysine 4 methylation (H3K4me) is crucial in the

transcription of genes for the synthesis of both compounds [197]. Yet, the relationship between the pigment and DON requires further biochemical and genetic investigation. Thus far, as has been shown here, *F. graminearum* surface color can be used in microbiological studies to predict DON concentration at a_w = 0.99 but it is not applicable for use at lower a_w.

3.5.5 Conclusion

The current experiment suggested that all RGB channels obtained from photos of *F. graminearum* are correlated and can be used to predict DON concentration produced by the fungus at a_w = 0.99. However, the colors were not effective predictors at a_w = 0.97 and 0.94 because these conditions appeared to stimulate the production of white mycelia, barely changing in color. Thus, the results indicate that *F. graminearum* surface color can only be used as a predictor of DON concentration at a_w as high as 0.99. Future analyses will determine ways to overcome the limitation caused by the superficial white mycelium. One alternative would be to take photos from the bottom or the medium or to analyze the color of the *F. graminearum* extract in acetonitrile prior to HPLC because the solvent would contain the pigments.

Chapter 4 Analysis of color change in *F. graminearum* contaminated grains and the predictability of DON contamination

4.1 RGB imaging as tool to analyze the growth of *Fusarium graminearum* in infected oats (*Avena sativa*) and rice (*Oryza sativa*)

4.1.1 Introduction

Fusarium spp. are the most common pathogens in many cereal crops, causing ear rot or head blight diseases and mycotoxin contamination [9, 11]. In the case of *F. graminearum*, its host range includes oats, rice, wheat, barley and other plants in which they do not cause disease [11]. There have been recent outbreaks of *Fusarium* head blight (FHB) in several areas including Asia, Canada, United States, Europe and South America, and the disease has been expanding worldwide [50]. In the United States, FHB has caused losses of around US$2.7 billion from 1998 to 2000, and it continues to reduce the yield and quality of cereals considerably, forcing a reduction in prices [200, 201]. In Japan, there were several outbreaks during the 20th century, including a record-breaking outbreak in 1998 of rice with deoxynivalenol (DON), a toxin associated with the disease, following a typhoon [44]. The Japanese Government has set a provisional limit for DON in grains and derivatives to 1.1 μg/g [175].

To better understand how *F. graminearum* propagates, it is important to analyze its growth pattern. According to Garcia*, et al.* [28], the most commonly used growth models for fungi are have been borrowed from bacterial studies, namely the lineal model and the ones developed by Gompertz and Baranyi. For molds, these models use their spatial expansion (e.g. radius or diameter) as a growth measure,

assuming that the organism matures as it becomes larger, following the same rationale applicable to plants, animals and other organisms. However, this approach has several limitations because it provides little information about the organism's metabolism and may result in misinterpretations if the mold grows irregularly or if the mold attains the maximum size in a closed system [26, 202]. A viable alternative to this issue is digital imaging combined with statistics, an approach gaining relevance in studies of FHB because of their potential to monitor the extent and severity of *Fusarium* infection in grains [19, 25]. For instance, some authors have utilized RGB (red, green and blue) imaging to distinguish wheat with symptoms of FHB from apparently healthy grains [6, 19, 25]. Furthermore, these methods require computers and digital color cameras, the latter having been described by Dammer*, et al.* [19] as cheap, small and lightweight.

When *F. graminearum* is grown in yeast extract agar in a Petri dish, the so-called stationary phase starts when it reaches the plate's border and stops expanding, keeping the same size until it eventually depletes the nutrients and its spores remain in a state of dormancy [26, 197]. However, phases like lag and stationary, represented by size-based models as apparently less active, are exactly the circumstances at which the fungus has to employ the highest effort to ensure its survival. In the lag phase, the organism needs to adapt to a new medium and in the stationary phase it has to adapt to the medium being exhausted. Besides the established fact that molds produce secondary metabolites during the stationary phase [32], a previous experiment demonstrated that *F. graminearum* changes its surface color (and the color of the agar medium) even during the stationary phase [26]. Change in pigmentation is an indicator of active metabolism [197], and it implies that the fungus is indeed substantially active, even when there is no more size expansion. Thus, a color-based

growth model might provide valuable information regarding the mold's maturation pattern, reflecting its variation in metabolic activity.

The predictability of color change in *F. graminearum* as it grows has already been demonstrated in yeast extract agar [26] but not yet in food matrices. Therefore, the current study aims to verify if oats and rice infected with *F. graminearum* present predictable patterns of color variation if incubated for 16 days at different a_w settings. Awareness of these patterns will allow farmers, researchers and other personnel working in agricultural fields to accurately analyze the mold's growth with better awareness about its state of maturity and possibly associate it with particular metabolic activity according to the stage of its lifecycle.

4.1.2 Material and methods

A. Mold isolate

This study was performed using an *F. graminearum* isolate from the Catalogue of the Japan Collection of Microorganisms (JCM). It is registered as the teleomorph *Giberella zeae* (Schwabe) Petch, strain TH-5, isolated by Sugiura [16] from rice stubble in Hirosaki, Aomori Prefecture, Japan. It is a known producer of deoxynivalenol, 15-acetyldeoxinivalenol, and zearalenone [17].

B. Grain samples

All samples of raw oats (*Avena sativa*) and rice (*Oryza sativa*) were obtained locally in Hokkaido. 250 g each of sealed and dried oats were purchased from a local store, with husk in plastic bags. Dry rice was obtained from local producers in plastic bags at 500 g each, with 90% husk and the remaining brown. All grains with husk showed the ability to germinate. Thus, they were autoclaved to inactivate the embryos and eliminate possible microbial contamination. After autoclaving, the color did not

seem to change considerably. For the current experiment, nine samples of oats and nine samples of rice, all containing 25 g, were placed in Petri dishes. Water activity was empirically set using distilled water, and for each grain the range started with the lowest value at which growth was observed. The cereals were split into three groups of three replicates each. For oats, the groups had a_w = 0.94, 0.97 and 0.99 and for rice, the values were 0.97, 0.98 and 0.99.

C. Incubation and RGB determination

F. graminearum was inoculated in the Petri dishes and left at room temperature (fluctuating between 18 °C and 26 °C). The fungi were photographed daily for 17 days in a black bucket, from the moment of inoculation onwards, from a vertical distance of 30 cm. The cameras used for the photographs were Nikon D3200 with a DX SWM VR (Nikon Corporation, Tokyo, Japan) lens and an iPhone 6 (Apple Inc., Cupertino, California, USA). The only source of light was a round LED attached to the bucket's lid. The photos were then processed on the ImageJ software (FIJI edition, National Institutes of Health, Bethesda, MD, USA) [41] using the method described by Cambaza*, et al.* [26]. ImageJ allowed the determination of average intensities of the RGB components from the photos. The variables analyzed were incubation time (in days) and RGB parameters, converted from the 8-bit notation (0 – 255) to the arithmetic index (0.0 – 1.0).

D. Statistical analysis

The statistical analysis was performed on JASP 0.9 (The JASP Team, Amsterdam, The Netherlands), Jamovi 0.9 (Jamovi Project, Amsterdam, The Netherlands) and Microsoft Excel (Version 14.5.8, Microsoft, Redmond, Washington, WA, USA). All the hypotheses were tested with $\alpha = 0.05$. The distribution of intensities of red, green, and blue were compared through analysis of covariance

(ANCOVA) to determine if their differences were significant. Some plots illustrated the variation of the RGB components at distinct a_w over a period of 16 days. Finally, Adobe Photoshop CC 2018 (Adobe Inc., San Jose, California, U.S.) was used to generate an RGB-based growth model for *F. graminearum* in grains.

4.1.3 Results

A. Qualitative description

All photos were successfully taken for 16 consecutive days. For a comprehensive analysis of the appearance of heavily infected grains, this report first shows photos taken using a smartphone, presenting the grains in the final phase of infection (Figure 34). The smartphone seemed to present photos much brighter than the ones taken using the professional camera, facilitating visualization of the grains.

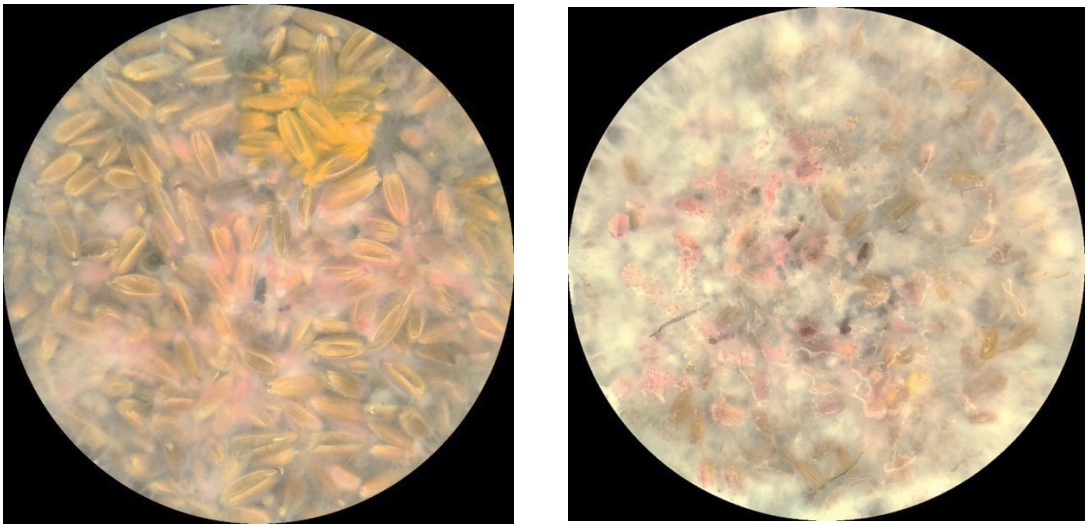

(a) (b)

Figure 34. Contaminated (a) oats at a_w = 0.97 and (b) rice at a_w = 0.98 with *F. graminearum* after 16 days, taken from a smartphone. The contrast was reduced to 40% to facilitate visualization.

As the photos show, heavily contaminated grains have a whitish mycelium and it was possible to notice some pigmentation, particularly in oat grains because the rice presents a higher density of the white mycelium. There are three pigment colors orange-yellow, pink and black. Colors such as pink to salmon-orange are frequently

found in infected spikes, and they result from the formation of spore masses in prolonged periods of high humidity [11]. Although the photos do not show clearly but even the more extreme cases of contamination presented several dark dots, perhaps black perithecia [31] or, in some cases, necrotic lesions, described by Goswami and Kistler [11] as brown, dark purple to black. The abundance of white and pinkish colors was expected as they are common visual features in infected kernels [11, 25].

The remainder of this study will be based on the photos taken through the professional camera because they significantly differ from the ones taken through the smartphone, as paired t-tests between the images acquired through both devices at the end of the experiment showed, with a consistent p-value < 0.001 (Table 8).

Table 8. Differences between RGB measurements of the photos of *F. graminearum* growing in cereal grains after 16 days.

Commodity	Color	$p_{\text{t-test}}$	Device	N	Mean	Median	SD	SE
Oats	R	< 0.001	Camera	9	0.16	0.16	0.02	0.01
			Smartphone	9	0.92	0.90	0.08	0.03
	G	< 0.001	Camera	9	0.12	0.12	0.02	0.01
			Smartphone	9	0.80	0.79	0.03	0.01
	B	< 0.001	Camera	9	0.01	0.01	0.01	0.00
			Smartphone	9	0.52	0.54	0.10	0.03
Rice	R	< 0.001	Camera	9	0.20	0.20	0.03	0.01
			Smartphone	9	0.92	0.91	0.03	0.01
	G	< 0.001	Camera	9	0.18	0.19	0.04	0.01
			Smartphone	9	0.87	0.86	0.02	0.01
	B	< 0.001	Camera	9	0.12	0.16	0.08	0.03
			Smartphone	9	0.66	0.71	0.10	0.03

N - sample size; SD - standard deviation; SE - standard error

Although the number of samples was considerably small (N = 9), the average and median RGB values between the devices presented very different orders of

magnitude, and both standard deviation and standard error were small compared to the measures of central tendency. There is a considerable body of research demonstrating the potential of smartphones for use in scientific applications [203-205] and it would be a good idea in future considering the widespread use of smartphones, but for studies like the current one, validation would be required.

All infected grains exhibited similar patterns of variation, regardless of the type of grain or a_w it was subjected to (Figure 35 – oats; Figure 36 – rice). The color variation in oats was more evident in comparison to rice because the grains were brighter and presented less contrast throughout the experiment although both showed similar behavior. Both grains were relatively bright initially and darkened until the 15th day. There was a notable reduction in brightness between the 1st and 2nd day, followed by slight darkening with fluctuations until the 8th day, when brightness declined substantially and the grains exhibited dark brown shades. This shade prevailed with some fluctuations up to the end of the experiment.

Part of the color change observed seems very consistent with the well-known models described by Garcia*, et al.* [28], presenting lag, log and stationary phases. It has been also observed in a previous study, on which the current is based [26]. The first day involves the mold's adaptation to the new medium (lag). Following this, it expands in the form of whitish mycelium, corresponding to the exponential growth frequently described in the literature [25]. This explains the increased paleness of the grains from an initial bright brown color.

The mycelium expands exponentially as much as possible, maximizing its surface for nutrient uptake. After reaching maximum expansion, it faces stress, possibly caused by limited access to nutrients with the grain's resistant husk certainly contributing to this situation.

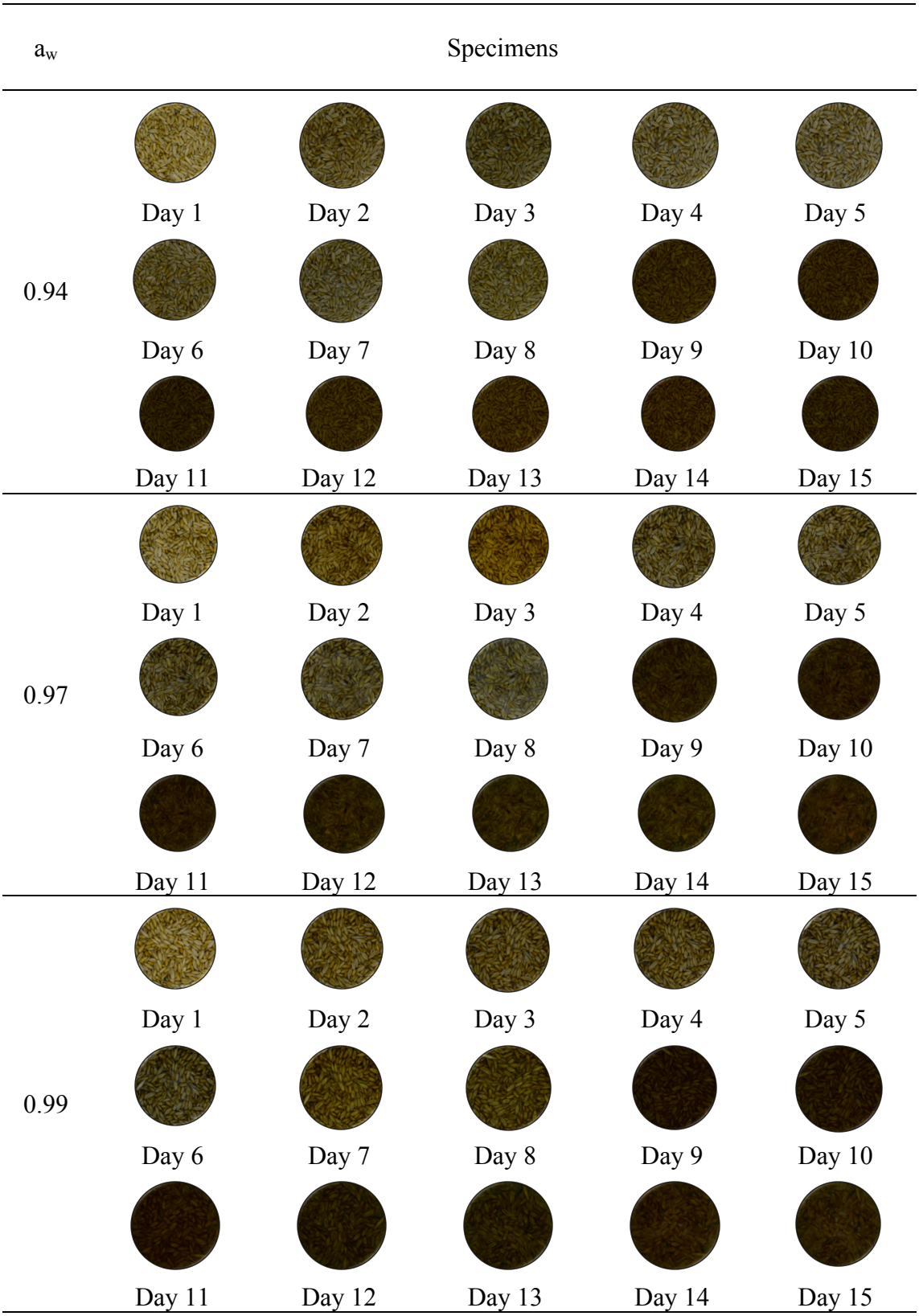

Figure 35. Color variation of oats contaminated with *F. graminearum* at different a_w for 15 days.

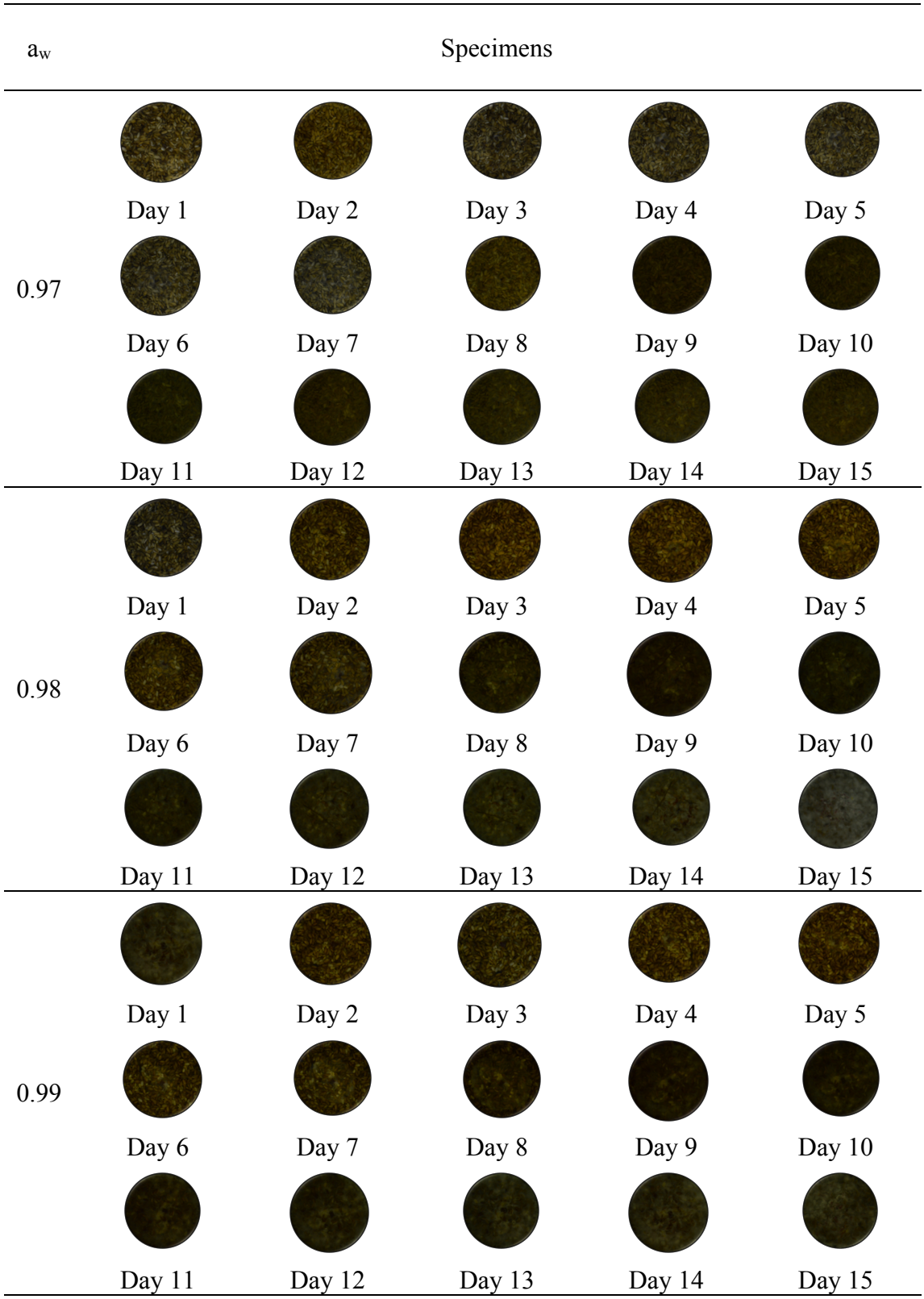

Figure 36. Color variation of rice contaminated with *F. graminearum* at different a_w for 15 days.

Therefore, on the 8th day, the mold starts producing spores to ensure its survival. *F. graminearum* has high competitive saprophytic ability (CSA) [11] and rapid production of spores, with toxin synthesis possibly contributing to this situation as well.

Spores can explain why the color declines in paleness between days 8 and 9. This change corresponds to the beginning of the stationary phase, when part of the mold enters dormancy. The following differences were observed between this growth pattern and the one observed in the previous study using yeast extract agar (Figure 37) [26]: (1) the easiest differences to notice are perhaps the shape and colors of the fungus, which are more pronounced in specimens grown in agar; (2) the grains are initially pale due to the increasingly dense mycelial network, while the specimens grown in agar expanded on the surface forming concentric layers of contrasting colors (3) though the lag phase took a single day, the exponential phase took longer in agar (seemingly up to the 14th day) and the transition to the stationary phase was smoother.

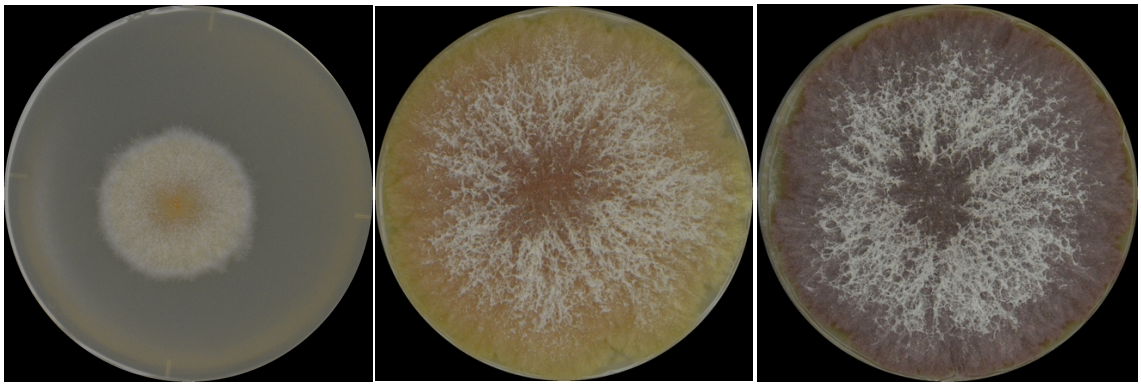

(a) (b) (c)

Figure 37. *F. graminearum* grown in yeast extract agar after (a) 4 days, (b) 8 days and (c) 12 days. These photos were taken for previous experiments [26, 202, 206].

The differences in growth strategy can be explained through the concept of *r* and *k* selection discussed in detail by Taylor*, et al.* [207], but it is first important to understand the differences between cereals and agar as media. The major difference is

perhaps the fact that agar has nutrients readily accessible to the mold while grains have husk as a polysaccharide barrier [208]. Fungi growing on cereals opt for a *k*-strategy, in which the organism becomes stronger and more capable to face adversity by itself, rather than producing a high quantity of conidia. In the current experiment, *F. graminearum* maintained a mature form (mycelium) in order to create structures such as haustoria, which are able to penetrate the kernels [32]. Moreover, mycelial growth also provides the fungus with the potential to search for cracks or other openings from which it can invade the grains. This can explain its increased density, resulting in the observed paleness. In agar, the specimens adopted an *r*-strategy, producing high quantity of conidia. It might seem counterintuitive since the mold has high nutrient availability and therefore would not need to propagate, but in the field, nutrient abundance provides the fungus with an opportunity to disperse the spores so that they can try to colonize more habitats around. The high quantity of spores maximizes the possibility for at least some to thrive. Assuming the veracity of the *r* and *k* theory, once the fungus is able to penetrate the kernels, it rapidly shifts its strategy to *r* and starts producing spores. This phenomenon can explain the sudden reduction in paleness between the 8th and 9th day until the end of the experiment. In the end, there is a mixture of spores and mycelium all around the grains.

Another difference to examine is the relatively wider surface area in cereals due to their granular nature. Wider surface offers more space for the fungus to expand and for that, mycelial growth is intuitively better than spore production. It is important to know that spores do not move by themselves, except the zoospores of chytridiomycota, oomycote and slime molds [32]. In the field, wind, insects, water and other agents can spread them [11], but that is not the case in a Petri dish. *F. graminearum* never seemed to "dive" into the layer of agar. Instead, they grow on the

surface and remain there, absorbing the nutrients until the agar runs dry. It perhaps uses a similar mechanism in grains, involving all the grains but never going beyond the surface. These facts and the high quantity of available nutrients, can explain the presence of a bulky organism growing on the surface of yeast extract agar while the same organism grows in the form of dispersed hyphae in grains.

One final aspect to consider is the homogeneous distribution of water and nutrients in agar. Each grain has a hull, layered bran, endosperm and an embryo, with individual grains differing in size and weight. Moreover, their spatial disposition or superposition is also likely to affect the overall distribution of nutrients. Thus, there is certainly a remarkable difference between the nutrient homogeneity of cereals and agar. A major feature of mycelial fungi is their tendency to grow towards areas with the highest concentration of nutrients [32]. This is perhaps one of the reasons why *F. graminearum* presented a radial growth (in ring-like concentric layers) in agar and an apparently irregular pattern in the grains.

In conclusion, the color of infected grains changed accurately and consistently over time. Therefore, although the experiment was performed in two different types of cereals and distinct water activity, a pattern of color change can be assumed thereby confirming the suitability of color as a reliable approach to analyze the growth or state of maturity of *F. graminearum*. Through observation, it was possible to visualize the lag (very bright grains), exponential growth (where the grains became pale) and stationary phases (when the grains became darker and with a less pale tone). Furthermore, the onset of the phases had exactly the same timing.

B. RGB analysis

In general, the oats presented balanced predominance over all three RGB components throughout the experiment, with all colors showing positive skewness.

On the other hand, rice exhibited almost neutral skewness for red and green and positive for blue. For both oats and rice, all colors were significantly correlated ($p < 0.001$), exhibiting Pearson coefficients above 0.5 (Figure 38). In general, the oats presented balanced predominance over all three RGB components throughout the experiment, with all colors showing positive skewness. On the other hand, rice exhibited almost neutral skewness for red and green and positive for blue. For both oats and rice, all colors were significantly correlated ($p < 0.001$), exhibiting Pearson coefficients above 0.5 [26, 202, 206] and are likely due to the fact that very few pigments (aurofusarin, rubrofusarin and carotenoids) contribute to the overall colors of *F. graminearum* and their colors do not differ substantially, all ranging from orange-yellow to wine-red [197, 206]. The dark perithecia do not contribute as much as the other pigments to the overall color [197].

Table 2 shows the impact of distinct a_w settings on the colors. All RGB components presented highly significant differences ($p < 0.001$ for most, 0.003 for the B channel in rice), though visual observation did not provide such an impression. This is another reason why sole reliance on visual evaluation of kernels may not be a prudent idea. According to Jirsa and Polišenská [25], sometimes differences can hardly be noticeable with the naked eye and digital imaging combined with statistical methods can perform this task more accurately.

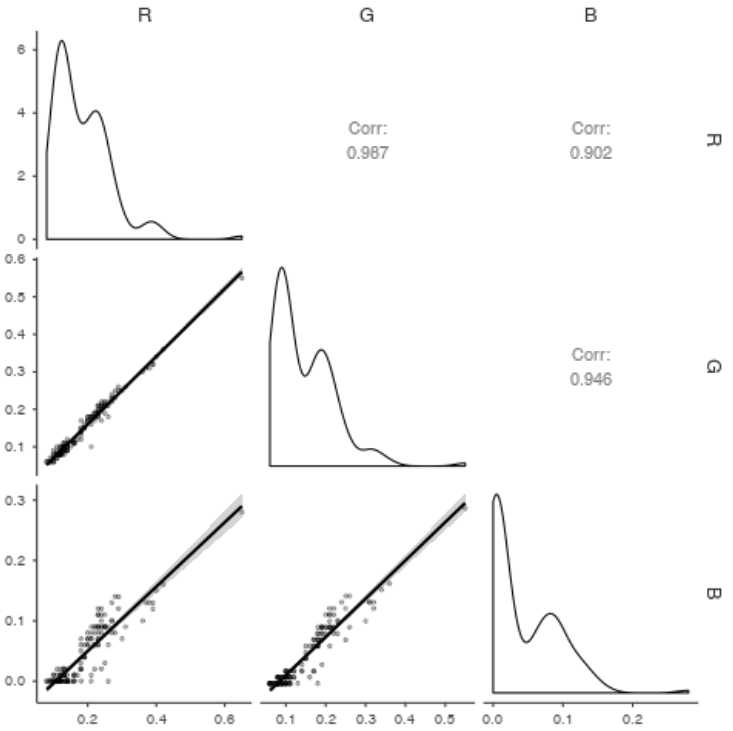

(a)

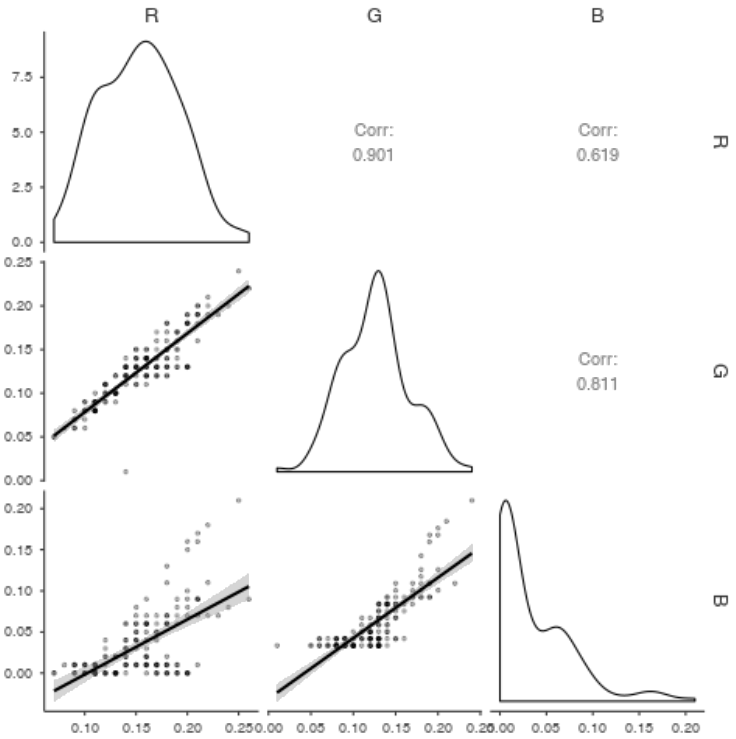

(b)

Figure 38. Correlations between the RGB components of *F. graminearum* grown in (a) oats and (b) rice.

Table 9. RGB differences between the infected grains at different a_w.

Commodity	Color	p_{ANCOVA}	a_w		Post Hoc Comparisons				
					MD	SE	df	t	p_{Tukey}
Oats	R	< 0.001	0.94	0.97	0.01	0.01	102	2.64	0.026
				0.99	0.03	0.01	102	6.37	< .001
			0.97	0.99	0.02	0.01	102	3.72	< .001
	G	< 0.001	0.94	0.97	0.01	< 0.01	102	1.95	0.130
				0.99	0.03	< 0.01	102	6.55	< .001
			0.97	0.99	0.02	< 0.01	102	4.6	< .001
	B	< 0.001	0.94	0.97	0.00	< 0.01	102	0.88	0.649
				0.99	0.02	< 0.01	102	5.28	< .001
			0.97	0.99	0.02	< 0.01	102	4.39	< .001
Rice	R	< 0.001	0.97	0.98	0.00	< 0.01	102	1.65	0.230
				0.99	0.02	< 0.01	102	5.77	< .001
			0.98	0.99	0.01	< 0.01	102	4.12	< .001
	G	< 0.001	0.97	0.98	1.96e-4	< 0.01	102	0.06	0.998
				0.99	0.02	< 0.01	102	4.68	< .001
			0.98	0.99	0.02	< 0.01	102	4.62	< .001
	B	0.003	0.97	0.98	-0.01	< 0.01	102	-2.41	0.046
				0.99	0.00	< 0.01	102	0.95	0.609
			0.98	0.99	0.01	< 0.01	102	3.36	0.003

MD - mean difference; SE - standard error; df - degrees of freedom

The major differences occurred between specimens incubated at $a_w = 0.99$ and the others, except in the case of blue component measurements in rice, which can also be noticed from the difference in skewness in Figure 38b, where the specimens grown at $a_w = 0.98$ were the ones with significant differences in relation to the others. First, the most frequent pattern of differences will be examined in detail followed by analysis of the blue component in rice. It is also important to bear in mind that a_w ranged from 0.94 to 0.99 in oats, with 0.97 as the intermediate value recorded, while the interval was narrower in rice (0.97 to 0.99, with 0.98 as intermediate).

A recent publication about RGB variation of *F. graminearum* grown in agar [206] provides valuable insights into the cause of the difference as the authors have

found exactly the same pattern of differences (Figure 39). Indeed, the experiment on agar stressed the color differences to such an extent that RGB imaging analysis did not initially seem adequate in predicting the mold's growth and toxin production at a_w below 0.99.

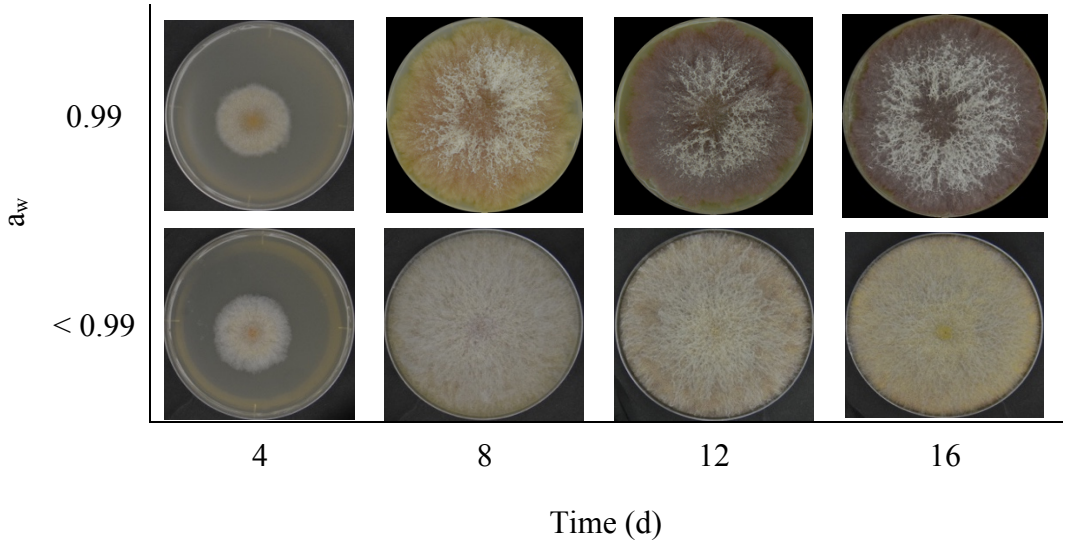

Figure 39. *F. graminearum* growth strategies at a_w = 0.99 and below, as observed in a previous experiment [206]. Note: the mold did not show any growth at a_w < 0.94.

When grown at a_w = 0.99, *F. graminearum* behaved exactly as it has already been described in this thesis, but at lower a_w the mold produces high volume of white mycelium, completely covering the surface of the medium, thus providing a barrier in visualization of the pigments.

A major distinctive feature of the kingdom Fungi is the organisms' extracellular digestion and nutrient uptake through pinocytosis, which makes fungi highly dependent on water [32]. Considerably low a_w might have led the mold to prioritize the *k*-selection survival strategy by growing an increased quantity of white hyphae, thus enhancing its CSA. In grains, the mycelia did not produce a drastic color variation perhaps due to the wider surface of the cereals compared to the same weight of agar.

The case of blue color in rice is unique, considering that it was not observed in oats, agar, or in the other channels, even though they are correlated. Another noticeable fact is the *p*-value (0.003) of the differences in blue component in the specimens incubated in rice, based on an analysis of covariance (ANCOVA), which was higher than similar calculations for other colors and in oats, implying the existence of some abnormality large enough to differ from the others. Furthermore, this group of measurements of the blue component showed the lowest correlations with red and green, even when compared with results from previous experiments [26, 202, 206].

A plausible explanation can be the abundance of dark perithecia or necrotic lesions in the specimens grown in rice at $a_w = 0.99$, particularly towards the end of the experiment. These pigments are frequently described as dark blue, violet, or purple [197], likely affecting the blue channel more than the others. The higher mycelial density in rice samples in relation to oats is perhaps related to the presence of dehusked rice among the grains, allowing *F. graminearum* to more readily access amylose, proteins and other easily digestible nutrients. According to Goswami and Kistler [11], high moisture and favorable conditions promote the development and maturation of conidia and perithecia.

For the following analysis of RGB variation in the grains, it is important to highlight the fact that the specimens described so far as photographed on the first day correspond to the initial time immediately after inoculation, i.e., time = 0 d (days). Thus, day 2 corresponds to time = 1 d (after 1 day of incubation) and so on. It implies that observations between days 8 and 9 correspond to observations in the interval $t \in [7\ d; 8\ d]$. It also implies that the only photos of the last day are the ones in the Figure 34 (the ones taken from a smartphone). The photos from day 17 were accounted in the

daily analysis, though they are not in Figure 35 and Figure 36. This would not have a made a difference to the results because the photos presented sufficiently demonstrated the predictability of *F. graminearum* color change in infected grains, through visual observation. Furthermore, any specific information obtained from the photos not shown, will be explained as accurately if necessary.

The nomenclature for the phases viz. lag, log (or exponential) and stationary phases derived from size based growth models, have been retained for comparison with the current state of knowledge [209-212]. The senescence or death phase has not been mentioned because the fungus did not die until the end of the experiment and *F. graminearum* can also thrive easily under extreme stress as a saprophyte, in nature [11]. However, new names will be proposed to more accurately reflect the observation. It is important to bear in mind that growth should not be seen simply as spatial expansion of an organism, but rather as a combination of physiological changes. In any case, it is more prudent to observe the changes in oats and rice before proposing the names.

All RGB values in oats showed an overall decreasing tendency, regardless of a_w (Figure 40). Variations seemed more consistent among the red component values, followed by green and finally blue, where the discrepancies between the specimens at different a_w seemed more evident. Yet, the overall shapes of all graphs are remarkably similar, thereby confirming the existence of a pattern of *F. graminearum* color variation as previously demonstrated by cultivating the fungus in yeast extract agar [26]. The current observation adds to the fact that this phenomenon also occurs in oats and across a_w (within the range where growth is possible).

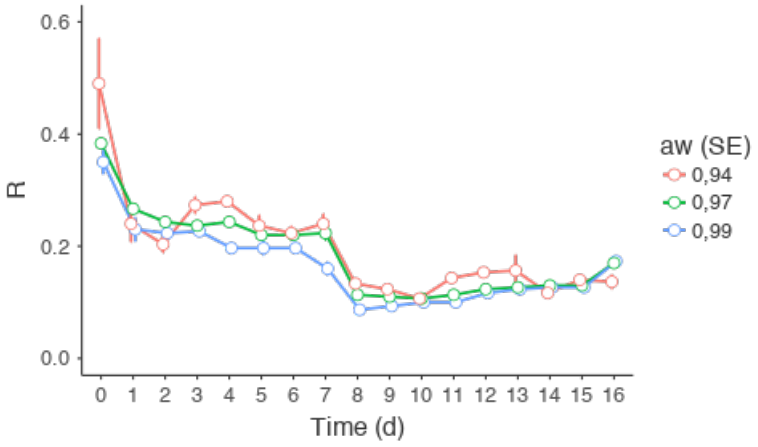

(a)

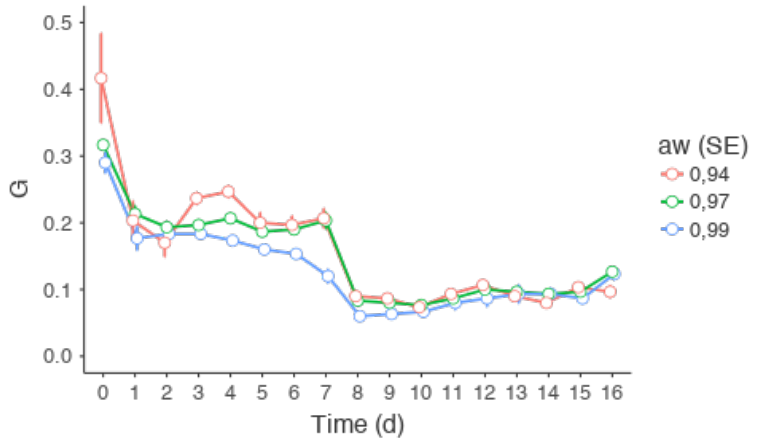

(b)

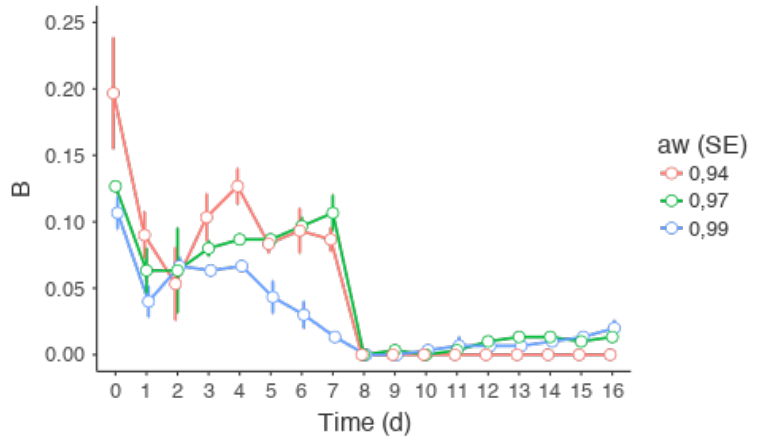

(c)

Figure 40. Variations of RGB components in oats infected with *F. graminearum* during 16 days.

The RGB-based growth curves for *F. graminearum* in oats seemed to decline in color intensity, with three distinguishable growth phases, during the same periods, regardless of the color component and a_w. They accurately reflect the information

obtained from visual analyses. The lag phase lasted for one day, where all components declined remarkably in intensity. The exponential phase comprised of the following six days, during which the quantity of pigments was mostly constant, yet showing some fluctuations. This was the phase of dominance of the mycelial paleness. The transition for the following phase lasted one day at which the color intensity further declined. During the stationary phase, a slight increasing trend was observed for all color components and this was due to spore production and the consequent accumulation of pigments [11, 25].

The transitions between the phases seemed smoother as a_w increased, perhaps due to the previously mentioned reason that water-borne stress leads the fungus to rapidly expand the mycelia through the medium, thus affecting the color more drastically [206]. An interesting observation is that although the colors were initially different due to the different humidity levels, in the end they all seemed to converge, especially from the 8th day until the end of the experiment. This suggests that *F. graminearum* shapes its microenvironment or substrate according to its needs until it presents the same characteristics, independent of the initial state. Several molds are known to affect the colors of grains [213-215] and in case of the current experiment, the grains acquired very similar colors after 8 to 10 days. This process has also been observed in agar and according to Dufosse*, et al.* [63], *Fusarium* usually releases pigments in the medium.

In rice (Figure 41), the trends presented some similarities and differences with respect to oats, but the basic shape prevails with the color declining on the 1st day, except the red component at a_w = 0.98 and 0.99, both values not changing much. The green component under the same treatments declined a little. Subsequently, it

fluctuates around a certain range of values for around 6 days, following which it quickly declines for approximately one day and finally rises.

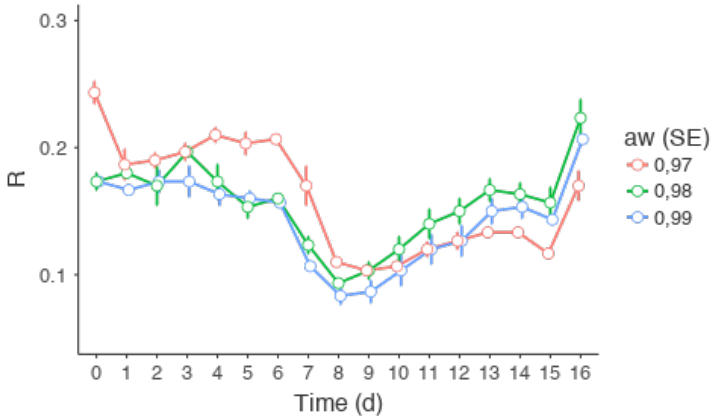

(a)

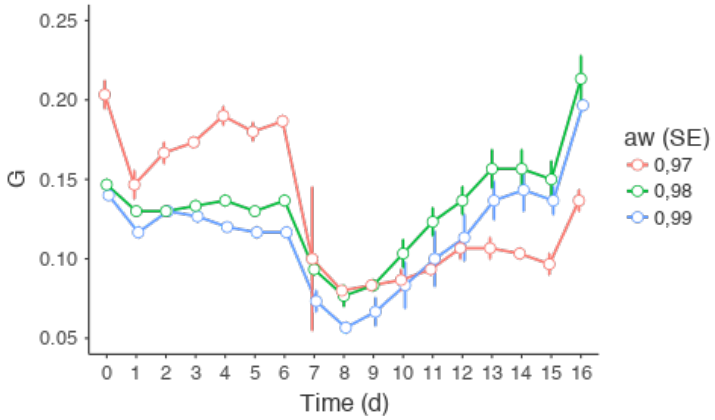

(b)

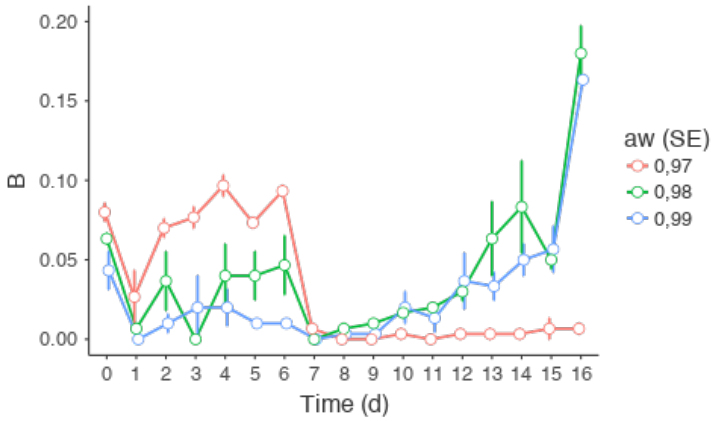

(c)

Figure 41. Variations of RGB components in rice infected with *F. graminearum* during 16 days.

Unlike oats, there was an exponential growth in all components on the last day of the experiment, except for the blue component at a_w = 0.97. This rapid RGB increase in intensity would likely have happened in oats too if the experiment was performed for a longer duration, even if a day more. It corresponds to a phase at which the grains are completely covered with white mycelium as Figure 34b shows. It is reasonable to believe that Figure 34a represents a previous step and the rice samples showed a more rapid increase in color intensity from day 8 until the end of the experiment. The variations are also more extreme as a_w decreases around the second half (perhaps from the 7^{th} to 9^{th} day) with the trends becoming similar for the different color components. However, blue was different (as already seen and explained) and now it is possible to see that the samples incubated at a_w = 0.97 exhibited a pattern of variation of the blue component more similar to what happened in oats, in relation to the other colors in rice. After the second decline, the intensity grew very smoothly, in an almost constant manner. The new observation allows postulation of theory opposed to the previous one, as the reason for the difference between the blue component in specimens grown in rice. There was considerably less quantity of perithecia and necrotic spots at this condition but there was high production of conidia, noticeable through the increase of the red component and perhaps green. Indeed, *F. graminearum* requires high humidity to start producing perithecia, which is one of the reasons for maturation of such structures occurring during spring [11].

In contrast to the infected oats, rice showed a smoother decline in colors, possibly due to the existence of some dehulled grains and consequent less stress on the mold to acquire the nutrients. The presence of dehulled grains is also expected to affect the dynamics of water distribution throughout the medium [216, 217], because

the cellulose barrier certainly affects the speed at which the grains absorbed the water. Thus, the fungus did not have to employ as much effort, as in the case of oats to ensure survival and it was much easier to modify its microenvironment to suit its needs, as part of the medium was already ideal for growth. For instance, in yeast extract agar, *F. graminearum* started producing spores from the 3rd day of incubation [26] instead of the 7th or 8th day, as observed in the current experiment. Thus, one can conclude from these observations that nutrient availability favors smoother color transitions between different growth phases.

By observing RGB changes in both oats and rice, the following features become apparent: (1) as a_w decreases, the RGB components tend to fluctuate more and the graph presents a wider co-domain (range of ordinates); (2) the blue component presents more fluctuations, possible due to the fact that its values are frequently low in relation to the others and thus more susceptible to noise or slight variations; (3) the specimens at the lowest a_w always start with higher color intensity in relation to the others but then equalize to the others or become lower and (4) the two highest a_w conditions presented almost the same behavior throughout the entire experiment.

Considering existing knowledge regarding microbial growth models and the observations from the current study along with the ones in yeast extract agar [26, 202, 206], the authors propose the model showed in Figure 42 to represent the growth of *F. graminearum* regardless of a_w, based on the variation of the RGB components and stressing on the alternation of the *k* and *r* selection strategies as a response to changes in the microenvironment.

Unlike the models widely used to describe bacterial growth [166, 209-211, 218], which have been borrowed to explain fungal growth patterns [28], the current

model presents two lag phases, one before a mycelial phase and another before the sporular phase. Also, in contrast to the stationary-like lag phases observed in size-based growth models, these lag phases present a decrease in coloration. The first decrease is due to the mycelium forming a transparent layer masking the "shiny" grains, and the second is due to the mature hyphae initiating the production of spores, thereby reducing the color intensity established by the mycelia.

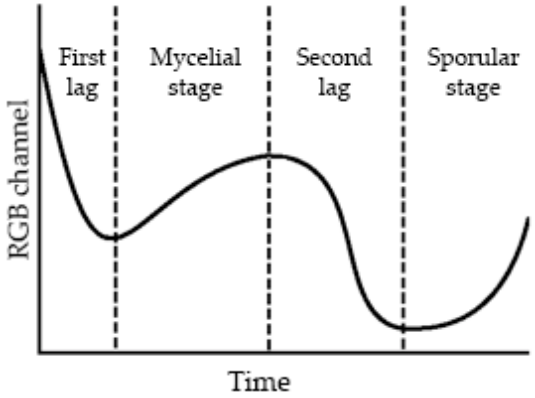

Figure 42. *F. graminearum* growth curve based on RGB measurements of contaminated cereals.

Immediately after the first lag (logarithmic negative), the paleness of hyphae restores the intensity of all colors as the mycelial network becomes denser (mycelial phase, logistic). After the second lag (logarithmic with negative coefficient of the abscissa), color intensity increases as yellow and pink pigments spread through the media, and the mycelia attain their maximum thickness (sporular phase, exponential). The model presents two valleys, each after the respective lag. They could be named valleys of re-adaptation (first and second), as these are circumstances in which a particular selection strategy (*r* or *k*) starts to dominate the microenvironment.

4.1.4 Conclusion

The current report is a follow-up to the study on RGB imaging as an alternative tool to size-based models to analyze *F. graminearum* growth. The first was performed using yeast extract agar and demonstrated the predictability of the mold's

variation of the RGB channels through digital photos taken on successive days using a professional camera and a smartphone. The current study validated the idea for cases in which the fungus grows in oats and rice. Furthermore, it was performed at distinct a_w settings. Thus, the visual analysis of digital photos, as well as statistical calculations and plotting of the graphs confirmed the existence of a growth pattern over time when *F. graminearum* infects oats and rice, and that such patterns occur across different a_w conditions at which the fungus can grow in a fairly similar fashion, for both grains. The mold begins colonization of the grains using a *k*-selection strategy, at which the fungus quickly develops a mycelium to survive in the new medium, and later an *r*-selection strategy, comprising of high sporulation that in field would ensure its propagation to new habitats or simply a dormant survival for long periods. From the observed pattern, a 4-phased model was proposed, containing a mycelial and a sporular phases preceded by lags or phases of adaptation.

4.2 Analysis of color change and DON synthesis in contaminated oat and rice

4.2.1 Introduction

Fusarium graminearum Schwabe is among the major cereal parasites, causing *Fusarium* head blight (FHB) in species including oats and rice and contaminating the grains with deoxynivalenol (DON) and several other mycotoxins. DON, also known as vomitoxin, inhibits protein synthesis and its ingestion causes several biological disturbances, such as gastrointestinal disorders and hematological changes [15]. According to the World Health Organization, the chemical is also teratogenic and an immunosuppressive neurotoxin [206]. There have been outbreaks of human gastrointestinal illness in Japan, China and India [15, 23], and this toxin also compromises animal production, affecting pigs, chicken and equines [50, 219]. For

these reasons, Japan has set a provisional limit of 1.1 μg/g [8]. Like many other mycotoxins, DON is resistant to several processing methods such as milling, baking, boiling, fermentation, etc., thereby ending up in processed food if initially present in the grains [12, 220-222]. Thus, control of *F. graminearum* seems to be the best strategy to prevent DON contamination, and therefore it is necessary to understand its growth pattern.

So far, size-based measurements (e.g., radius or diameter) have been the gold standard in describing fungal growth and predicting mycotoxin production [28], perhaps because they were developed when there were few alternatives which were as inexpensive, quick or even technologically feasible. These study methods were borrowed from bacterial studies [28, 166] and were undoubtedly suitable to describe fungi in several circumstances, but present some constraints with a potential to result in inaccuracies due to peculiarities in mycelial growth [26]. For instance, when grown in a closed system such as a Petri dish, the so-called stationary phase is actually forced by the container's barriers and might create the illusion that the mold stops growing at this stage [26, 202], but it is well-known that the metabolism does not really stop at this stage [32]. Indeed, stages at which the fungus is not expanding in size are more likely to be the ones at which the mold performs the most important processes to ensure its survival [26]. For instance, in the lag stage, the fungus has to adapt to a new environment and in the stationary phase, it faces the stress of nutrient depletion. Furthermore, radius and diameter have little practicality in the field because the fungus is not likely to present a regular growth pattern if the substrates do not present regular shape or if factors such as water or nutrients are not evenly distributed throughout the environment.

Optical methods have recently been used as tools to monitor growth of *F. graminearum* and its damage in grains, with increasing success [25], and also in the detection of DON [1, 9]. These tools have the advantage of being rapid, non-destructive, non-labor intensive and in some cases very cheap [19, 25], requiring only a digital camera and statistical analysis tools. Recent studies have demonstrated the predictability of *F. graminearum* growth pattern and also DON contamination in yeast extract agar (YEA), based on the variation of the mold's superficial colors through the measurement of the average red, green and blue (RGB) components of digital photos at different temperatures and a_w [26, 202]. If this method is applied to grains, it will be possible to ensure their quality and prevent DON contamination in a cheap, reliable, non-subjective and non-destructive method.

The current study was aimed to analyze the relationship between average RGB variation in digital photos of oats (*Avena sativa*) and rice (*Oryza sativa*) infected with *F. graminearum* and DON concentration which were accumulated for 16 days at different temperatures and water activity (a_w).

4.2.2 Material and methods

A. Mold isolate

This study was performed using a *F. graminearum* isolate from the Catalogue of the Japan Collection of Microorganisms (JCM). It is registered as the teleomorph *Giberella zeae* (Schwabe) Petch, strain TH-5, isolated by Sugiura*, et al.* [167] from rice stubble in Hirosaki, Aomori Prefecture, Japan. It is a known producer of deoxynivalenol, 15-acetyldeoxinivalenol, and zearalenone [72].

B. Grain samples

All samples of raw oats (*Avena sativa*) and rice (*Oryza sativa*) were obtained locally in Hokkaido. Dried and sealed oats were purchased from a local store, with husk in plastic bags, at 250 g each. Dried rice was obtained from local producers, in plastic bags containing 500 g each, with 90% husk and the remaining brown. All grains with husk showed the ability to germinate. Thus, they were autoclaved to inactivate the embryos and eliminate possible microbial contamination. After autoclaving, the color did not seem to change considerably. For the current experiment, nine samples each of oats and rice, each containing 25 g, were placed in Petri dishes. Water activity was empirically set using distilled water, and for each grain the starting range was the lowest value at which growth was observed.

C. Incubation and RGB determination

The cereals were split into three groups, each with distinct water activity (a_w). For oats, the groups had a_w = 0.94, 0.97 and 0.99 and for rice they were 0.97, 0.98 and 0.99. In total, each cereal was used to prepare 153 media in Petri dishes, 144 to grow the molds and 9 as control to determine the colors in the beginning on the experiment. Thus, 288 specimens of *F. graminearum* were sown, one in each medium. In the end, there were three replicates per water activity at which five repetitions were incubated at four different temperatures: 15 °C, 20 °C, 25 °C and 30 °C. From the fourth day of incubation, three replicates per temperature, cereal, and a_w were taken for DON quantification. Before the extraction, the fungi were photographed in a black bucket, from a vertical distance of 30 cm. The camera model used was Nikon D3200 with a DX SWM VR lens (Nikon Corporation, Tokyo, Japan), which was used without flash or any automation affecting illumination. The only source of light was a round LED attached to the bucket's lid. The photos were then processed using the method

described by Cambaza*, et al.* [26] on ImageJ software (FIJI edition, National Institutes of Health, Bethesda, Maryland, United States), developed by the National Institutes of Health and the Laboratory for Optical and Computational Instrumentation (LOCI, University of Wisconsin) [41]. ImageJ allowed the determination of average intensities of the RGB components from the photos.

The analysis considered only the fungal surface, excluding any background including the plate borders or agar. In the end, the variables analyzed were incubation time (in days), a_w and the RGB parameters, converted from the 8-bit notation (0−255) to the arithmetic index (0.0−1.0).

2.2.2. Extraction and High-Performance Liquid Chromatography (HPLC)

For extraction, each sample was mixed with 100 mL of water:acetonitrile (84:16) and blended in a Seward Stomacher 400 machine (Seward Ltd., Singapore). Approximately 15 mL of the filtered extract was transferred to a tube and 2 mL of this filtrate were purified using Supel™ TOX DON cartridges [19]. These cartridges eliminate undesirable fat, pigment, and carbohydrate and retain large molecules. HPLC was run through a Jasco CrestPak C18T-5 affinity column using (a) water:acetonitrile:methanol (92:4:4) and (b) acetonitrile as mobile phase with a flow rate of 0.2 mL/min at 35 °C and ultraviolet detection at 220 nm. The DON peak consistently appeared at an elution of 8 min.

D. Statistical analysis

Statistical analysis was performed on JASP 0.9 (The JASP Team, Amsterdam, The Netherlands), Jamovi 0.9 (Jamovi Project, Amsterdam, The Netherlands) and Microsoft Excel (Version 14.5.8, Microsoft, Redmond, Washington, United States). All the hypotheses were tested at $\alpha = 0.05$. The distribution of intensities of red, green, and blue and DON concentration were compared using analysis of covariance

(ANCOVA) to determine if their differences were significant, followed by Tukey's post-hoc comparisons if necessary. The correlations between the colors and DON concentration were then analyzed through scatter plot matrices.

4.2.3 Results and discussion

The samples were successfully grown and photographed at all settings. The average RGB values were measured and DON was quantified. The first subsection of the results will focus on the visual impression of the specimen photos followed by the statistical analysis.

A. Qualitative description

Infection of oats (Figure 43) and rice (Figure 44) were quite similar, with regards to color variation. Rice samples were generally the most heavily infected, perhaps because in rice some grains were hulled, thereby providing nutrients to the mold more readily. Hull is one of the most important natural barriers for the cereal, and its absence facilitates colonization [208]. Moreover, rice husk presented higher water permeability [223] and it might have facilitated the mold's process of digestion. In order to feed, a mold has to secrete enzymes capable of externally decomposing the substrate with the organism then absorbing the resulting nutrients [32].

In all cases, the grains were relatively dark in the beginning, especially rice. The difference in tone between the samples immediately after inoculation and on the 4^{th} day was consistently remarkable. As time passed, the color became increasingly pale, regardless of the temperature or a_w. Paleness resulted from mycelial growth, and it increaseed as the hyphal network became denser [11, 25].

One exception can be noticed in oats at $a_w = 0.94$, where mycelial growth was slower, perhaps because such condition is suboptimal for growth.

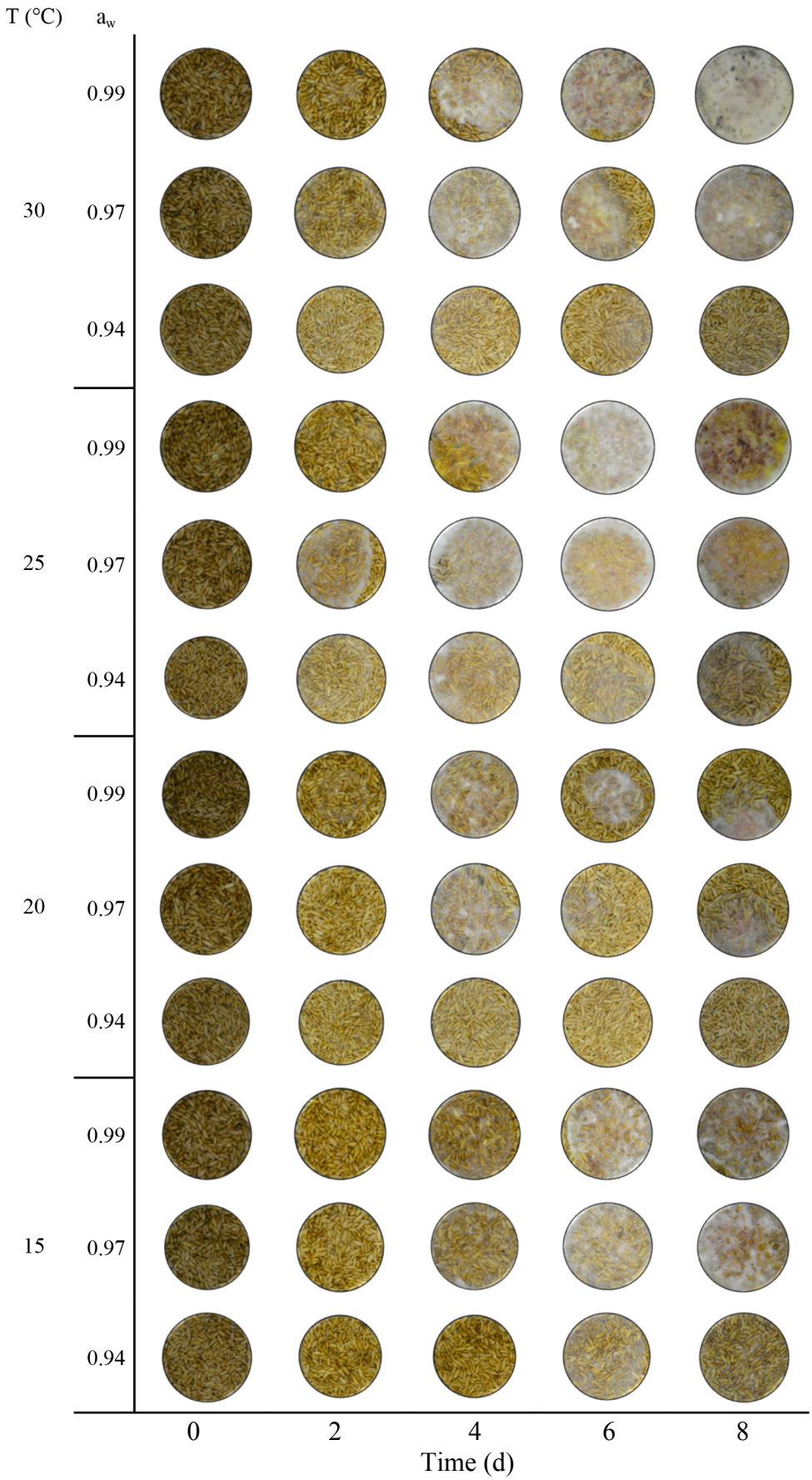

Figure 43. Color variation of oats infected with *F. graminearum* at different a_w during 16 days.

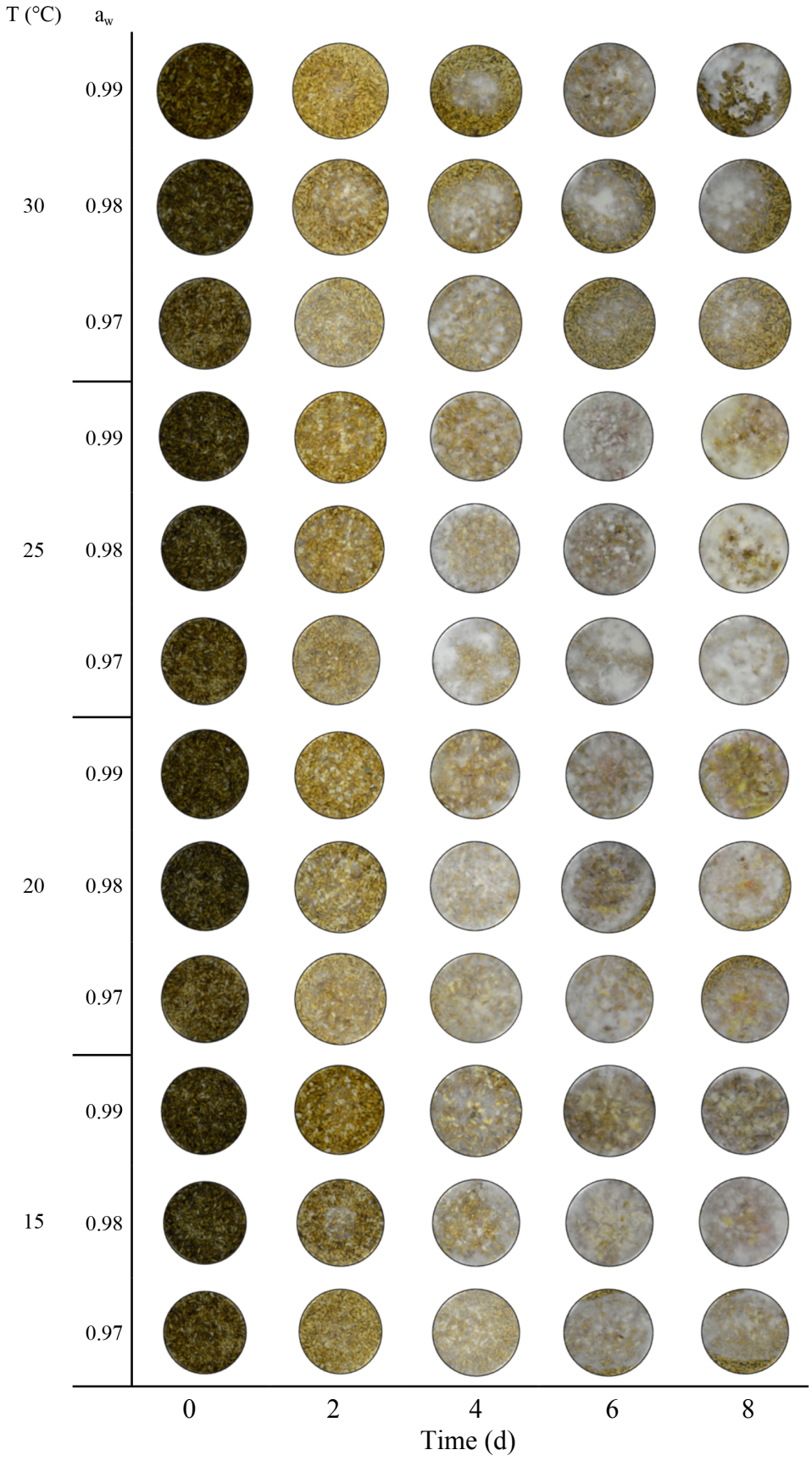

Figure 44. Color variation of rice infected with *F. graminearum* at different a_w during 16 days.

According to Ramirez*, et al.* [195], based on measurements at 25 °C, *F. graminearum* grows optimally at a_w settings between 0.95 and 0.995. However, the authors have used different strains (RC 17-2 and RC 22-2) from the current study (TH-5) and a previous experiment had showed high mycelial growth at a_w = 0.95 in yeast extract agar (YEA). Molds rely on environmental water for their external digestion [32, 224].

Some cases show grains less infected than the ones from the previous day of collection at the same conditions of a_w and temperatures. This might have happened due to irregularities in the samples resulting in different patterns of distribution of nutrients and water. Fungi present chemotropism towards nutrients [32, 224]. This explains why in some cases, such as oats incubated in Petri dishes at 25 °C and a_w = 0.97 measured on the 4^{th} day, a clear delimitation of the extent of hyphae growth in high density was observed. For instance, individual grains are expected to present slight differences in size, weight or even shape. Variations might also have resulted from the particular mass of each inoculum or the exact position in the Petri dish where they were placed.

In most cases, regardless of the cereal or temperature, higher a_w leads to faster mycelial growth and formation of pigments varying from very dark purple to magenta or pink and yellow. Direct proportionality between a_w and growth rate are intuitive, assuming that fungi highly rely on water to obtain nutrients which has been already demonstrated [8,28]. In oats, the pigments are considerably easier to see at all temperatures except at 20 °C, and in rice they can be seen virtually at all temperatures. In case of oats at 20 °C, the impression of low contamination in relation to other temperatures is likely due to the distribution of humidity, as previously mentioned. More water might have accumulated on one side of the Petri dish. Yet, it

is possible to notice some pigmentation in the areas more heavily infected in these grains at 20 °C. The colors of the pigments are consistent with the most common descriptions throughout literature [11, 25]. The purple or dark pigments are likely to be melanin present in perithecia [31, 71, 197], usually produced when there is high humidity and favorable temperature [11], pinkish or reddish can be aurofusarin (more likely) or rubrofusarin, possibly torulene, and the orange-yellow also aurofusarin (also more likely) or neurosporaxanthin [197].

It is reasonable to make the following conclusions: (1) rice shows the highest level of infection, perhaps due to the peeled grains and higher digestibility, (2) all temperatures were suitable for the growth of *F. graminearum*, (3) the level of infection seems directly proportional to a_w, and (4) this was more easily noticable in the oat samples, possibly because of a wider range of a_w. The samples became paler over time because of mycelial growth, and perhaps from the 8th day the mold started developing spores and perithecia.

B. Impact of temperature on color and DON concentration

According to an analysis of covariance (ANCOVA), samples incubated at distinct temperatures exhibited values of all RGB components to be significantly different ($p < 0.05$). Such differences were difficult to observe through visual analysis since in most cases the behavior of the mold seemed very similar. Perhaps the statistical differences arose from the combination of irregularities in the distribution and intensity of colors, particularly at the later stages. For instance, there are differences in the density of mycelia, hue, quantity and saturation of the pigments, or even irregularities in the colors of the grains, especially rice since some grains were hulled. Nevertheless, a previous experiment in yeast extracts agar showed very similar results [202], suggesting that the difference is more likely to arise from the mold's

pigmentation as a response to temperature variation. Moreover, there are more studies confirming the impact of temperature on the pigmentation of *F. graminearum* and other molds [185, 186]. For instance, *F. graminearum* requires a favorable temperature in order to start producing spores during spring [11].

It is also relevant to consider that differences in color between the specimens incubated at distinct temperatures might be in part related to the variations in a_w, but it seems unlikely because the visual analysis suggested that a_w had similar effect on the mold across temperatures, especially in oats. Nevertheless, the color skewness caused by a_w in each temperature might have been different in magnitude but the analysis of covariance showed $p < 0.05$ for all RGB components, with the level of difference being too extreme with reference to visual impression. In YEA, the impact of a_w on the visual characteristic of the fungus was very consistent and easily noticeable [206]. Specimens at $a_w = 0.99$ presented the typical and predictable color variation previously demonstrated by Cambaza*, et al.* [26], while $a_w < 0.99$ stimulated dense mycelial growth, masking pigmentation. The contrast between colorful and whitish samples was therefore visually clear, although for the red component the difference was not significant ($p = 0.169$). If the same happened in the grains for all temperatures, the differences would not be expected to be as remarkable as the analysis of covariance showed in the current experiment. Furthermore, in agar, significant color differences were observed between specimens grown at the same temperatures when a_w was the same [202]. This implies that temperature by itself was the major cause of the differences. However, the role of a_w will certainly be better understood with careful examination of how a_w affects color at each particular temperature, which remains to be examined in detail.

Considering post-hoc comparisons, rice presented more cases of RGB differences (11 instances) compared to oats (5 instances). In both cereals, the specimens incubated at 15 °C and 25 °C presented the major differences, with significant differences for all RGB components. Such differences were more remarkable in rice, with *p*-value consistently lower than 0.001, and no case presenting differences at such magnitude in oats. The second more frequent differences were between specimens at 20 °C and 25 °C, present in both cereals but absent for the green component in oats. The following differences occurred only in rice: 20 °C and 30 °C for all RGB components, 25 °C and 30 °C also for all components, and finally 15 °C and 20 °C only for the red component. The following aspects are noticeable: (1) red component was the one with most frequent differences (7 instances, 2 in oats and 5 in rice), followed by blue (6 circumstances, 2 in oats and 4 in rice) and green (5 cases, 1 in oat and 4 in rice); (2) samples incubated at 25 °C presented more frequent cases of differences (11 instances), followed by 20 °C, 30 °C (6 instances for both) and 15 °C (7 cases).

In the previous experiments, the red component had always shown more fluctuations [26, 202, 206], which is justified since the most characteristic pigments of *F. graminearum*, especially at the later stages of its lifecycle (when there is high quantity of spores), are shades of red or related colors such as pink [11, 25, 197]. Since sporulation is affected by the temperature [11], the differences in this component are a reflection of variations in quantity of spores. The fact that blue was the second in the incidence of differences, might follow the same logic as red but melanin is not as frequent as aurofusarin or rubrofusarin [197].

The samples incubated at 25 °C were more frequently different from the others perhaps because this is the optimal temperature for growth of *F. graminearum*

[195], resulting in the production of more spores and consequently a unique color profile, compared to other temperatures. The suboptimal temperatures presented lesser differences between them because moldy samples without spores were mostly whitish for all samples. It is interesting to note that specimens at 20 °C and 30 °C presented exactly the same frequency of differences (6 instances each) and both have exactly the same difference in temperature with 20 °C. In case of 15 °C, which is the most distant from the optimal state, 7 instances of differences were observed. Yet, most differences were between 25 °C and the lowest temperatures, which the fact that warm temperatures are more favorable for the development of spores in relation to cooler conditions [11].

So far, from the observations with respect to the colors, it might be concluded that red is the most sensitive color component across temperatures and this quality seems desirable if slight variations are to be detected. Green, on the other side, was the most resistant to temperature variations, and this quality might be advantageous to develop a color based approach without the need for validation at every temperature, or when the temperature is not being monitored. The choice of the best component seems to be a case of sensitivity versus stability.

Table 10 showed time and temperature variations are related to concentration of DON in the Petri dishes containing oats and rice. The amount of toxin varied significantly over time. The samples incubated at different temperatures, on the other hand, did not present significant differences in general, except in pairwise comparisons with respect to time, in case of rice samples. Yet, such observations are still to be discussed in more detail in this subsection and even more in the following subsections with particular focus on how temperature and a_w both affect the dynamics of color variation and DON production.

Table 10. Analysis of covariance showing the significance of the differences in DON production, between samples, over time and incubated at different temperatures.

Commodity	Variable	Sum of Squares	df	Mean Square	F	p_{ANCOVA}
Oats	Time (d)	2.08e+6	4	519864	21.28	< 0 .001
	Temperature (°C)	134044	3	44681	1.83	0.145
	Time (d) * Temperature (°C)	308417	12	25701	1.05	0.406
	Residuals	3.32e+6	136	24434		
Rice	Time (d)	2.44e+6	4	610426	89.09	< 0.001
	Temperature (°C)	51483	3	17161	2.50	0.062
	Time (d) * Temperature (°C)	312039	12	26003	3.80	< 0.001
	Residuals	931843	136	6852		

df - degrees of freedom

Figure 45 shows variation of RGB components and DON concentration at different temperatures, during the course of the experiment, in oat samples. It is better to first consider Figure 45a-c, which are related to the RGB channels and compare them with the visual analysis of oats (Figure 43) and post-hoc comparisons.

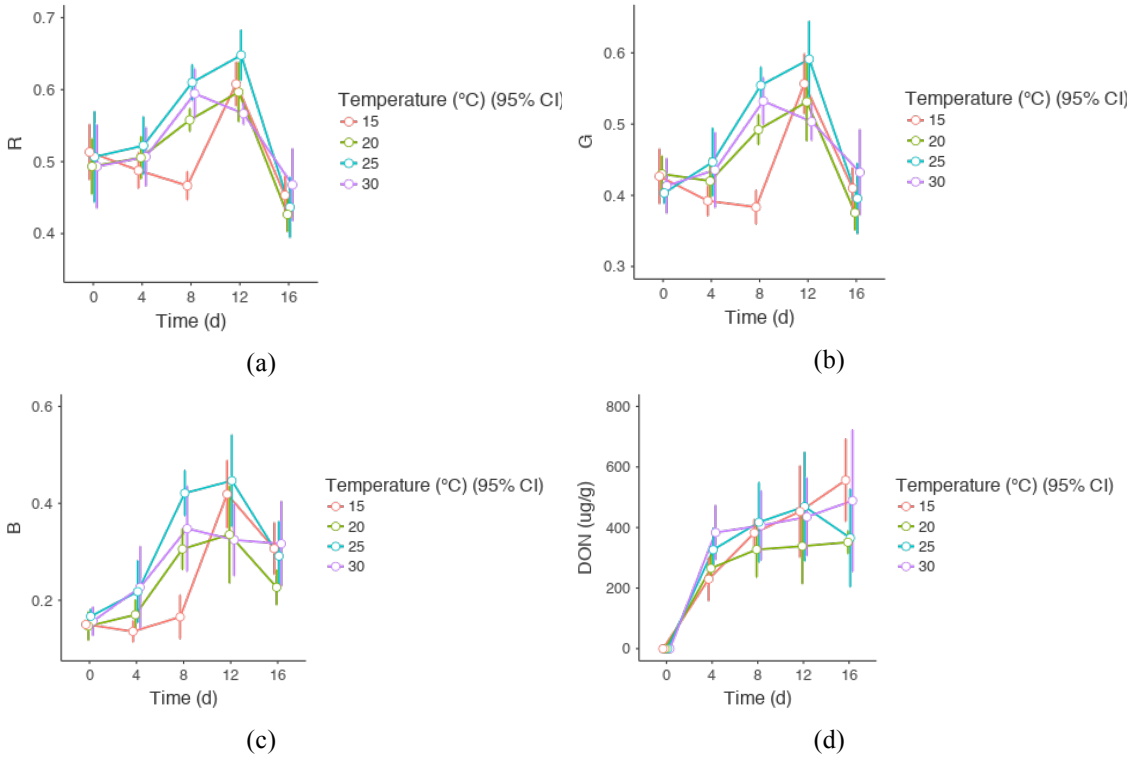

Figure 45. Variation of the RGB components and DON concentration in oats infected with *F. graminearum* at different temperatures for 16 days.

It has already been shown that temperature significantly affects the variation of all RGB channels. At first glance, the samples incubated at 20 °C almost consistently presented the highest intensity for all RGB components, followed by 20 °C and 30 °C (both without significant differences, as already seen). The samples at 15 °C presented the lowest intensities until the 8th day and then rose to the second highest intensities. Initially, specimens at 15 °C might have taken longer than the others to adapt to the new environment as the temperature was suboptimal [8, 11], but after catching up with the others, they started producing spores as well. The fact that the samples at the lowest temperature seemed to lower in color intensity is more likely related to individual fluctuations, because the visual analysis implied a rise in color intensity, except between the sample from the 4th and 8th days at a_w = 0.94. Though all samples had initially almost the same coloration, there were noteworthy discrepancies, especially in the middle of the experiment. This observation is consistent with the visual analysis, as all samples were almost equally dark in the beginning and, in the end, with high density of white mycelium, although some samples presented more pigmentation than others on the 16th day. It has been seen in post-hoc comparisons that samples incubated at 25 °C presented significant differences with the ones at 15 °C (all RGB components) and 20 °C (red and blue). The difference with 15 °C was easy to notice because the trends are different, but at 20 °C it can be seen that the graph never crosses the line representing 25 °C.

From these graphs, it can be concluded that the color initially declines as the temperature rises from the optimal, until the 8th day, but the red and green components in particular, tend to converge. In most cases, the intensity increased to a peak on the 12th day followed by decrease. The increase in intensity is due to the

mycelial growth [206] and the decline is likely due to the noise caused by the presence of pigments on the white background [26].

DON concentration (Figure 45d) increased in all cases, except in samples incubated at 25 °C. However, this reduction is likely due to fluctuations in individual samples, possibly related to the pattern of distribution of water through the grains, initial position of the inoculum, the proportion water:acetonitrile during the extraction of the DON samples, or differences in weight or shape of the grains. However, there were 136 degrees of freedom and the confidence intervals are wide enough to accommodate the possibility that DON concentration kept increasing throughout the experiment. There is sufficient evidence, with some of it being specific to DON, that mycotoxins are stable and accumulate over time [28, 35, 195].

As pointed out in the post-hoc comparisons, temperature had a stronger impact on the colors and DON production, in rice in comparison to oats. With respect to temperature, colors in infected rice (Figure 46a-c), exhibited patterns remarkably similar for all color components. These observations along with observations in oats, suggest the existence of a high correlation between all RGB components. Such correlations have been demonstrated in previous experiments [26, 202, 206], and have been explored in further detail. The rice samples incubated at 25 °C presented the highest intensity of all RGB channels for most of the experiment, although the ones at 30 °C had the highest values until the 4th day and the lowest immediately after that, until the end of the experiment. All colors showed rapid increase in intensity in the beginning for all samples, except the ones at 30 °C, which continued to rise until the 8th day, following which the colors did not change considerably, although there were fluctuations. Visual analyses of most samples support these observations.

The rapid increase in color intensity from the start is perhaps due to the ready availability of nutrients in rice samples as it has been already discussed. The almost sudden reduction after the 8th day is probably because of nutrient depletion, when the fungus initiates the so-called stationary phase [26].

Incubation at different temperatures resulted in different trends in DON production (Figure 46d), particularly after the 8th day, likely due to the same errors causing discrepancy in oats at 25 °C, as previously mentioned. Furthermore, though the peeled rice seemed uniformly distributed throughout the samples, it was difficult to determine with certainty and the differences between the samples might have affected the availability of nutrients and the overall dynamics of DON synthesis. Sorensen and Sondergaard [74] demonstrated that slight differences in nutrients, even between considerably similar media, can lead *F. graminearum* to produce different quantities of DON and other secondary metabolites.

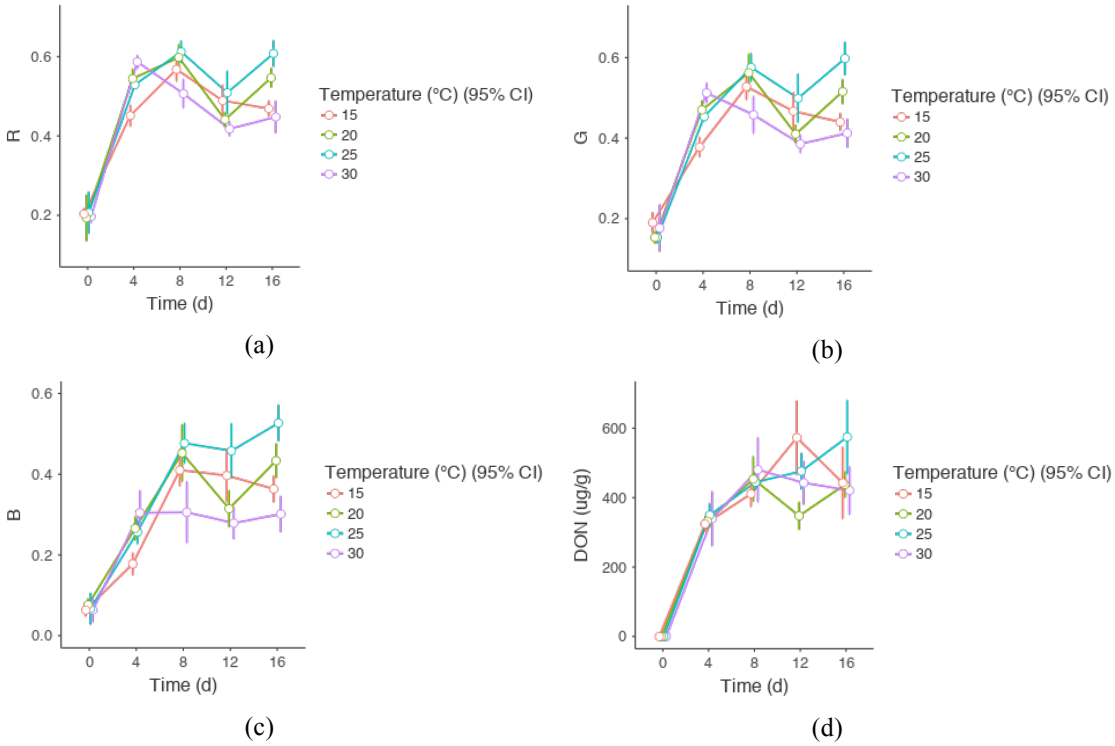

Figure 46. Variation of the RGB components and DON concentration in rice infected with *F. graminearum* at different temperatures during 16 days.

So far, it seems that an optimal temperature promotes the development of higher color intensity and suboptimal tends to reduce it and beyond a certain point (in this case it was below 20 °C) the color measurement follows a different pattern. This is likely to be related to growth strategy and in this case the major factors influencing were temperature and nutrient source, a dynamics well-explained by Leplat*, et al.* [5] and Goswami and Kistler [11]. It is also important to bear in mind that rice has a husk more permeable to water in relation to oats [223] and there was some brown rice. Though the temperature was similar, the specimens growing in oats faced higher nutrient stress and it led them to adopt a saprophytic strategy frequent in the winter (*k*-strategy) [207], with minimal biomass to save energy but highly capable mycelia in terms of ability to colonize the grains (e.g., by developing haustoria). This is the reason why the color did not increase considerably until the 12th day. Just after some degree of success, the fungus shifted to *r*-strategy, quickly maturing, thickening the mycelia (maximizing nutrient absorption) and producing spores. In rice, the fungus directly opted for *r*-strategy, similar to what happens during spring because the conditions seemed favorable, even under a relatively cool environment. *F. graminearum* is frequent in temperate climates [15], though higher temperatures favor its growth [16].

C. At 15 °C

ANCOVA tests demonstrated significant differences ($p < 0.05$) between all RGB components for all oat samples incubated at distinct a_w with Figure 47 a-c showing the color variations. All colors showed very similar trends and samples at a_w = 0.97 presenting the highest intensity throughout the experiment, except in the beginning.

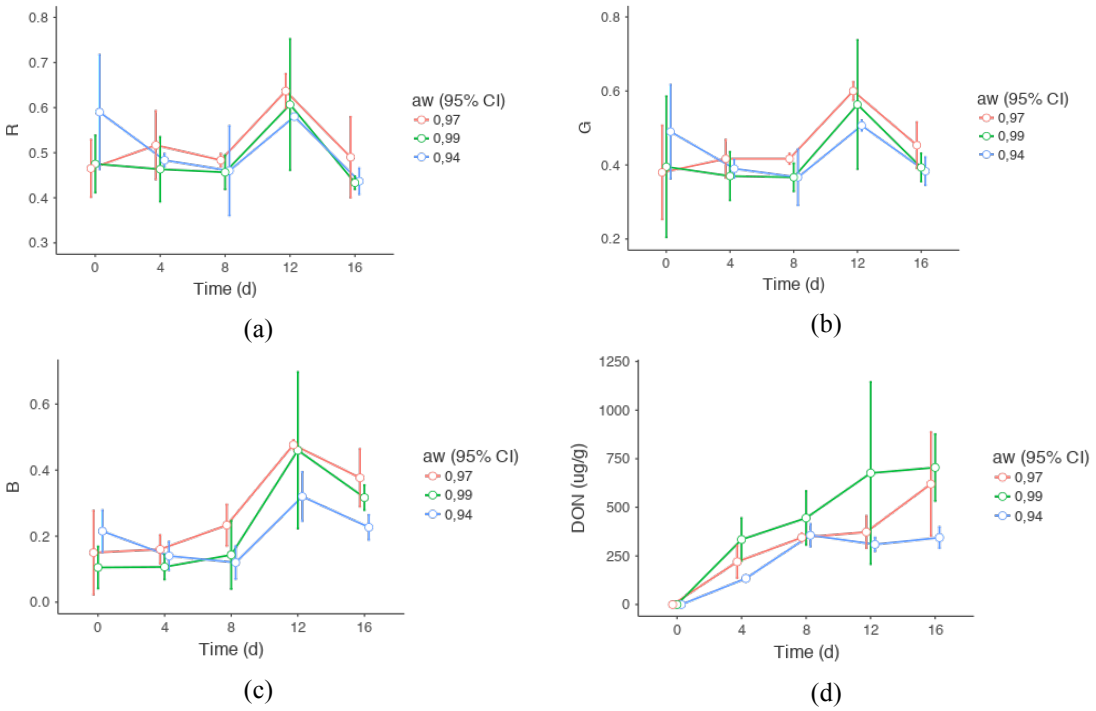

Figure 47. Variation of the (a) red, (b) green and (c) blue color components and (d) DON concentration in oats infected with *F. graminearum* at 15 °C during 16 days, as a function of a_w.

Post-hoc comparisons did not show significant differences between the samples incubated at a_w = 0.94 and 0.99 in any RGB channel. At distinct a_w settings, the colors presented very similar pattern of change, almost constant until the 8th day, increasing to a maximum on the 12th day and then decreasing. The increase reflects rising paleness, with the formation of pigments reducing the whiteness. In these samples, mycelial growth took longer than expected to become noticeable [26, 206], regardless of the humidity, most likely due to the temperature being suboptimal [11, 35].

DON concentration increased in general (Figure 47d), though there was a fluctuation between days 8 and 16 among samples at a_w = 0.94. Yet, the data suggested that that a_w was directly proportional to DON concentration (p_{ANCOVA} < 0.001; p_{Tukey} < 0.05 for all comparisons). This result is consistent with findings by

Ramirez, *et al.* [195] and is due to the fact that high humidity is favorable for the fungus to mature and start secondary metabolism [11].

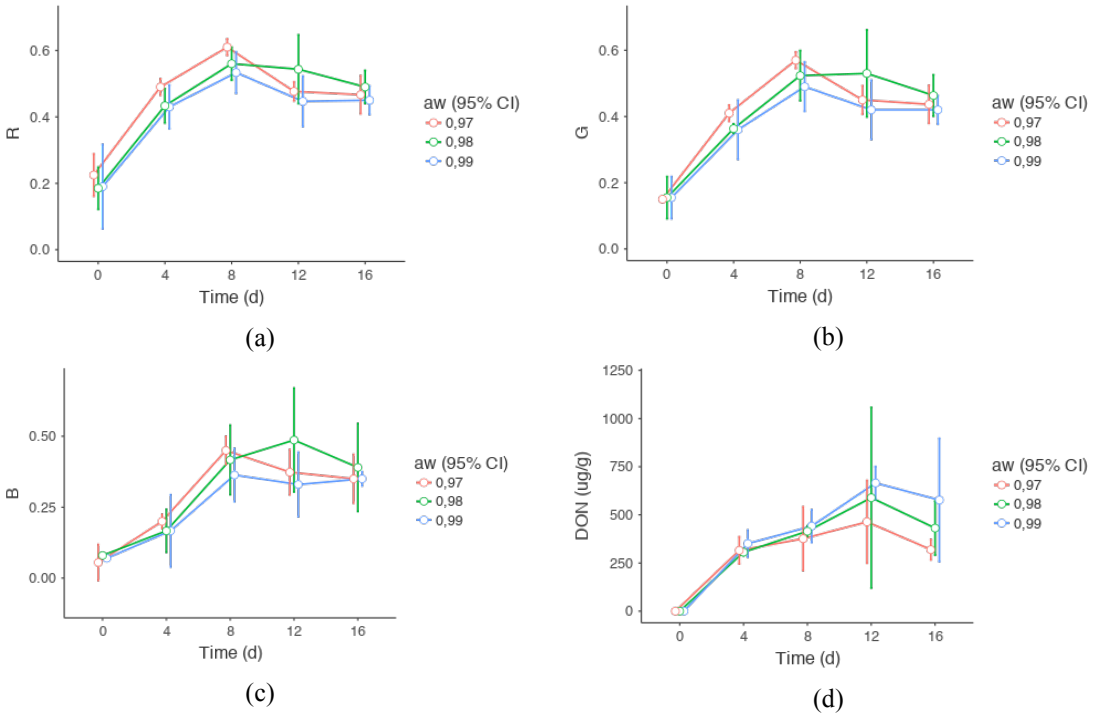

Figure 48. Variation of the (a) red, (b) green and (c) blue color components and (d) DON concentration in rice infected with *F. graminearum* at 15 °C during 16 days as a function of a_w.

In rice, the pattern of color change (Figure 48a-c) was not exactly similar to oats. The color differences of samples at different a_w were also significant, according to an ANCOVA test, and post-hoc analyses showed that the major significant differences were between the samples at $a_w = 0.97$ and the others ($p < 0.05$). In most cases, RGB components increased until reaching a maximum on the 8th day and then decreased slightly or remained constant. The only exception was the blue component measured from specimens incubated at $a_w = 0.98$, showing the highest intensity on the 12^{th} day. The overall trend was easily noticeable through visual analysis, with the RGB component again showing rapid growth at 15 °C when compared to the measurements in oats, for reasons mentioned in the previous subsection.

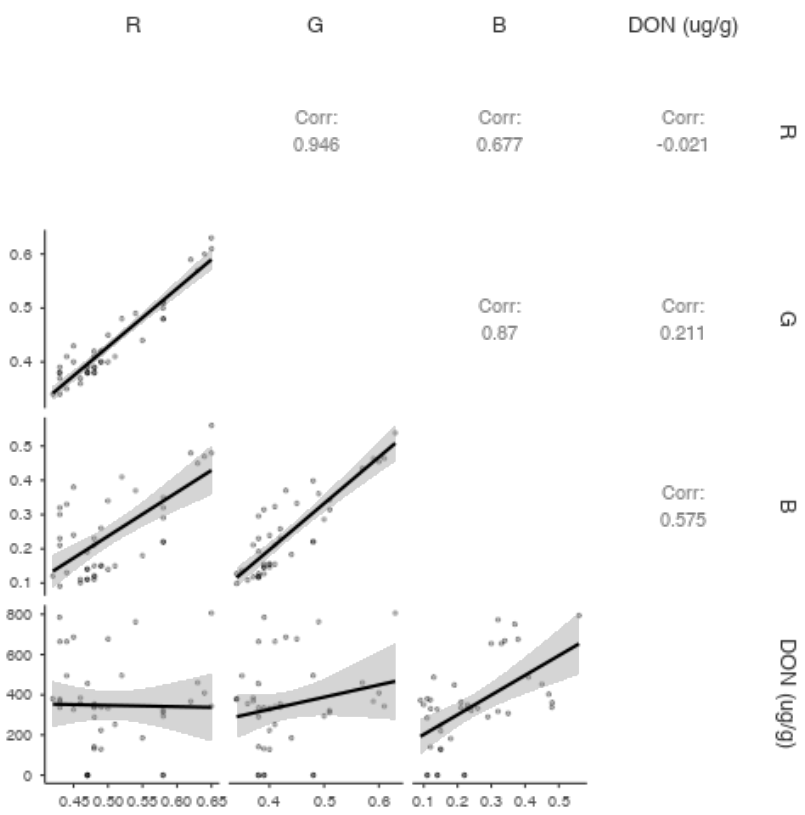
R
G
B
DON (ug/g)
Corr:
0.946
Corr:
0.677
Corr:
-0.021
R
Corr:
0.87
Corr:
0.211
G
Corr:
0.575
B
DON (ug/g)

(a)

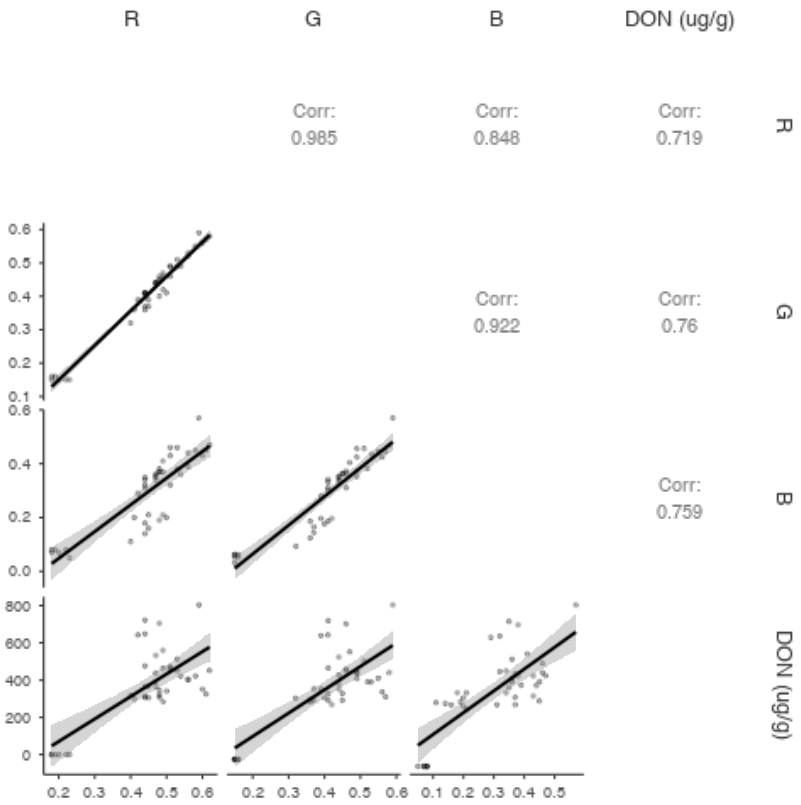
R
G
B
DON (ug/g)
Corr:
0.985
Corr:
0.848
Corr:
0.719
R
Corr:
0.922
Corr:
0.76
G
Corr:
0.759
B
DON (ug/g)

(b)

Figure 49a shows Person's correlations between RGB components and DON measured in the samples of oats and rice at 15 °C. In the case of oats, all correlations were significant with $p < 0.001$ between the colors but only blue presenting such level of significance with DON. Furthermore, only the latter exhibited a Pearson's correlation higher than 0.5. These observations suggest that at 15 °C the colors are highly correlated with only blue showing potential to be used as a predictor of DON contamination at 15 °C in oats ($r = 575$), and being directly proportional to DON concentration. However, when the mold was grown in YEA at 15 °C, a fitting analysis showed high coefficient of determination (R^2), none below 0.8, between all colors and DON concentration, with the relationship between the amount of toxin showing quadratic relationships with all the colors. This might have been because the colors are much more visible, as the mold grows on the surface of YEA.

Unlike in oats, all correlations in the from the rice samples at 15 °C between the RGB channels and between them and DON concentration were significant for $p < 0.001$, all of them showing direct proportionality and no Pearson's

coefficient was below 0.7 (

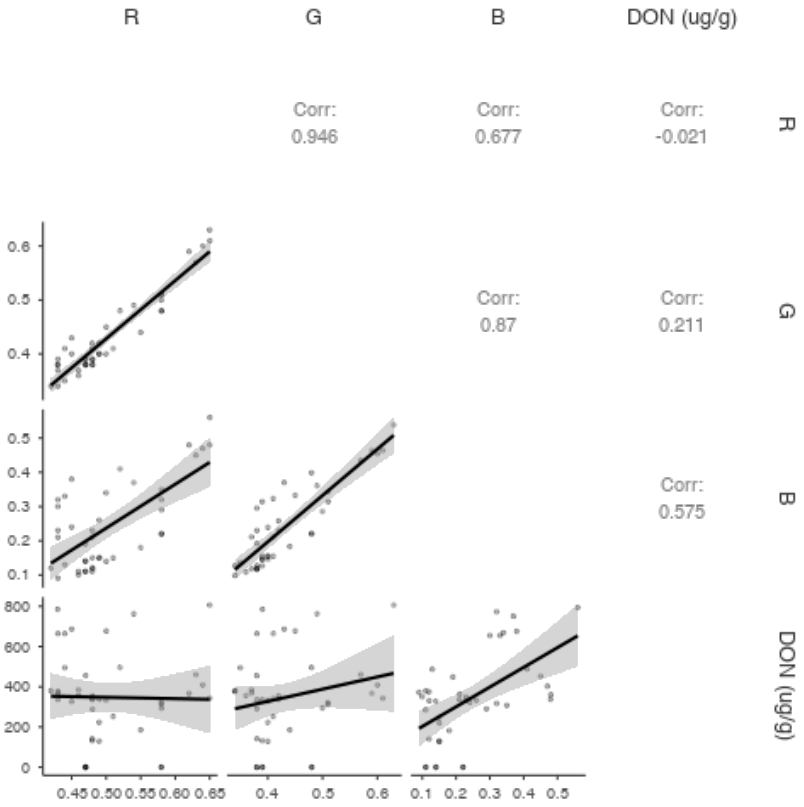

(a)

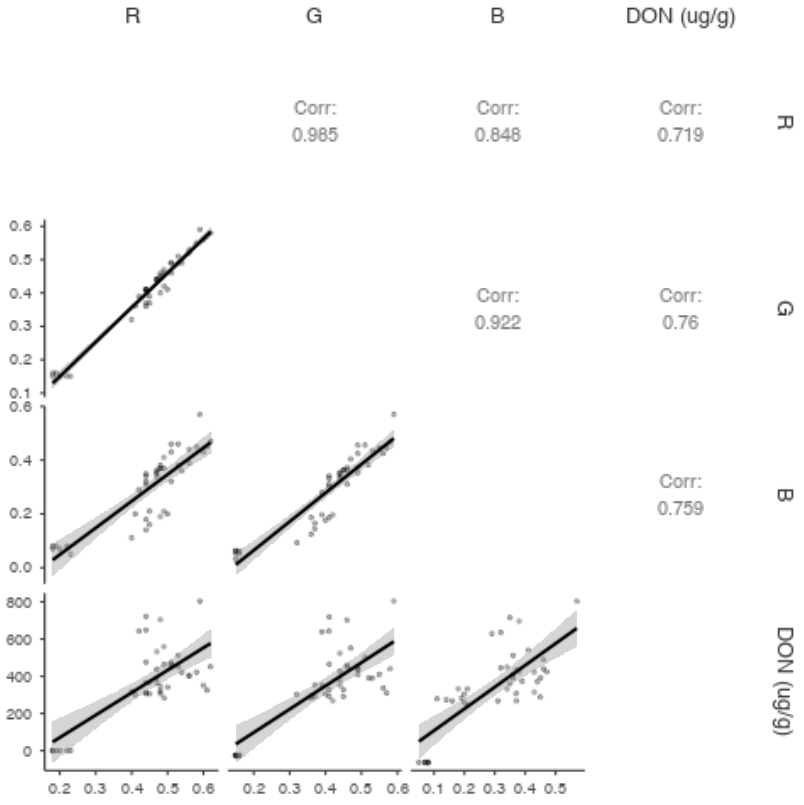

(b)

Figure 49b). The strongest correlation with DON was with the green (r = 0.76) and blue (r = 0.759) components, with almost the same value. The difference between what happened in oats and rice might have been due to the fact that *F. graminearum* was able to mature and produce spores earlier in the rice samples, exhibiting earlier the paleness of the mycelium and also the spores' more vivid colors, and for this reason it was easier to obtain more information about the color variation and relate it to DON production.

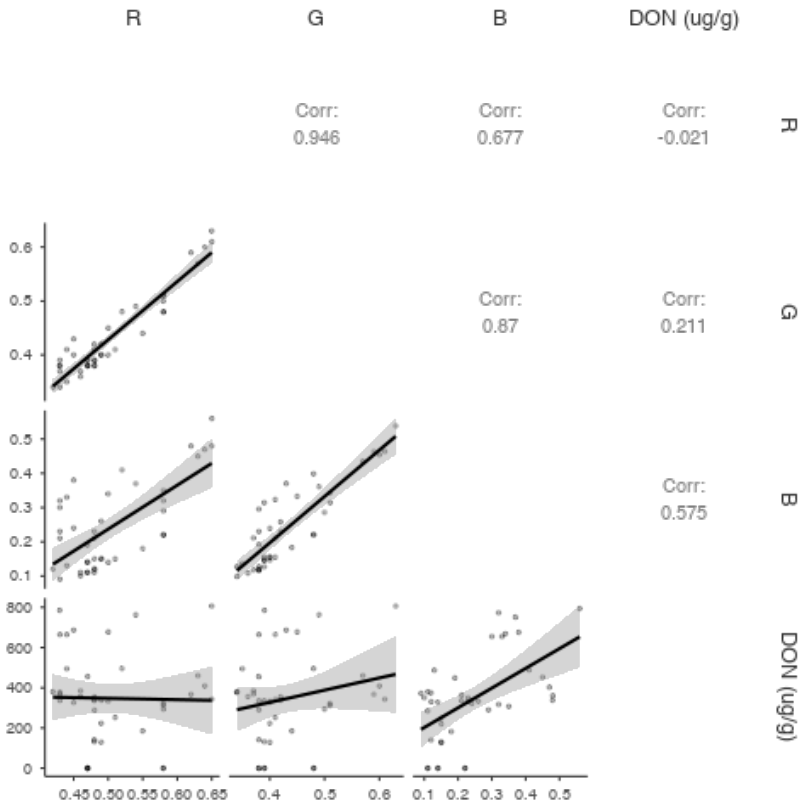

(a)

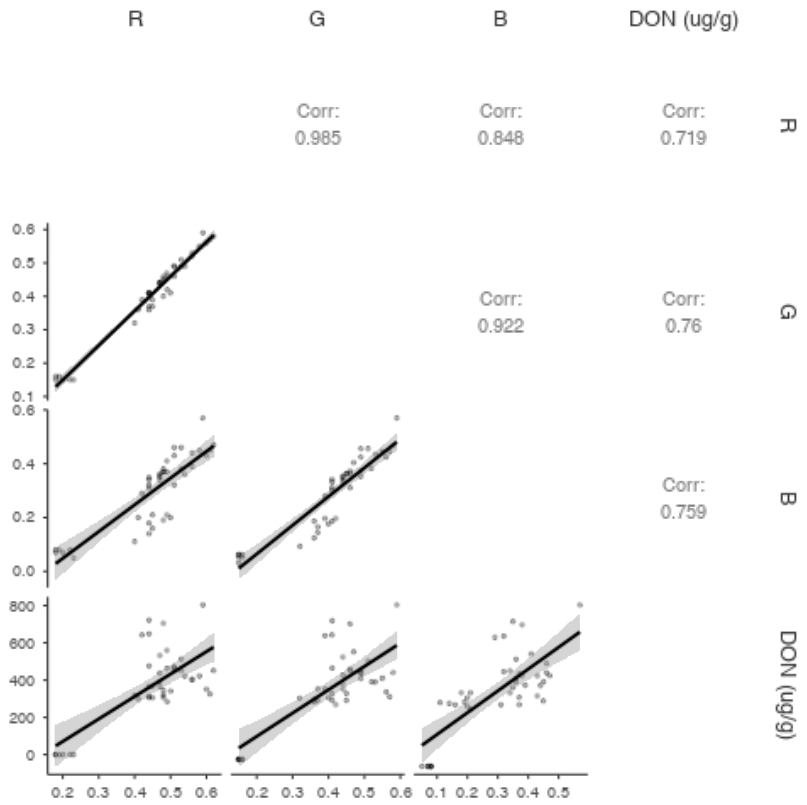

(b)

Figure 49. Correlations between RGB components and DON concentration in infected (a) oats and (b) rice at 15 °C.

D. At 20 °C

In general, there were very few significant RGB differences between the samples incubated at different a_w, at 20 °C. According to an ANCOVA test, only the red component in oats presented significant differences ($p < 0.005$), for only the samples incubated at $a_w = 0.94$, with respect to the others. There were no cases of significant differences in rice.

Color and DON measurements in oats, however, showed considerable fluctuations with the confidence intervals being quite high in some cases (Figure 50a-c).

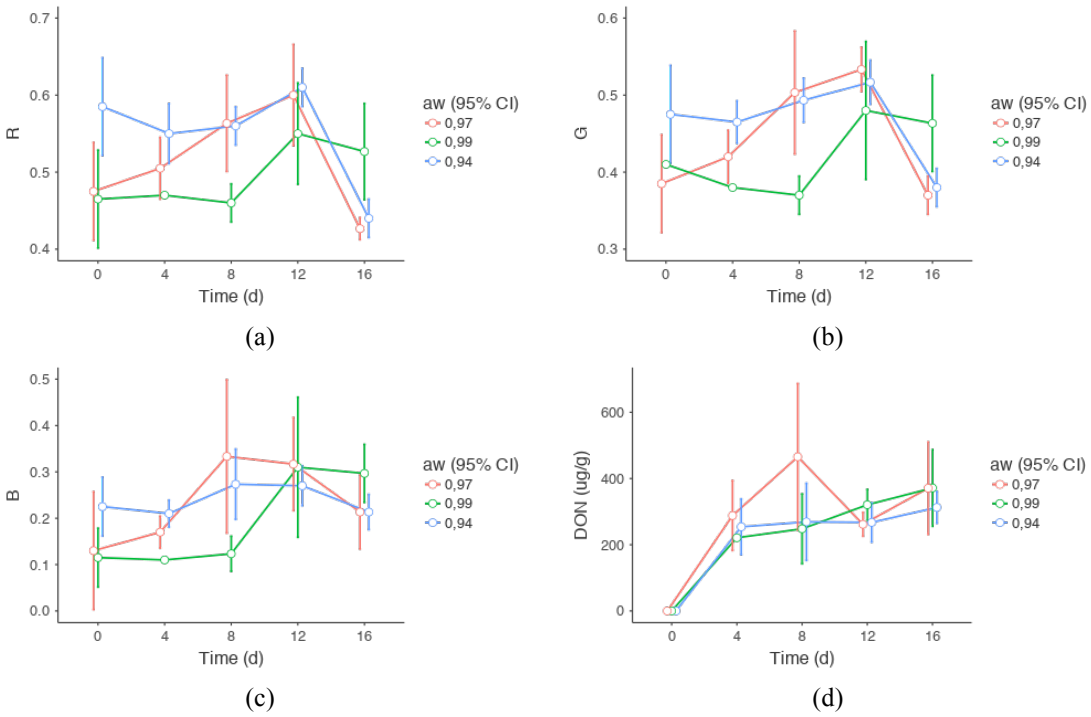

Figure 50. Variation of the (a) red, (b) green and (c) blue color components and (d) DON concentration in oats infected with *F. graminearum* at 20 °C during 16 days considering a_w.

RGB graphs loosely resemble the ones from oats in the previous subsection but there are considerable variations between the different a_w, especially in samples incubated at $a_w = 0.97$ on the 8th day.

It is difficult to explain why the samples at $a_w = 0.97$ exhibited rapid color change in the beginning while the others did not present such level of variation until the 8th day, although there is a rationale to explain this based theory and observation from other specimens rather than from evidence obtained here alone. It might be that the mold was in a very critical, almost optimal condition, which led the organism to change its survival strategy as it was growing. The a_w was intermediate between 0.94 (the lowest for growth) and 0.99 (optimal), as also the temperature, which was suboptimal but not very different from the optimal (20 °C). Thus, in the beginning of the experiment, it was in a condition similar to the one observed at 0.99 (the colors are initially very similar) and it would follow the same strategy, growing slowly until

the 8th day. However, the stress, due to the relatively low quantity of water and the barrier of the grains' husk, forced the fungus to act similarly to the specimens growing at a_w = 0.94. It may be noted that from day 8 it behaved similar to the fungi at the lowest a_w. The specimens at a_w = 0.94 and 0.99 behaved mostly like the ones at 15 °C and it confirms the existence of a pattern in which the *F. graminearum*, when in oats, does not change considerably the color of the medium until the 8th day of incubation.

DON concentration also increased (Figure 50d), but there was high fluctuation, particularly for the samples incubated at a_w = 0.97 on the 8th day. The high instability at this level of humidity might indeed be an indication that the fungus was at a critical condition, trying to select between survival strategies for the suitable microenvironments.

On the other hand, the colors and DON concentration in rice (Figure 51), changed almost exactly the same way and exhibited a pattern very similar to the one observed at 15 °C, with fewer discrepancies, as seen in the ANCOVA tests ($p > 0.05$). Red and green seemed to be the most consistent components across a_w with blue also showing consistent trends.

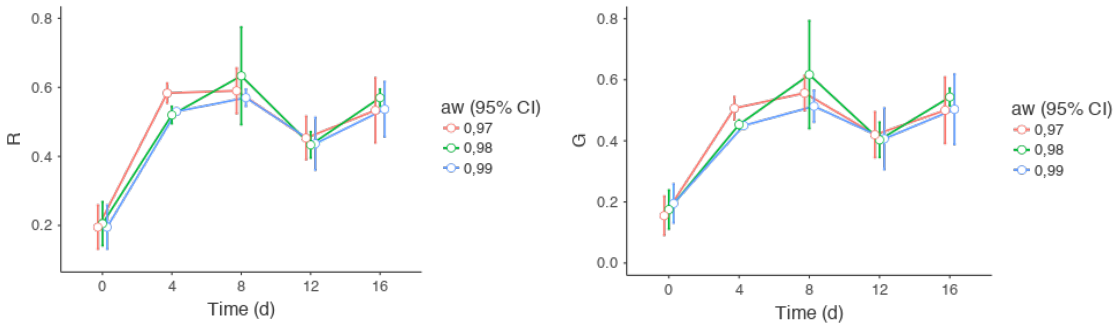

(a) (b)

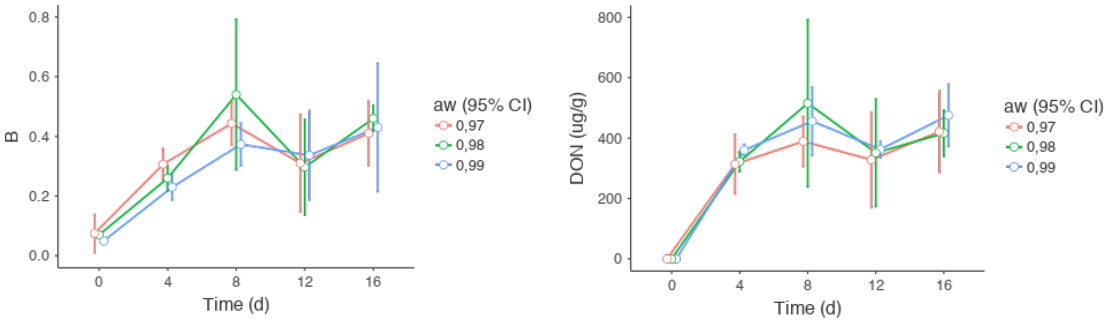

(c) (d)

Figure 51. Variation of the (a) red, (b) green and (c) blue color components and (d) DON concentration in rice infected with *F. graminearum* at 20 °C during 16 days as a function of a_w.

At 20 °C, correlations between the colors and DON concentration seemed to increase when compared to the ones at 15 °C, in general (

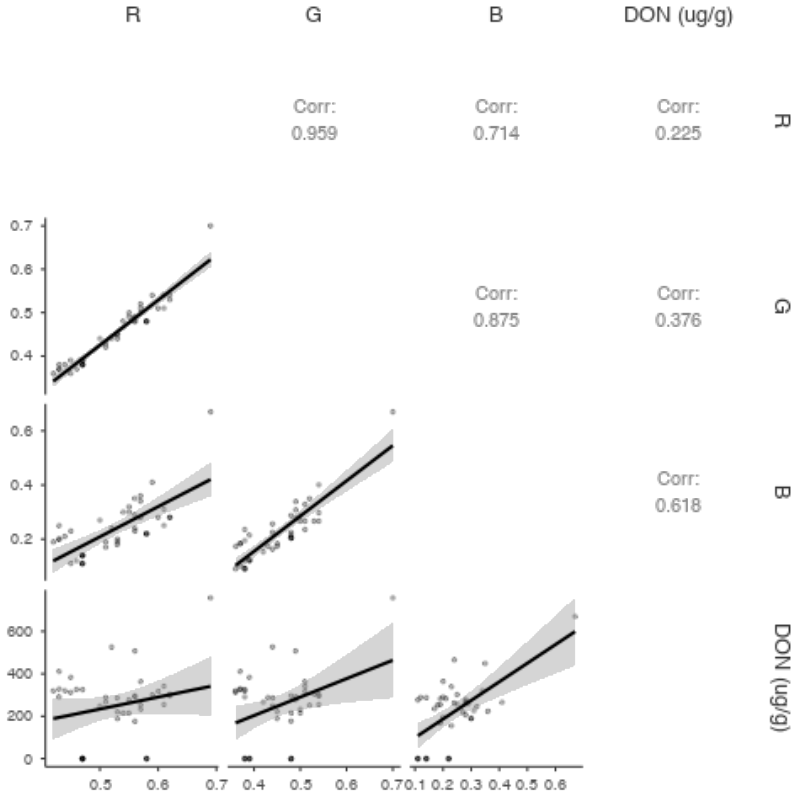

(a)

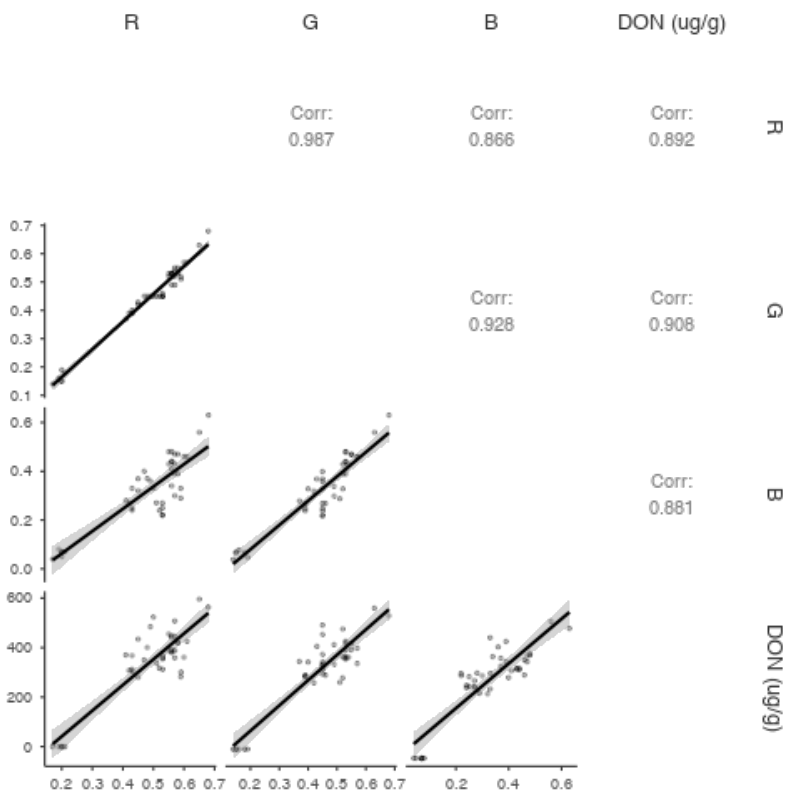

(b)

Figure 52). This might be due to 20 °C being more suitable for normal metabolic activity compared to the previous temperature [8, 35, 195]. In oats, all RGB components were highly correlated, with only blue showing a significant Pearson's correlation with DON concentration at $p < 0.001$. However, at this temperature, green was also correlated with DON at $p < 0.05$. Thus, green can be used to fairly predict DON concentration when *F. graminearum* is incubated in oats at 20 °C, although its Pearson's correlation with DON concentration seems weak ($r = 0.376$).

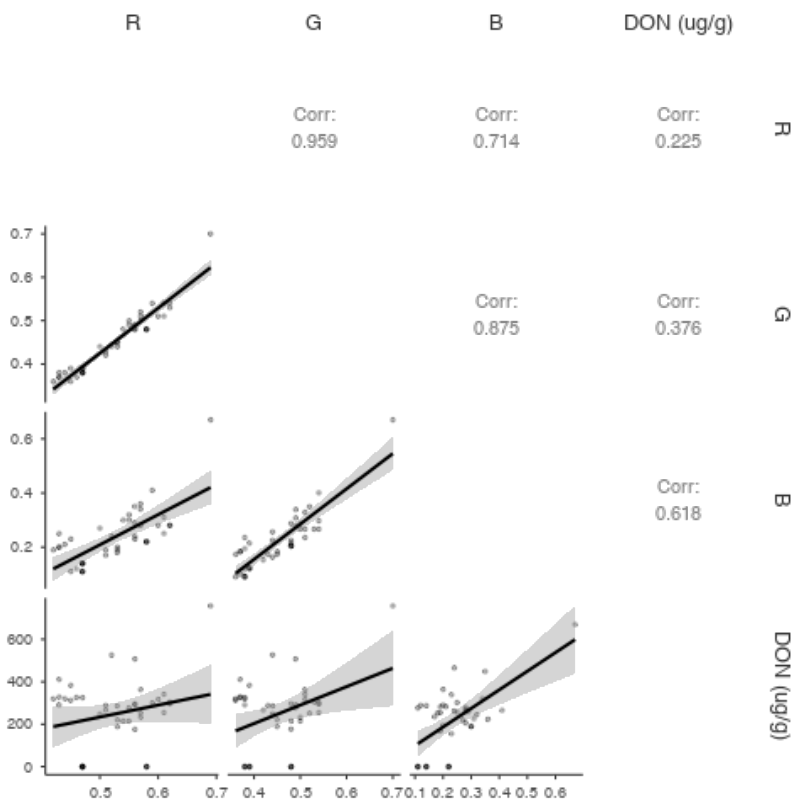

(a)

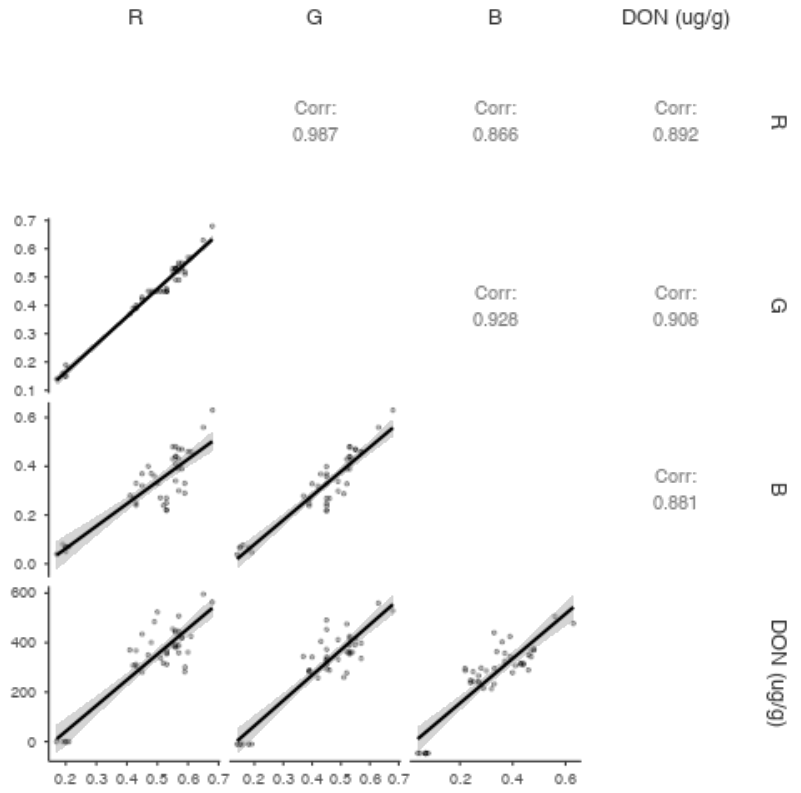

(b)

Figure 52. Correlations between RGB components and DON concentration in infected (a) oats and (b) rice at 20 °C.

In the case of rice, the correlations were all significant at $p < 0.001$ between the RGB components and also between them and the DON level. The correlation between green and DON concentration presented the highest Pearson's coefficient ($r = 0.908$) but again, no color had a coefficient lower than 0.8. Thus, any RGB component seems fit to predict DON quantity in infected rice, given the conditions analyzed.

E. At 25 °C

The ANCOVA test showed significant RGB differences between the samples incubated at distinct a_w in measurements of red ($p = 0.035$) and green ($p = 0.049$) intensities in oat samples at 25 °C (Figure 53a-c).

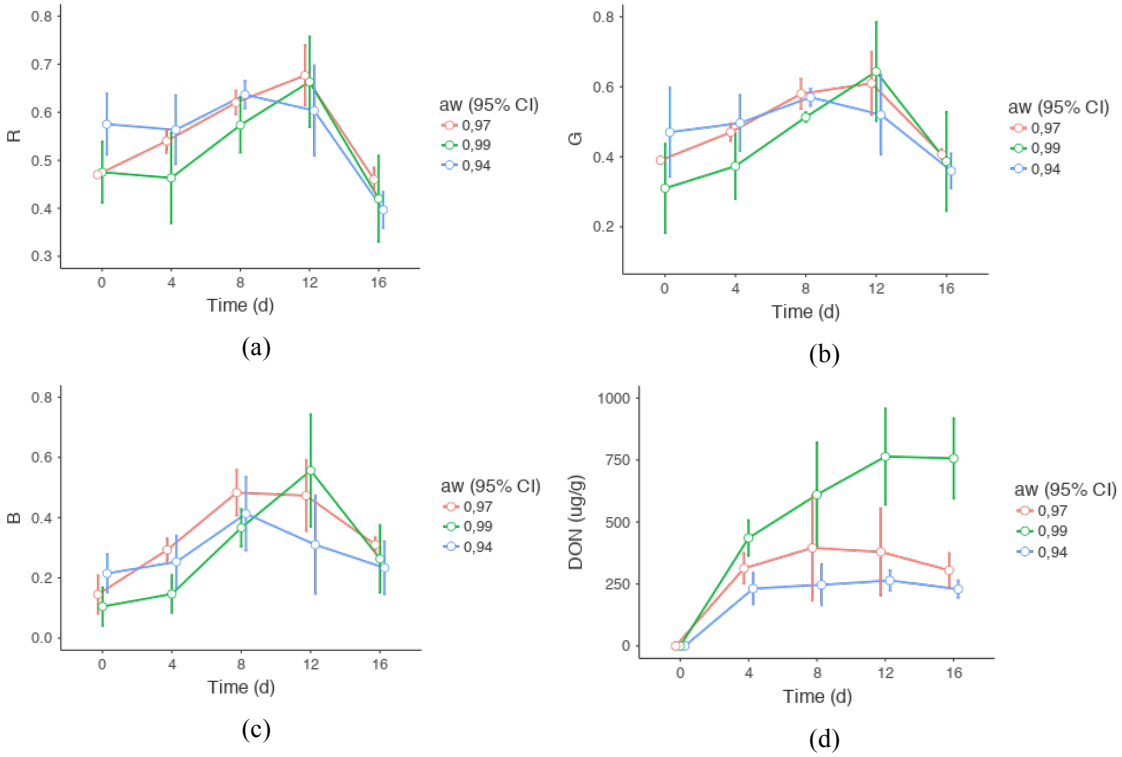

Figure 53. Variation of the (a) red, (b) green and (c) blue color components and (d) DON concentration in oats infected with *F. graminearum* at 25 °C during 16 days considering a_w.

Tukey's post-hoc comparisons showed that the differences in red were between the samples incubated at $a_w = 0.94$ and 0.99, and the differences in blue were

between the samples incubated at a_w = 0.94 and 0.97. Yet, the graphs displayed the same trends as observed in the previous temperatures, indicating that the molds manifested the same color variations over time, with a fairly constant or slightly increasing slope between the first 4 to 8 days, but showing, a peak on day 12 in most cases. Once again, this increase in all color intensities seems related to the augmentation in paleness with mycelial growth and the end spots of pigmentation masking part of the pale layer, thus decreasing the overall color intensity.

Figure 53d, shows significant differences ($p_{ANCOVA} < 0.001$) in DON concentration between specimens grown at different a_w. As the figure illustrates, a_w was directly proportional to DON level, which is a frequent occurrence [195]. The concentrations seem to decline towards the end of the experiment, but this might be due to experimental errors or occasional fluctuations between the samples.

In the case of rice, all colors were significantly different ($p < 0.05$) for samples incubated at distinct a_w, according to an ANCOVA test. Post-hoc Tukey's comparisons show that the significant differences are between the samples incubated at a_w = 0.97 and the others ($p < 0.05$). Visual analysis of the photos suggests that the samples at a_w = 0.97 present higher hyphal density, but with the higher a_w conditions a higher level of pigmentation is displayed. Thus a slightly darker pigmentation is observed, particularly at the end of the experiment. Yet, all graphs (Figure 54a-c) showed mostly the same trend for all the settings, also similar to the shapes observed showed mostly the same trend for all the conditions, similar to the shapes observed when examining other temperatures, except at a_w = 0.99 on day 12, which shows a peak.

The charts, as well as the trends of DON variation (Figure 54d), were as expected. DON measurement of samples at a_w = 0.97 showed the average value

declining from day 12 to 16, which was likely to be a fluctuation resulting from human errors during the preparation of the sample or DON extraction, as already mentioned.

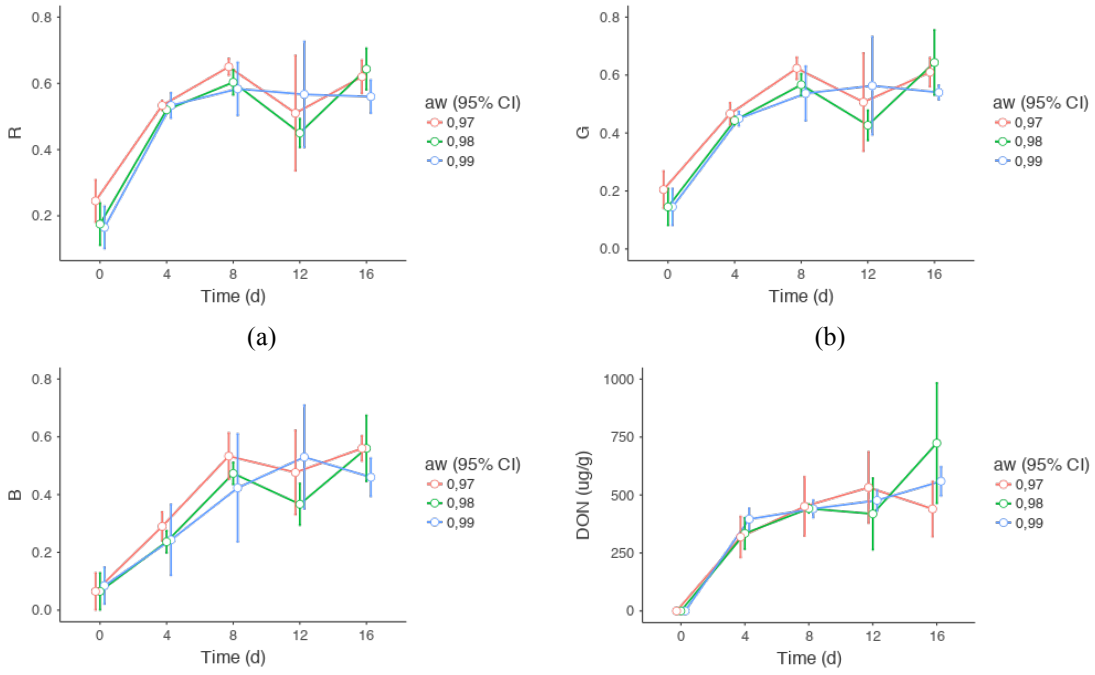

Figure 54. Variation of the (a) red, (b) green and (c) blue color components and (d) DON concentration in rice infected with *F. graminearum* at 25 °C during 16 days as a function of a_w.

Once again, most Pearson's correlations between the RGB components and between them and DON concentration increase with increase in temperature from 20 °C to 25 °C (Figure 55). By now, it seems acceptable to postulate that the correlations are likely to increase as the temperature increases towards the one optimal for growth. If this is true, then the correlations are expected to decrease if the temperature rises beyond 25 °C. It would also be prudent do develop future experiments to analyze more temperatures within or beyond the range considered for this study.

Regarding the Figure 55a, the correlations not only increased but the correlation of blue and DON concentration retained the magnitude of its significance ($p < 0.001$).

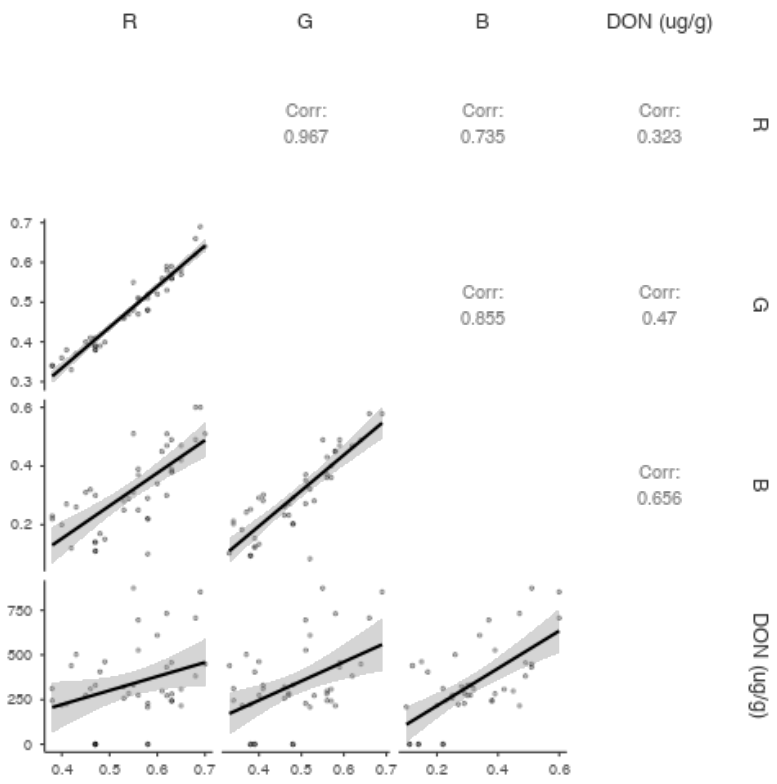

(a)

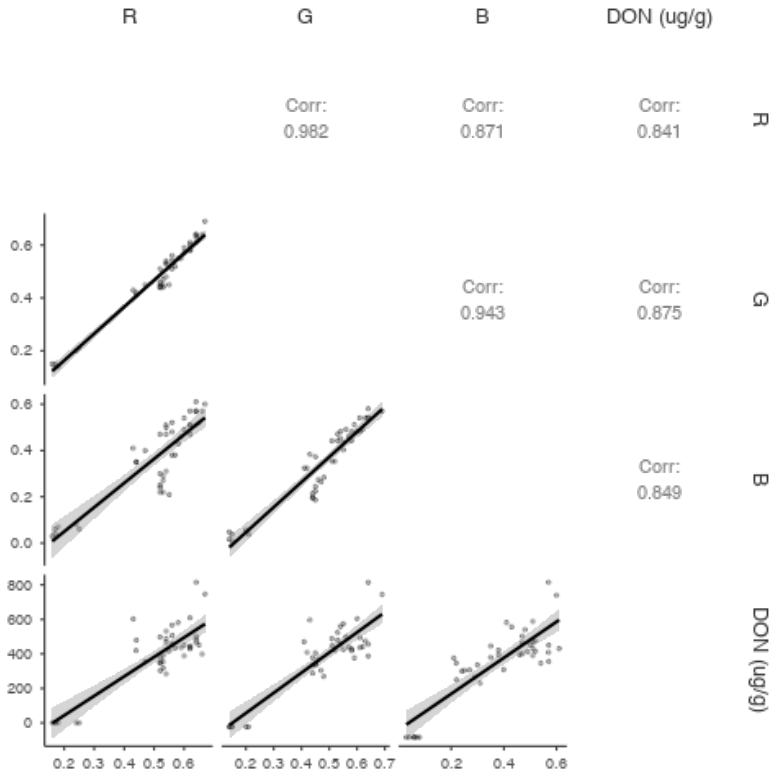

(b)

Figure 55. Correlations between RGB components and DON concentration in infected (a) oats and (b) rice at 25 °C.

The correlations of green and red with DON level increased their significances to $p < 0.01$ and $p < 0.05$, respectively.

It is perhaps possible to improve this model by measuring the RGB and toxin variations daily. In case of rice (figure 13b), all correlations were above 0.8 and highly significant ($p < 0.001$). This information suggests that it is possible to predict DON concentration with acceptable accuracy in rice infected with *F. graminearum* at 25 °C, at least under the a_w conditions tested in the current experiment.

F. At 30 °C

The samples incubated at 30 °C presented several similarities with the ones at 20 °C and 25 °C, though there are remarkable fluctuations (figure 14a-c).

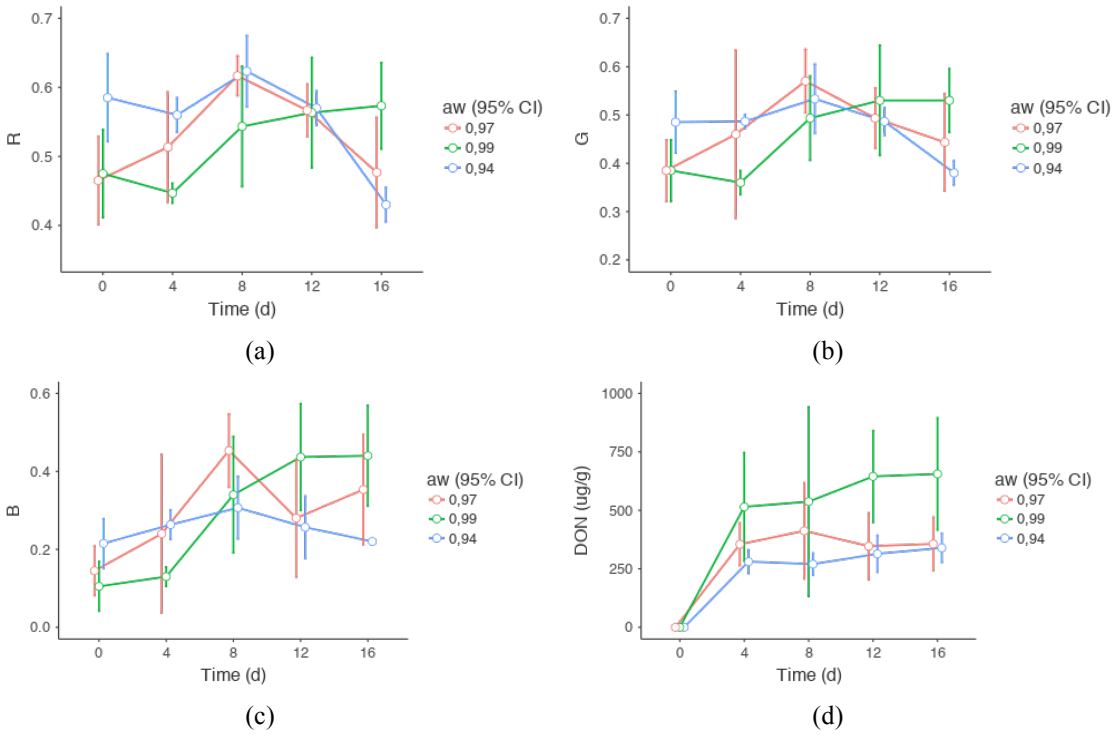

Figure 56. Variation of the (a) red, (b) green and (c) blue color components and (d) DON concentration in oats infected with *F. graminearum* at 30 °C during 16 days considering a_w.

The only significant RGB differences were in the red channel ($p = 0.006$) and Tukey's comparisons identified the only significant RGB difference ($p = 0.049$) between the samples incubated at 0.94 and 0.99. The trends, however, show

considerable fluctuations. The concentration of DON also presented some fluctuations but it did not change significantly for each a_w condition from day 4 until the end of the experiment. According to an ANCOVA test, the differences in DON considering the distinct a_w ($p < 0.001$) and humidity was directly proportional to the quantity of toxin. This difference was consistent with the information available in literature [35, 195].

All RGB and color measurements between the rice samples incubated at 30 °C presented significant differences between the samples with different a_w ($p_{ANCOVA} < 0.05$), and the following Tukey's comparisons demonstrated that the major differences were between the samples at $a_w = 0.97$ and the remaining conditions. However, it was difficult to notice such differences by observing the RGB graphs in the Figure 57a-c.

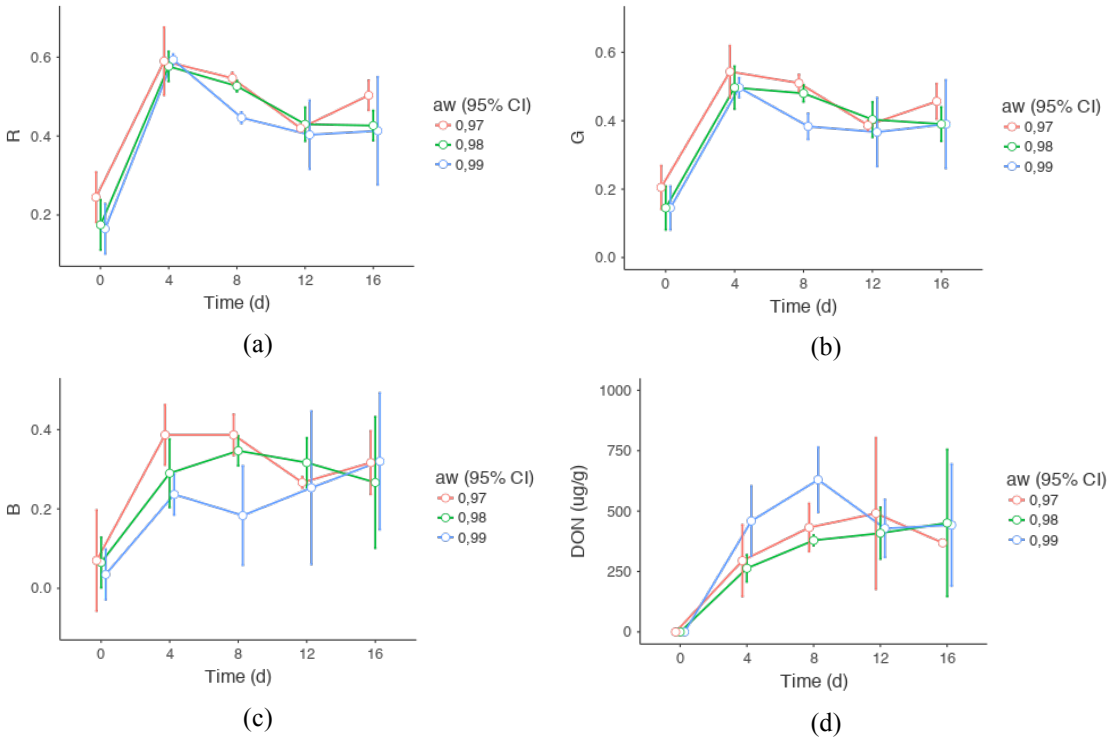

Figure 57. Variation of the (a) red, (b) green and (c) blue color components and (d) DON concentration in rice infected with *F. graminearum* at 30 °C during 16 days as a function of a_w.

It was even harder to observe in cases of red and green because these colors did not only show very similar trends, but also showed patterns of variation very similar to the ones already seen at all other temperatures. Even the Figure 57c arguably exhibited the same pattern.

The repetition of RGB color patterns across all temperatures and a_w analyzed is another confirmation of the predictable color variation in *F. graminearum* which was recently demonstrated [26, 202], stressing the fact that it not only occurs in YEA but also in cereals.

The correlation profile (

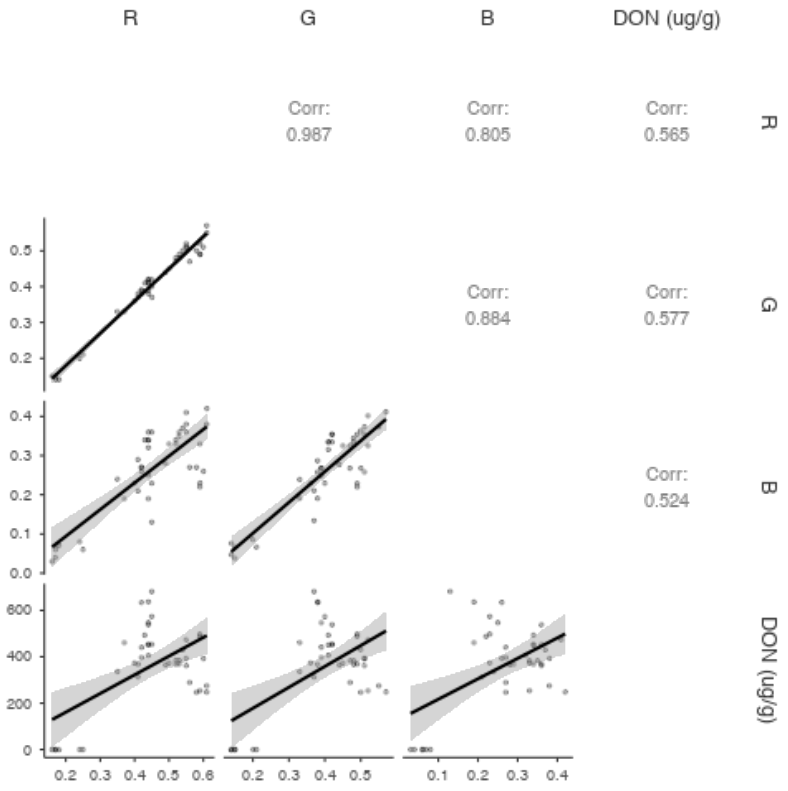

(a)

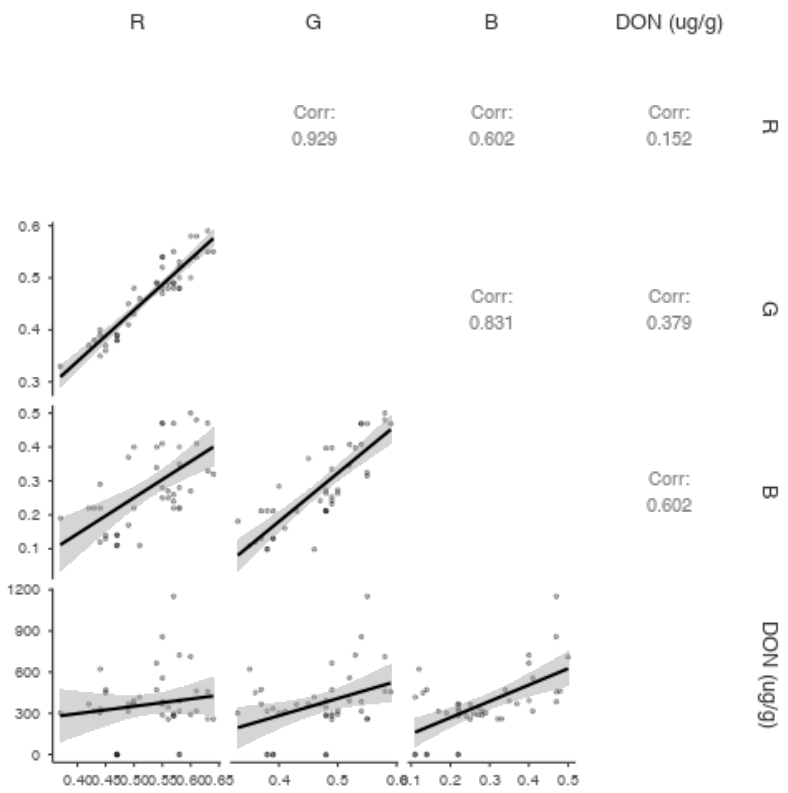

(b)

Figure 58) between RGB and DON concentration was very similar to the one at 20 °C. For instance, in the case of oats, blue was the RGB component with the highest (r = 645) and most significant (p < 0.001) correlation with DON concentration, and it was followed by the green component (r = 365; p < 0.05).

Rice samples presented highly significant correlations (p < 0.001) and acceptable Pearson's coefficients (r > 0.5) although lower that the ones determined for samples grown at 25 °C. This is strong evidence that correlations between average RGB components from photos of grains infected with *F. graminearum* increase as the temperature reaches 25 °C, regardless of the cereal. This is relevant because temperature also favors propagation of the microorganism [35, 195], thereby posing the highest risk of FHB outbreak and possible DON contamination.

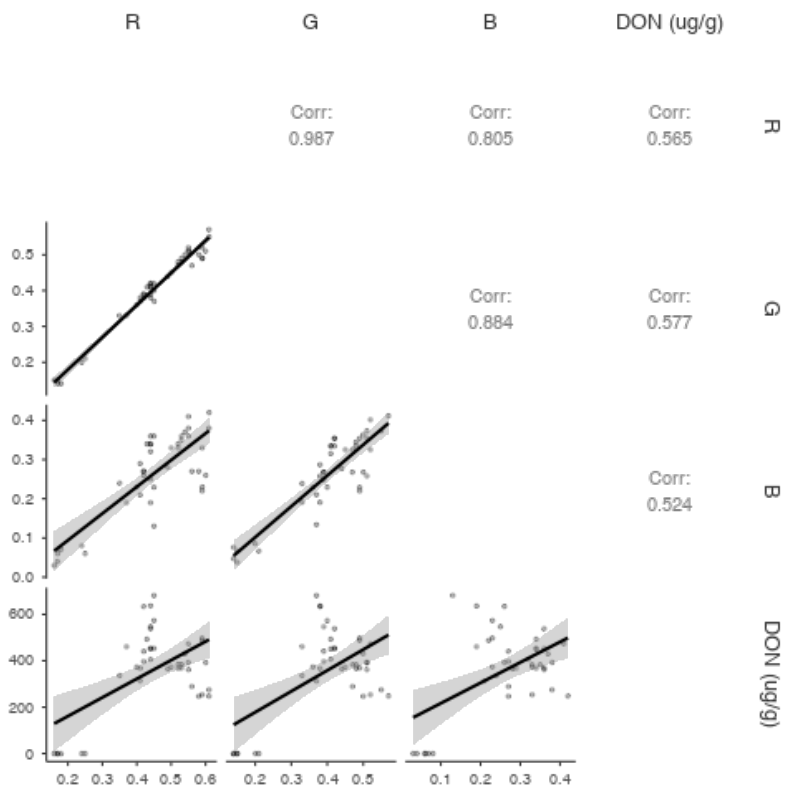

(a)

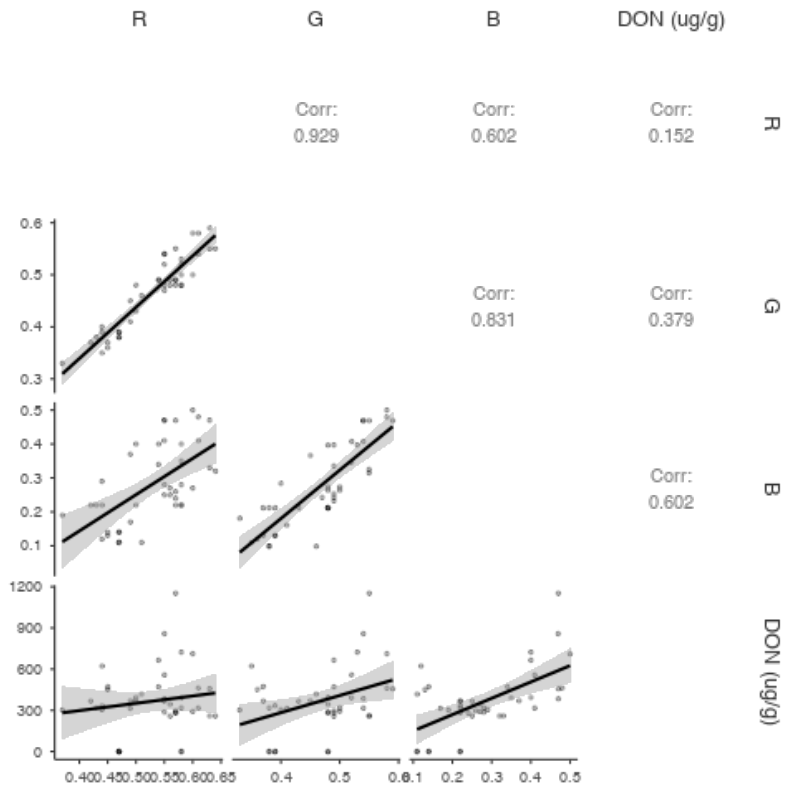

(b)

Figure 58. Correlations between RGB components and DON concentration in infected (a) oats and (b) rice at 30 °C.

4.2.4 Conclusion

The current experiment demonstrates that a combination of temperature and a_w affects RGB components of *F. graminearum* and DON levels in infected oats and rice, especially the latter. As optimal conditions are approached (25 °C and $a_w = 0.99$) the mold tends to increase the intensity of all colors (due to mycelial growth) up to a point in time between the 8th and 12th day, and then reduce, sometimes only subtly (as sporulation starts). In the case of rice, the process happens more quickly and it tends to rise again after the reduction in intensity perhaps because the density of the mycelium keeps increasing, covering the entire Petri dish. Optimal conditions also promote increased production of DON, possibly because of increased biomass. Most importantly, as the temperature approaches 25 °C, the correlation between RGB components and DON becomes stronger and increases in significance. In oats, blue was the only RGB component consistently presenting highly significant correlation with DON ($p < 0.001$) and acceptable Pearson's coefficient, within the range of 25 ± 10 °C. In rice, all correlations were highly significant ($p < 0.001$) and presented Pearson's coefficient sufficiently high to assume that RGB components can be used as predictor of levels of DON contamination. In general, colors were shown to be effective predictors of DON concentration in grains but in oats it would be better to increase the number of measurements (e.g. by performing daily measurements) to improve the models.

Chapter 5 Synthesis

5.1 Revisiting the hypotheses

As the current thesis is based on the premise that color intensity has the potential to function as alternative to size measurements, two outcomes (alternative hypotheses) not yet observed were proposed to come as evidence from the current experiment:

- First, size-based measurements are known to be predictable as the mold grows [28] and for this reason they are used in mold growth models. If colors are to be used for the same purpose, they have to be predictable as the mold grows. If this is true, we should expect that periodic digital photos of *F. graminearum* throughout its lifecycle would present predictable variation of RGB channels;
- Second, DON accumulates as the fungus grows and its variation can be predicted given the conditions (temperature and a_w) [195]. If the first alternative hypothesis is verified and both RGB channels and DON concentration present predictable patterns throughout the mold's lifecycle, they present some correlation.

The experiments presented in the sections 3.3 and 4.1 and virtually all others demonstrated the veracity of the first alternative hypotheses. The first (section 3.3) demonstrated that in agar, different replicates grown under the same conditions present exactly the same pattern of color change during three weeks in yeast extract agar (YEA). This experiment was consubstantiated by further experiments under different temperatures and a_w (sections 3.4 and 3.4, respectively). Moreover, the sections 4.1 and 4.2 also demonstrated the consistency of color variation in oats and

rice infected with *F. graminearum*, even when a_w and temperature vary. Furthermore, all RGB channels presented similar trends and were highly correlated. The verification of the first hypothesis points towards the possibility that color can be an alternative to size in *F. graminearum* growth studies

Regarding the second hypothesis, RGB components were acceptably correlated with DON concentration in most cases, though this hypothesis was somewhat more difficult to verify in relation to the first due to technical issues. For instance, *F. graminearum* produced high quantity of mycelia when grown at $a_w < 0.99$ in YEA, "hiding" the spore-borne pigmentation (section 3.4). But this issue was demystified in sections 4.1 and 4.2 (in grains) as there was higher growth surface for the mold and the high mycelial growth seemed to be associated to the mold's choice of survival strategy. Under stress, it favors mycelial growth as an attempt to better explore the local environment, opposed to the propagation through spores when easy survival is assured. The most important to consider is the fact that in the remaining experiments where DON was quantified it was frequently correlated to RGB channels, though some color components more than others and suboptimal growth conditions remarkably reduced such correlations. In summary, despite of the fluctuations, the evidences favor the second alternative hypotheses, meaning that as far as the current experiments were held, RGB measurements of digital photos of *F. graminearum* throughout its lifecycle presented acceptable relationships with the quantity of DON accumulated in the media. Yet, there shall be reservations to this observation, and it would be a good idea to keep searching for evidences in order to support this idea.

5.2 Remarks

The development of viable imaging tools to analyze the growth pattern of *F. graminearum* and production of DON and other relevant metabolites requires mastery of basic principles underlying the mold's ecology, optics and statistics. This seems highly feasible but requires very careful scrutiny. The following intriguing aspects were observed from the current study : (1) colors of *F. graminearum* result from a combination of unpigmented biomass and a considerably small variety of pigments, all produced according to the organism's adaptive strategies, (2) there is a predictable pattern of color variation throughout the mold's lifecycle which is easy to analyze through RGB imaging, (3) *F. graminearum* is highly sensitive to temperature, a_w, nutrients and several other environmental factors, (4) the growth pattern of this mold is basically the same across types of substrates, but the ease of obtaining nutrients affects the mold's growth strategy and the speed at which the organism thickens the mycelium or produces spores.

F. graminearum quickly adapts to different environments. Some authors [5, 11] have provided valuable accounts of the mold's lifecycle and have facilitated comprehension of the phenomena observed in the current experiment. The fungus has two basic growth strategies which can be related to *r* and *k* survival strategies well-described by Taylor*, et al.* [207]. As the organism reaches a substrate, it quickly produces a mycelium and spreads through the medium (*k*-strategy). If the medium is rich in nutrients, the fungus favors the production of spores (*r*-strategy). *K*-strategy results in increase in levels of all RGB components as the mold becomes white. *R*-strategy increases the RGB components if the medium is dark or acidic (the mold producing yellow pigments under low pH), or highly illuminated (light stimulating the production of carotenoids), or decreases RGB if the medium is bright, for instance

if there is high mycelial biomass. Toxin production occurs mainly when the fungus adopts the *r*-strategy, i.e., when there are live colors [11] and this is indeed one of the ways to detect Fusarium head blight. Since the growth stages or strategies are always associated to particular colors, they are predictable.

It is also important to consider the role of temperature and a_w in the dynamics of RGB changes during growth of *F. graminearum* [225]. There are two major profiles determined by either of these environmental factors (with intermediate states): harsh or optimal conditions. When the conditions tend to be optimal (25 °C and a_w = 0.99), the fungus favors rapid growth and production of spores (*r*-strategy). Thus, one can expect a very rapid rise in all RGB values (either from pigmentation or high mycelial biomass) and also DON concentration. RGB imaging is highly reliable in these situations, especially if there are no strong natural barriers for colonization such as husk. It explains why there were high correlations between colors and DON concentration in rice sample containing peeled grains and in agar, but not as much in oats. Under harsh conditions, the fungus is as rapid at colonizing, but it does not thicken the mycelium as much (possibly to save energy), and it might even be hardly noticeable in grains. In these cases, imaging analysis might not help much, but the chances for the grains to be contaminated are also rare. Thus, RGB analysis seems to be a low cost and rapid approach when the conditions seem unfavorable.

5.3 Conclusion

After careful examination of pros and cons regarding the use of color alternative to size-based growth measurements of *F. graminearum* and prediction of DON production at a particular time, RGB imaging seems to bear potential to perform the task under several circumstances. Colors of *F. graminearum* are very predictable because they are derived from considerably few sources, with aurofusarin and the

white mycelium being the most influential among them. Their properties and how most important environmental factors affect them seem to be sufficiently well known to allow the development of reliable RGB imaging approaches. Favorable temperature, a_w and availability of nutrients stimulate high density of biomass and production of pigmented spores and perithecia. It was possible to design an RGB imaging based growth model including four stages consisting of a mycelial and a sporular stage, both initiated by two lag stages. The speed at which each stage starts appears to be a function of the type of nutrient. The intensity is likely to respond to how optimal or harsh the temperature and a_w conditions are for growth.

5.4 Recommendations

RGB based methods have high potential, which are beyond the scope of this particular study. Future researchers must consider the expansion of this idea to other strains of *F. graminearum* or even other species or genera, for the analysis of other toxins, metabolites, plant diseases, growth media, and temperature and a_w ranges. Furthermore, several other factors such as pH, oxygen, carbon dioxide [16] or fungicides (organic or synthetic) [3] can be included in future experiments. Color-based models can be further explored and possibly be incorporated with sorters to separate grains with high likelihood of having mycotoxins.

Other technical features of the experiment can also be improved. For instance, a very good light isolating chamber could replace the bucket used to better control the possible interference. Even the illumination itself could be further optimized. The experiment could be reproduced using simpler everyday cameras, such as smartphones so that the farmer or common citizen are able to monitor *Fusarium* infection or DON contamination at home.

Good agricultural practices are very important. According to French investigators such as Leplat*, et al.* [5] and Jaillais*, et al.* [6], the reemergence of FHB is mostly due to anthropogenic factors such as crop rotation between cereals, reduce tillage or crop management. Langseth and Stabbetorp [24] added lodging and time of harvest. *F. graminearum* is highly resistant and sometimes grains can look safe but the mold is there. For instance, there were cases when grains with low water activity did not show any growth until the 8^{th} day of incubation and were contaminated. Therefore, it is better to maintain the grain at suboptimal conditions to avoid moldiness. If the grains are heavily infected or exhibit pink or yellow colors at the surface, it is better to avoid them.

Bibliography

[1] F. A. Saccon, D. Parcey, J. Paliwal, and S. S. Sherif, "Assessment of *Fusarium* and deoxynivalenol using optical methods," *Food and Bioprocess Technology,* vol. 10, no. 1, pp. 34-50, 2017.

[2] D. Ryu, and L. B. Bullerman, "Effect of cycling temperatures on the production of deoxynivalenol and zearalenone by *Fusarium graminearum* NRRL 5883," *Journal of Food Protection,* vol. 62, no. 12, pp. 1451-1455, 1999.

[3] A. Velluti, V. Sanchis, A. J. Ramos, C. Turon, and S. Marin, "Impact of essential oils on growth rate, zearalenone and deoxynivalenol production by *Fusarium graminearum* under different temperature and water activity conditions in maize grain," *J Appl Microbiol,* vol. 96, no. 4, pp. 716-24, 2004.

[4] E. Fredlund, A. Gidlund, M. Sulyok, T. Borjesson, R. Krska, M. Olsen, and M. Lindblad, "Deoxynivalenol and other selected *Fusarium* toxins in Swedish oats--occurrence and correlation to specific *Fusarium* species," *Int J Food Microbiol,* vol. 167, no. 2, pp. 276-83, Oct 15, 2013.

[5] J. Leplat, H. Friberg, M. Abid, and C. Steinberg, "Survival of *Fusarium graminearum*, the causal agent of *Fusarium* head blight. A review," *Agronomy for sustainable development,* vol. 33, no. 1, pp. 97-111, 2013.

[6] B. Jaillais, P. Roumet, L. Pinson-Gadais, and D. Bertrand, "Detection of *Fusarium* head blight contamination in wheat kernels by multivariate imaging," *Food Control,* vol. 54, pp. 250-258, 2015.

[7] W. Langseth, and O. Elen, "Differences between barley, oats and wheat in the occurrence of deoxynivalenol and other trichothecenes in Norwegian grain," *Journal of phytopathology,* vol. 144, no. 3, pp. 113-118, 1996.

[8] E. M. Cambaza, S. Koseki, and S. Kawamura, "Meta-analytic review on the impact of temperature and water activity in deoxynivalenol synthesis by *Fusarium graminearum*," *Food Research,* vol. 2, no. 5, pp. 443-446, 2018.

[9] V. Dvořáček, A. Prohasková, J. Chrpová, and L. Štočková, "Near infrared spectroscopy for deoxynivalenol content estimation in intact wheat grain," *Plant Soil Environ,* vol. 58, pp. 196-203, 2012.

[10] M. Sabater-Vilar, H. Malekinejad, M. H. Selman, M. A. van der Doelen, and J. Fink-Gremmels, "*In vitro* assessment of adsorbents aiming to prevent deoxynivalenol and zearalenone mycotoxicoses," *Mycopathologia,* vol. 163, no. 2, pp. 81-90, Feb, 2007.

[11] R. S. Goswami, and H. C. Kistler, "Heading for disaster: *Fusarium graminearum* on cereal crops," *Molecular plant pathology,* vol. 5, no. 6, pp. 515-525, 2004.

[12] M. Shahin, D. Hatcher, and S. Symons, "Development of multispectral imaging systems for quality evaluation of cereal grains and grain products," *Computer vision technology in the food and beverage industries*, pp. 451-482: Elsevier, 2012.

[13] M. Wiwart, I. Koczowska, and A. Borusiewicz, "Estimation of *Fusarium* head blight of triticale using digital image analysis of grain." pp. 563-569.

[14] S. Cavret, N. Laurent, B. Videmann, M. Mazallon, and S. Lecoeur, "Assessment of deoxynivalenol (DON) adsorbents and characterisation of

their efficacy using complementary *in vitro* tests," *Food Addit Contam Part A Chem Anal Control Expo Risk Assess,* vol. 27, no. 1, pp. 43-53, Jan, 2010.

[15] M. L. Martins, and H. M. Martins, "Influence of water activity, temperature and incubation time on the simultaneous production of deoxynivalenol and zearalenone in corn (*Zea mays*) by *Fusarium graminearum*," *Food Chemistry,* vol. 79, no. 3, pp. 315-318, Nov, 2002.

[16] R. Greenhalgh, G. A. Neish, and J. D. Miller, "Deoxynivalenol, acetyl deoxynivalenol, and zearalenone formation by Canadian isolates of *Fusarium graminearum* on solid substrates," *Appl Environ Microbiol,* vol. 46, no. 3, pp. 625-9, Sep, 1983.

[17] J. He, R. Yang, T. Zhou, R. Tsao, J. C. Young, H. Zhu, X. Z. Li, and G. J. Boland, "Purification of deoxynivalenol from *Fusarium graminearum* rice culture and mouldy corn by high-speed counter-current chromatography," *J Chromatogr A,* vol. 1151, no. 1-2, pp. 187-92, Jun 1, 2007.

[18] N. Morooka, N. Uratsuji, T. Yoshisawa, and H. Yamamoto, "Studies on the toxic substances in barley infected with *Fusarium* spp," *Food Hygiene and Safety Science (Shokuhin Eiseigaku Zasshi),* vol. 13, no. 5, pp. 368-375, 1972.

[19] K.-H. Dammer, B. Möller, B. Rodemann, and D. Heppner, "Detection of head blight (*Fusarium* ssp.) in winter wheat by color and multispectral image analyses," *Crop Protection,* vol. 30, no. 4, pp. 420-428, 2011.

[20] D. Ryu, and L. B. Bullerman, "Effect of cycling temperatures on the production of deoxynivalenol and zearalenone by Fusarium graminearum NRRL 5883," *J Food Prot,* vol. 62, no. 12, pp. 1451-5, Dec, 1999.

[21] M. I. Almeida, N. G. Almeida, K. L. Carvalho, G. A. Goncalves, C. N. Silva, E. A. Santos, J. C. Garcia, and E. A. Vargas, "Co-occurrence of aflatoxins

B(1), B(2), G(1) and G(2), ochratoxin A, zearalenone, deoxynivalenol, and citreoviridin in rice in Brazil," *Food Addit Contam Part A Chem Anal Control Expo Risk Assess,* vol. 29, no. 4, pp. 694-703, 2012.

[22] B. Bergsjo, W. Langseth, I. Nafstad, J. H. Jansen, and H. J. Larsen, "The effects of naturally deoxynivalenol-contaminated oats on the clinical condition, blood parameters, performance and carcass composition of growing pigs," *Vet Res Commun,* vol. 17, no. 4, pp. 283-94, 1993.

[23] T. Yoshizawa, "Thirty-five Years of Research on Deoxynivalenol, a Trichothecene Mycotoxin: with Special Reference to Its Discovery and Co-occurrence with Nivalenol in Japan," *Food Safety,* vol. 1, no. 1, pp. 2013002-2013002, 2013.

[24] W. Langseth, and H. Stabbetorp, "The effect of lodging and time of harvest on deoxynivalenol contamination in barley and oats," *Journal of Phytopathology,* vol. 144, no. 5, pp. 241-245, 1996.

[25] O. Jirsa, and I. Polišenská, "Identification of *Fusarium* damaged wheat kernels using image analysis," *Acta Universitatis Agriculturae Et Silviculturae Mendelianae Brunensis,* vol. 59, no. 5, pp. 125-130, 2014.

[26] E. Cambaza, S. Koseki, and S. Kawamura, "The Use of Colors as an Alternative to Size in Fusarium graminearum Growth Studies," *Foods,* vol. 7, no. 7, Jun 27, 2018.

[27] S. Benaliaa, B. Bernardi, S. Cuberob, A. Leuzzic, M. Larizzac, and J. Blascob, "Preliminary trials on hyperspectral imaging implementation to detect mycotoxins in dried figs," *CHEMICAL ENGINEERING,* vol. 44, 2015.

[28] D. Garcia, A. J. Ramos, V. Sanchis, and S. Marin, "Predicting mycotoxins in foods: a review," *Food Microbiol,* vol. 26, no. 8, pp. 757-69, Dec, 2009.

[29] E. Olivares Diaz, "Physical and Chemical Properties of Multiple Varieties of NERICA, Indica and Japonica Types of Rice for Assessing and Enhancing Quality," Division of Environmental Resources, Graduate School of Agricultural Research, Hokkaido University, Sapporo, Hokkaido, Japan, 2018.

[30] R. Ruan, S. Ning, A. Song, A. Ning, R. Jones, and P. Chen, "Estimation of *Fusarium* scab in wheat using machine vision and a neural network," *Cereal chemistry,* vol. 75, no. 4, pp. 455-459, 1998.

[31] R. J. N. Frandsen, S. A. Rasmussen, P. B. Knudsen, S. Uhlig, D. Petersen, E. Lysøe, C. H. Gotfredsen, H. Giese, and T. O. Larsen, "Black perithecial pigmentation in *Fusarium* species is due to the accumulation of 5-deoxybostrycoidin-based melanin," *Scientific Reports,* vol. 6, pp. 26206, 05/19/online, 2016.

[32] J. W. Deacon, *Fungal biology*, 4th ed., Malden, MA: Blackwell Pub., 2006.

[33] L. Dufossé, Y. Caro, and M. Fouillaud, "Fungal Pigments: Deep into the Rainbow of Colorful Fungi," *J. Fungi,* vol. 3, no. 45, Aug 7, 2017.

[34] S. Marin, V. Sanchis, and N. Magan, "Water activity, temperature, and pH effects on growth of *Fusarium moniliforme* and *Fusarium proliferatum* isolates from maize," *Canadian Journal of Microbiology,* vol. 41, no. 12, pp. 1063-1070, Dec, 1995.

[35] M. L. Ramirez, S. Chulze, and N. Magan, "Impact of environmental factors and fungicides on growth and deoxinivalenol production by *Fusarium graminearum* isolates from Argentinian wheat," *Crop Protection,* vol. 23, no. 2, pp. 117-125, 2004.

[36] S. D. Gupta, Y. Ibaraki, and P. Trivedi, "Applications of RGB color imaging in plants," *Plant Image Analysis: Fundamentals and Applications*, pp. 41, 2014.

[37] K. Padmavathi, and K. Thangadurai, "Implementation of RGB and grayscale images in plant leaves disease detection–comparative study," *Indian Journal of Science and Technology,* vol. 9, no. 6, 2016.

[38] M. Teena, A. Manickavasagan, A. M. Al-Sadi, R. Al-Yahyai, and M. Deadman, "RGB color imaging to detect *Aspergillus flavus* infection in dates," *Emirates Journal of Food and Agriculture*, pp. 683-688, 2016.

[39] S.-C. Yoon, T.-S. Shin, G. W. Heitschmidt, K. C. Lawrence, B. Park, and G. Gamble, "Hyperspectral imaging using a color camera and its application for pathogen detection." p. 940506.

[40] M. D. Abràmoff, P. J. Magalhães, and S. J. Ram, "Image processing with ImageJ," *Biophotonics international,* vol. 11, no. 7, pp. 36-42, 2004.

[41] C. A. Schneider, W. S. Rasband, and K. W. Eliceiri, "NIH Image to ImageJ: 25 years of image analysis," *Nat Methods,* vol. 9, no. 7, pp. 671-5, Jul, 2012.

[42] W. Burger, and M. J. Burge, *Digital image processing: an algorithmic introduction using Java*, p.^pp. 811: Springer, 2016.

[43] Wikimedia Commons. "File:*F. graminearum*.JPG," 29 December 2018, 2018; https://commons.wikimedia.org/wiki/File:F.graminearum.JPG.

[44] K. Tanaka, Y. Sago, Y. Zheng, H. Nakagawa, and M. Kushiro, "Mycotoxins in rice," *Int J Food Microbiol,* vol. 119, no. 1-2, pp. 59-66, Oct 20, 2007.

[45] Y. Kim, I. J. Kang, D. B. Shin, J. H. Roh, S. Heu, and H. K. Shim, "Timing of *Fusarium* Head Blight Infection in Rice by Heading Stage," *Mycobiology,* vol. 46, no. 3, pp. 283-286, 2018.

[46] J. J. Pestka, and A. T. Smolinski, "Deoxynivalenol: toxicology and potential effects on humans," *Journal of Toxicology and Environmental Health, Part B,* vol. 8, no. 1, pp. 39-69, Jan-Feb, 2005.

[47] L. M. Cahill, S. C. Kruger, B. T. McAlice, C. S. Ramsey, R. Prioli, and B. Kohn, "Quantification of deoxynivalenol in wheat using an immunoaffinity column and liquid chromatography," *Journal of Chromatography A,* vol. 859, no. 1, pp. 23-28, Oct 22, 1999.

[48] M. Pascale, and A. Visconti, "Overview of detection methods for mycotoxins," *Mycotoxins Detection Methods, Management, Public Health and Agricultural Trade.[CAB International*, pp. 171-83, 2008.

[49] A. Astoreca, L. Ortega, C. Fígoli, M. Cardós, L. Cavaglieri, A. Bosch, and T. Alconada, "Analytical techniques for deoxynivalenol detection and quantification in wheat destined for the manufacture of commercial products," *World Mycotoxin Journal,* vol. 10, no. 2, pp. 111-120, 2017.

[50] M. Weidenbörner, *Encyclopedia of Food Mycotoxins*, 1 ed.: Springer-Verlag Berlin Heidelberg, 2001.

[51] K. Kubo, N. Kawada, and M. Fujita, "Evaluation of *Fusarium* Head Blight Resistance in Wheat and the Development of a New Variety by Integrating Type I and II Resistance," *Jarq-Japan Agricultural Research Quarterly,* vol. 47, no. 1, pp. 9-19, Jan, 2013.

[52] J.-E. Kim, J. Jin, H. Kim, J.-C. Kim, S.-H. Yun, and Y.-W. Lee, "GIP2, a putative transcription factor that regulates the aurofusarin biosynthetic gene cluster in *Gibberella zeae*," *Applied and environmental microbiology,* vol. 72, no. 2, pp. 1645-1652, 2006.

[53] S. Malz, M. N. Grell, C. Thrane, F. J. Maier, P. Rosager, A. Felk, K. S. Albertsen, S. Salomon, L. Bohn, and W. Schäfer, "Identification of a gene cluster responsible for the biosynthesis of aurofusarin in the *Fusarium graminearum* species complex," *Fungal Genetics and Biology,* vol. 42, no. 5, pp. 420-433, May, 2005.

[54] E. Garcia-Cela, E. Kiaitsi, A. Medina, M. Sulyok, R. Krska, and N. Magan, "Interacting Environmental Stress Factors Affects Targeted Metabolomic Profiles in Stored Natural Wheat and That Inoculated with *F. graminearum*," *Toxins (Basel),* vol. 10, no. 2, Jan 29, 2018.

[55] I. M. Hueza, P. C. F. Raspantini, L. E. R. Raspantini, A. O. Latorre, and S. L. Górniak, "Zearalenone, an Estrogenic Mycotoxin, Is an Immunotoxic Compound," *Toxins,* vol. 6, no. 3, pp. 1080-1095, 2014.

[56] E. Lysoe, S. S. Klemsdal, K. R. Bone, R. J. Frandsen, T. Johansen, U. Thrane, and H. Giese, "The PKS4 gene of *Fusarium graminearum* is essential for zearalenone production," *Appl Environ Microbiol,* vol. 72, no. 6, pp. 3924-32, Jun, 2006.

[57] J. N. Ashley, B. C. Hobbs, and H. Raistrick, "Studies in the biochemistry of micro-organisms: The crystalline colouring matters of *Fusarium culmorum* (WG Smith) Sacc. and related forms," *Biochemical Journal,* vol. 31, no. 3, pp. 385, 1937.

[58] G. H. Stout, and L. H. Jensen, "Rubrofusarin: a structure determination using direct phase calculation," *Acta Crystallographica,* vol. 15, no. 5, pp. 451-457, 1962.

[59] P. M. Baker, and J. C. Roberts, "Studies in mycological chemistry. Part XXI. The structure of aurofusarin, a metabolite of some *Fusarium* species," *Journal of the Chemical Society C: Organic*, no. 0, pp. 2234-2237, 1966.

[60] D. H. R. Barton, and N. H. Werstiuk, "The constitution and stereochemistry of culmorin," *Chemical Communications (London)*, no. 1, pp. 30-31, 1967.

[61] S. Shibata, E. Morishita, T. Takeda, and K. Sakata, "Metabolic Products of Fungi. XXVIII. The Structure of Aurofusarin. (1)," *Chem Pharm Bull (Tokyo),* vol. 16, no. 3, pp. 405-410, 1968.

[62] R. J. N. Frandsen, N. J. Nielsen, N. Maolanon, J. C. Sørensen, S. Olsson, J. Nielsen, and H. Giese, "The biosynthetic pathway for aurofusarin in *Fusarium graminearum* reveals a close link between the naphthoquinones and naphthopyrones," *Molecular Microbiology,* vol. 61, no. 4, pp. 1069-80, Aug, 2006.

[63] L. Dufosse, M. Fouillaud, Y. Caro, S. A. Mapari, and N. Sutthiwong, "Filamentous fungi are large-scale producers of pigments and colorants for the food industry," *Curr Opin Biotechnol,* vol. 26, pp. 56-61, Apr, 2014.

[64] J. Avalos, J. Pardo-Medina, O. Parra-Rivero, M. Ruger-Herreros, R. Rodríguez-Ortiz, D. Hornero-Méndez, and M. C. Limón, "Carotenoid Biosynthesis in *Fusarium*," *J Fungi (Basel),* vol. 3, no. 3, Jul 7, 2017.

[65] H. Kim, H. Son, and Y. W. Lee, "Effects of light on secondary metabolism and fungal development of *Fusarium graminearum*," *J Appl Microbiol,* vol. 116, no. 2, pp. 380-9, Feb, 2014.

[66] Y. Liu, N. Liu, Y. Yin, Y. Chen, J. Jiang, and Z. Ma, "Histone H3K4 methylation regulates hyphal growth, secondary metabolism and multiple

stress responses in *Fusarium graminearum*," *Environ Microbiol,* vol. 17, no. 11, pp. 4615-30, Nov, 2015.

[67] A. G. Medentsev, A. Arinbasarova, and V. K. Akimenko, "[Biosynthesis of naphthoquinone pigments by fungi of the genus *Fusarium*]," *Prikl Biokhim Mikrobiol,* vol. 41, no. 5, pp. 573-7, Sep-Oct, 2005.

[68] S. Shibata, E. Morishita, T. Takeda, and K. Sakata, "The structure of aurofusarin," *Tetrahedron Letters,* vol. 7, no. 40, pp. 4855-4860, 1966/01/01/, 1966.

[69] J.-M. Jin, J. Lee, and Y.-W. Lee, "Characterization of carotenoid biosynthetic genes in the ascomycete *Gibberella zeae*," *FEMS microbiology letters,* vol. 302, no. 2, pp. 197-202, Jan, 2009.

[70] F. J. Leeper, and J. Staunton, "The biosynthesis of rubrofusarin, a polyketide naphthopyrone from *Fusarium culmorum*: 13 C NMR Assignments and incorporation of 13 C-and 2 H-labelled acetates," *Journal of the Chemical Society, Perkin Transactions 1*, pp. 2919-2925, 1984.

[71] R. H. Proctor, R. A. Butchko, D. W. Brown, and A. Moretti, "Functional characterization, sequence comparisons and distribution of a polyketide synthase gene required for perithecial pigmentation in some *Fusarium* species," *Food Addit Contam,* vol. 24, no. 10, pp. 1076-87, Oct, 2007.

[72] Y. Sugiura, "*Gibberella zeae* (Schwabe) Petch," *JCM Catalogue*, Japan Collection of Microorganisms, ed., Microbe Division (JCM), 1996.

[73] Sigma-Aldrich, "01497 Yeast Extract Agar," *Product Information*, S.-A. C. LLC., ed., Sigma-Aldrich, Inc., 2013.

[74] J. L. Sorensen, and T. E. Sondergaard, "The effects of different yeast extracts on secondary metabolite production in *Fusarium*," *Int J Food Microbiol,* vol. 170, pp. 55-60, Jan 17, 2014.

[75] M. S. Ammar, N. N. Gerber, and L. E. McDaniel, "New antibiotic pigments related to fusarubin from *Fusarium solani* (Mart.) Sacc. I. Fermentation, isolation, and antimicrobial activities," *J Antibiot (Tokyo),* vol. 32, no. 7, pp. 679-84, Jul, 1979.

[76] N. N. Gerber, and M. S. Ammar, "New antibiotic pigments related to fusarubin from *Fusarium solani* (Mart.) Sacc. II. Structure elucidations," *J Antibiot (Tokyo),* vol. 32, no. 7, pp. 685-8, Jul, 1979.

[77] K. Jarolim, K. Wolters, L. Woelflingseder, G. Pahlke, J. Beisl, H. Puntscher, D. Braun, M. Sulyok, B. Warth, and D. Marko, "The secondary *Fusarium* metabolite aurofusarin induces oxidative stress, cytotoxicity and genotoxicity in human colon cells," *Toxicol Lett,* vol. 284, pp. 170-183, Mar 1, 2018.

[78] A. G. Medentsev, A. N. Kotik, V. A. Trufanova, and V. K. Akimenko, "[Identification of aurofusarin in *Fusarium graminearum* isolates, causing a syndrome of worsening of egg quality in chickens]," *Prikl Biokhim Mikrobiol,* vol. 29, no. 4, pp. 542-6, Jul-Aug, 1993.

[79] Glentham Life Sciences, "GA7883 - Aurofusarin," *Product Datasheet*, G. L. S. Ltd, ed., Glentham Life Sciences, 2018.

[80] G. Beccari, V. Colasante, F. Tini, M. T. Senatore, A. Prodi, M. Sulyok, and L. Covarelli, "Causal agents of *Fusarium* head blight of durum wheat (*Triticum durum* Desf.) in central Italy and their in vitro biosynthesis of secondary metabolites," *Food Microbiol,* vol. 70, pp. 17-27, Apr, 2018.

[81] G. R. Birchall, K. Bowden, U. Weiss, and W. B. Whalley, "The chemistry of fungi. Part LVI. Aurofusarin," *Journal of the Chemical Society C: Organic*, no. 0, pp. 2237-2239, 1966.

[82] R. J. Frandsen, C. Schutt, B. W. Lund, D. Staerk, J. Nielsen, S. Olsson, and H. Giese, "Two novel classes of enzymes are required for the biosynthesis of aurofusarin in *Fusarium graminearum*," *J Biol Chem,* vol. 286, no. 12, pp. 10419-28, Mar 25, 2011.

[83] I. Gaffoor, D. W. Brown, R. Plattner, R. H. Proctor, W. Qi, and F. Trail, "Functional analysis of the polyketide synthase genes in the filamentous fungus *Gibberella zeae* (anamorph *Fusarium graminearum*)," *Eukaryotic Cell,* vol. 4, no. 11, pp. 1926-1933, Nov, 2005.

[84] J.-E. Kim, J.-C. Kim, J.-M. Jin, S.-H. Yun, and Y.-W. Lee, "Functional Characterization of Genes Located at the Aurofusarin Biosynthesis Gene Cluster in *Gibberella zeae*," *The Plant Pathology Journal,* vol. 24, no. 1, pp. 8-16, 2008, 2008.

[85] D. Hoffmeister, and N. P. Keller, "Natural products of filamentous fungi: enzymes, genes, and their regulation," *Natural Product Reports,* vol. 24, no. 2, pp. 393-416, Apr, 2007.

[86] J.-E. Kim, K.-H. Han, J. Jin, H. Kim, J.-C. Kim, S.-H. Yun, and Y.-W. Lee, "Putative polyketide synthase and laccase genes for biosynthesis of aurofusarin in *Gibberella zeae*," *Applied and environmental microbiology,* vol. 71, no. 4, pp. 1701-1708, Apr, 2005.

[87] J. E. Dvorska, P. F. Surai, B. K. Speake, and N. H. Sparks, "Effect of the mycotoxin aurofusarin on the antioxidant composition and fatty acid profile of quail eggs," *Br Poult Sci,* vol. 42, no. 5, pp. 643-9, Dec, 2001.

[88] C. N. Ezekiel, R. Bandyopadhyay, M. Sulyok, B. Warth, and R. Krska, "Fungal and bacterial metabolites in commercial poultry feed from Nigeria," *Food Addit Contam Part A Chem Anal Control Expo Risk Assess,* vol. 29, no. 8, pp. 1288-99, Aug, 2012.

[89] M. J. Nichea, S. A. Palacios, S. M. Chiacchiera, M. Sulyok, R. Krska, S. N. Chulze, A. M. Torres, and M. L. Ramirez, "Presence of Multiple Mycotoxins and Other Fungal Metabolites in Native Grasses from a Wetland Ecosystem in Argentina Intended for Grazing Cattle," *Toxins (Basel),* vol. 7, no. 8, pp. 3309-29, Aug 20, 2015.

[90] E. Streit, C. Schwab, M. Sulyok, K. Naehrer, R. Krska, and G. Schatzmayr, "Multi-mycotoxin screening reveals the occurrence of 139 different secondary metabolites in feed and feed ingredients," *Toxins (Basel),* vol. 5, no. 3, pp. 504-23, Mar 8, 2013.

[91] S. Tola, D. Bureau, J. Hooft, F. Beamish, M. Sulyok, R. Krska, P. Encarnação, and R. Petkam, "Effects of Wheat Naturally Contaminated with *Fusarium* Mycotoxins on Growth Performance and Selected Health Indices of Red Tilapia (*Oreochromis niloticus* × *O. mossambicus*)," *Toxins,* vol. 7, no. 6, pp. 1929, May 29, 2015.

[92] J. E. Dvorska, and P. F. Surai, "Yeast glucomannans prevent deterioration of quail egg quality during aurofusarinotoxicosis," in XVI European Symposium on the Quality of Poultry Meat and the X European Symposium on the Quality of Eggs and Egg Products, Sint-Brieuc - Ploufragan, France, 2003, pp. 93-101.

[93] J. E. Dvorska, P. F. Surai, B. K. Speake, and N. H. Sparks, "Antioxidant systems of the developing quail embryo are compromised by mycotoxin

aurofusarin," *Comp Biochem Physiol C Toxicol Pharmacol,* vol. 131, no. 2, pp. 197-205, Feb, 2002.

[94] J. E. Dvorska, P. F. Surai, B. K. Speake, and N. H. Sparks, "Protective effect of modified glucomannans against aurofusarin-induced changes in quail egg and embryo," *Comp Biochem Physiol C Toxicol Pharmacol,* vol. 135C, no. 3, pp. 337-43, Jul, 2003.

[95] BioViotica, "Rubrofusarin," *Product Data Sheet*, BioViotica Naturstoffe, ed., BioViotica Naturstoffe GmbH, 2012.

[96] C. Demicheli, H. Bcraldo, and L. Tosi, "Cu (Il) and Ni (II) Complexes of Rubrofusarin and 6-galactosyl Rubrofusarin," 1992.

[97] H. Tanaka, and T. Tamura, "The chemical constitution of Rubrofusarin, a pigment from *Fusarium graminearum*," *Agricultural and Biological Chemistry,* vol. 26, no. 11, pp. 767-770, 1962.

[98] B. Marazzi, P. K. Endress, L. P. De Queiroz, and E. Conti, "Phylogenetic relationships within *Senna* (Leguminosae, Cassiinae) based on three chloroplast DNA regions: patterns in the evolution of floral symmetry and extrafloral nectaries," *American Journal of Botany,* vol. 93, no. 2, pp. 288-303, Feb, 2006.

[99] L. M. Moreira, J. P. Lyon, A. Lima, L. Codognoto, A. E. Machado, F. de S Tiago, D. Araújo, E. L. Silva, N. Hioka, and M. R. Rodrigues, "Quinquangulin and Rubrofusarin: A Spectroscopy Study," *Orbital: The Electronic Journal of Chemistry,* vol. 9, no. 4, 2017.

[100] E. Pereira, C. Demicheli, and L. Peixoto, "A Spectrometric Study of the Chelating Properties of 6-Galactosyl-Rubrofusarin: Mg (II), Al (III), Fe (III), Ni (II) and," *J. Braz. Chem. Soc,* vol. 6, no. 4, pp. 381-386, 1995.

[101] A. Branco, A. C. Pinto, R. Braz-Filho, E. F. Silva, N. F. Grynberg, and A. Echevarria, "Rubrofusarina, um policetídeo natural inibidor da topoisomerase II-α humana," *Rev. bras. farmacogn,* vol. 18, no. supl, pp. 703-708, 2008.

[102] R. Mata, A. Gamboa, M. Macias, S. Santillan, M. Ulloa, and C. Gonzalez Mdel, "Effect of selected phytotoxins from *Guanomyces polythrix* on the calmodulin-dependent activity of the enzymes cAMP phosphodiesterase and NAD-kinase," *J Agric Food Chem,* vol. 51, no. 16, pp. 4559-62, Jul 30, 2003.

[103] European Molecular Biology Laboratory. "Rubrofusarin B (CHEBI:133805)," 4 September 2018, 2018; https://www.ebi.ac.uk/chebi/searchId.do?chebiId=CHEBI:133805.

[104] Y. C. Song, H. Li, Y. H. Ye, C. Y. Shan, Y. M. Yang, and R. X. Tan, "Endophytic naphthopyrone metabolites are co-inhibitors of xanthine oxidase, SW1116 cell and some microbial growths," *FEMS Microbiol Lett,* vol. 241, no. 1, pp. 67-72, Dec 1, 2004.

[105] S. Rangaswami, "Crystalline chemical components of the seeds of *Cassia tora* Linn. Identity of *Tora* Substance C with rubrofusarin and *Tora* Substance B with nor-rubrofusarin," *Proceedings of the Indian Academy of Sciences - Section A,* vol. 57, no. 2, pp. 88-93, February 01, 1963.

[106] A. B. Oliveira, M. L. M. Fernandes, V. T. Shaat, L. A. Vasconcelos, and O. R. Gottlieb, "Constituents of *Cassia* species," *Rev Latinoamer Quim,* vol. 8, pp. 82-85, 1977.

[107] Y. Jing, J. Yang, L. Wu, Z. Zhang, and L. Fang, "[Rubrofusarin glucosides of *Berchemia polyphylla* var. leioclada and their scavenging activities for DPPH radical]," *Zhongguo Zhong Yao Za Zhi,* vol. 36, no. 15, pp. 2084-7, Aug, 2011.

[108] R. G. Coelho, W. Vilegas, K. F. Devienne, and M. S. G. Raddi, "A new cytotoxic naphthopyrone dimer from *Paepalanthus bromelioides*," *Fitoterapia,* vol. 71, no. 5, pp. 497-500, 2000/09/01/, 2000.

[109] M. A. Ernst-Russell, C. L. L. Chai, J. H. Wardlaw, and J. A. Elix, "Euplectin and Coneuplectin, New Naphthopyrones from the Lichen *Flavoparmelia euplecta*," *Journal of Natural Products,* vol. 63, no. 1, pp. 129-131, 2000/01/01, 2000.

[110] B. H. Mock, and J. E. Robbers, "Biosynthesis of rubrofusarin by *Fusarium graminearum*," *Journal of pharmaceutical sciences,* vol. 58, no. 12, pp. 1560-1562, Dec, 1969.

[111] H. E. Hallen, and F. Trail, "The L-type calcium ion channel cch1 affects ascospore discharge and mycelial growth in the filamentous fungus *Gibberella zeae* (anamorph *Fusarium graminearum*)," *Eukaryot Cell,* vol. 7, no. 2, pp. 415-24, Feb, 2008.

[112] P. Rugbjerg, M. Naesby, U. H. Mortensen, and R. J. Frandsen, "Reconstruction of the biosynthetic pathway for the core fungal polyketide scaffold rubrofusarin in *Saccharomyces cerevisiae*," *Microb Cell Fact,* vol. 12, pp. 31, Apr 4, 2013.

[113] S. D. Alqahtani, H. A. Assiri, F. A. Al-Abbasi, A. M. El-Halawany, and A. M. Al-Abd, "Abstract 1205: Rubrofusarin and toralactone sensitize resistant MCF-7^{adr} cell line to paclitaxel via inhibiting P-glycoprotein efflux activity," *Cancer Research,* vol. 77, no. 13 Supplement, pp. 1205-1205, 2017.

[114] A. M. El-Halawany, M. H. Chung, N. Nakamura, C. M. Ma, T. Nishihara, and M. Hattori, "Estrogenic and anti-estrogenic activities of *Cassia tora* phenolic

constituents," *Chem Pharm Bull (Tokyo),* vol. 55, no. 10, pp. 1476-82, Oct, 2007.

[115] M. Ghebremeskel, and W. Langseth, "The occurrence of culmorin and hydroxy-culmorins in cereals," *Mycopathologia,* vol. 152, no. 2, pp. 103-8, 2001.

[116] J. C. Young, and D. E. Games, "Supercritical fluid chromatography of *Fusarium* mycotoxins," *J Chromatogr,* vol. 627, no. 1-2, pp. 247-54, Dec 25, 1992.

[117] iChemLabs. "2D Sketcher | ChemDoodle Web Components," 9 September 2018, 2018; https://web.chemdoodle.com/demos/sketcher/.

[118] Nara Institute of Science and Technology. "KNApSAcK Metabolite Information - Culmorin," 2 September 2018, 2018; http://kanaya.naist.jp/knapsack_jsp/information.jsp?word=C00021971.

[119] J. Weber, M. Vaclavikova, G. Wiesenberger, M. Haider, C. Hametner, J. Frohlich, F. Berthiller, G. Adam, H. Mikula, and P. Fruhmann, "Chemical synthesis of culmorin metabolites and their biologic role in culmorin and acetyl-culmorin treated wheat cells," *Org Biomol Chem,* vol. 16, no. 12, pp. 2043-2048, Mar 28, 2018.

[120] National Center for Biotechnology Information. "Culmorin," 5 September 2018, 2018; https://www.ncbi.nlm.nih.gov/pubmed/.

[121] J. D. Miller, and S. MacKenzie, "Secondary Metabolites of *Fusarium venenatum* Strains with Deletions in the Tri5 Gene Encoding Trichodiene Synthetase," *Mycologia,* vol. 92, no. 4, pp. 764-771, 2000.

[122] G. C. Kasitu, J. W. ApSimon, B. A. Blackwell, D. A. Fielder, R. Greenhalgh, and J. D. Miller, "Isolation and characterization of culmorin derivatives

produced by *Fusarium culmorum* CMI 14764," *Canadian Journal of Chemistry,* vol. 70, no. 5, pp. 1308-1316, 1992/05/01, 1992.

[123] W. Langseth, M. Ghebremeskel, B. Kosiak, P. Kolsaker, and D. Miller, "Production of culmorin compounds and other secondary metabolites by *Fusarium culmorum* and *F. graminearum* strains isolated from Norwegian cereals," *Mycopathologia,* vol. 152, no. 1, pp. 23-34, 2001.

[124] P. B. Pedersen, and J. D. Miller, "The fungal metabolite culmorin and related compounds," *Nat Toxins,* vol. 7, no. 6, pp. 305-9, 1999.

[125] T. Grafenhan, P. R. Johnston, M. M. Vaughan, S. P. McCormick, R. H. Proctor, M. Busman, T. J. Ward, and K. O'Donnell, "*Fusarium praegraminearum* sp. nov., a novel nivalenol mycotoxin-producing pathogen from New Zealand can induce head blight on wheat," *Mycologia,* vol. 108, no. 6, pp. 1229-1239, Nov/Dec, 2016.

[126] I. Laraba, H. Boureghda, N. Abdallah, O. Bouaicha, F. Obanor, A. Moretti, D. M. Geiser, H. S. Kim, S. P. McCormick, R. H. Proctor, A. C. Kelly, T. J. Ward, and K. O'Donnell, "Population genetic structure and mycotoxin potential of the wheat crown rot and head blight pathogen *Fusarium culmorum* in Algeria," *Fungal Genet Biol,* vol. 103, pp. 34-41, Jun, 2017.

[127] D. Strongman, J. Miller, L. Calhoun, J. Findlay, and N. Whitney, "The biochemical basis for interference competition among some lignicolous marine fungi," *Botanica Marina,* vol. 30, no. 1, pp. 21-26, 1987.

[128] S. P. McCormick, N. J. Alexander, and L. J. Harris, "CLM1 of *Fusarium graminearum* encodes a longiborneol synthase required for culmorin production," *Appl Environ Microbiol,* vol. 76, no. 1, pp. 136-41, Jan, 2010.

[129] I. National Center for Biotechnology. "*Gibberella zeae* strain GZ3639 longiborneol synthase (CLM1) gene, compl - Nucleotide - NCBI," 7 September 2018, 2018; https://www.ncbi.nlm.nih.gov/pubmed/.

[130] E. Humer, A. Lucke, H. Harder, B. U. Metzler-Zebeli, J. Bohm, and Q. Zebeli, "Effects of Citric and Lactic Acid on the Reduction of Deoxynivalenol and Its Derivatives in Feeds," *Toxins (Basel),* vol. 8, no. 10, Sep 28, 2016.

[131] S. Uhlig, G. S. Eriksen, I. S. Hofgaard, R. Krska, E. Beltran, and M. Sulyok, "Faces of a changing climate: semi-quantitative multi-mycotoxin analysis of grain grown in exceptional climatic conditions in Norway," *Toxins (Basel),* vol. 5, no. 10, pp. 1682-97, Sep 27, 2013.

[132] W. A. Abia, B. Warth, M. Sulyok, R. Krska, A. N. Tchana, P. B. Njobeh, M. F. Dutton, and P. F. Moundipa, "Determination of multi-mycotoxin occurrence in cereals, nuts and their products in Cameroon by liquid chromatography tandem mass spectrometry (LC-MS/MS)," *Food Control,* vol. 31, no. 2, pp. 438-453, 2013.

[133] S. Generotti, M. Cirlini, B. Sarkanj, M. Sulyok, F. Berthiller, C. Dall'Asta, and M. Suman, "Formulation and processing factors affecting trichothecene mycotoxins within industrial biscuit-making," *Food Chem,* vol. 229, pp. 597-603, Aug 15, 2017.

[134] K. Mastanjevic, B. Sarkanj, R. Krska, M. Sulyok, B. Warth, K. Mastanjevic, B. Santek, and V. Krstanovic, "From malt to wheat beer: A comprehensive multi-toxin screening, transfer assessment and its influence on basic fermentation parameters," *Food Chem,* vol. 254, pp. 115-121, Jul 15, 2018.

[135] R. M. Delgado, M. Sulyok, O. Jirsa, T. Spitzer, R. Krska, and I. Polisenska, "Relationship between lutein and mycotoxin content in durum wheat," *Food*

Addit Contam Part A Chem Anal Control Expo Risk Assess, vol. 31, no. 7, pp. 1274-83, 2014.

[136] P. F. Dowd, J. D. Miller, and R. Greenhalgh, "Toxicity and interactions of some *Fusarium graminearum* metabolites to caterpillars," *Mycologia,* vol. 81, no. 4, pp. 646-650, 1989.

[137] R. Rotter, H. Trenholm, D. Prelusky, K. Hartin, B. Thompson, and J. Miller, "A preliminary examination of potential interactions between deoxynivalenol (DON) and other selected *Fusarium* metabolites in growing pigs," *Canadian Journal of Animal Science,* vol. 72, no. 1, pp. 107-116, 1992.

[138] F. Trail, and R. Common, "Perithecial development by *Gibberella zeae*: a light microscopy study," *Mycologia*, pp. 130-138, 2000.

[139] K. Lawler, K. Hammond-Kosack, A. Brazma, and R. M. Coulson, "Genomic clustering and co-regulation of transcriptional networks in the pathogenic fungus *Fusarium graminearum*," *BMC Syst Biol,* vol. 7, pp. 52, Jun 27, 2013.

[140] L. Studt, P. Wiemann, K. Kleigrewe, H.-U. Humpf, and B. Tudzynski, "Biosynthesis of Fusarubins Accounts for Pigmentation of *Fusarium fujikuroi* Perithecia," *Applied and Environmental Microbiology,* vol. 78, no. 12, pp. 4468-4480, 03/12/received

03/25/accepted, 2012.

[141] D. Parisot, M. Devys, and M. Barbier, "Notizen: 5-Deoxybostrycoidin, a New Metabolite Produced by the Fungus *Nectria haematococca* (Berk. and Br.) Wr," *Zeitschrift für Naturforschung B*, 11, 1989, p. 1473.

[142] L. J. Ma, D. M. Geiser, R. H. Proctor, A. P. Rooney, K. O'Donnell, F. Trail, D. M. Gardiner, J. M. Manners, and K. Kazan, "*Fusarium* pathogenomics," *Annu Rev Microbiol,* vol. 67, pp. 399-416, 2013.

[143] K. O'Donnell, A. P. Rooney, R. H. Proctor, D. W. Brown, S. P. McCormick, T. J. Ward, R. J. Frandsen, E. Lysoe, S. A. Rehner, T. Aoki, V. A. Robert, P. W. Crous, J. Z. Groenewald, S. Kang, and D. M. Geiser, "Phylogenetic analyses of RPB1 and RPB2 support a middle Cretaceous origin for a clade comprising all agriculturally and medically important *Fusaria*," *Fungal Genet Biol,* vol. 52, pp. 20-31, Mar, 2013.

[144] E. Dadachova, R. A. Bryan, R. C. Howell, A. D. Schweitzer, P. Aisen, J. D. Nosanchuk, and A. Casadevall, "The radioprotective properties of fungal melanin are a function of its chemical composition, stable radical presence and spatial arrangement," *Pigment cell & melanoma research,* vol. 21, no. 2, pp. 192-199, Apr, 2008.

[145] J. Avalos, and A. F. Estrada, "Regulation by light in *Fusarium*," *Fungal Genet Biol,* vol. 47, no. 11, pp. 930-8, Nov, 2010.

[146] A. Prado-Cabrero, P. Schaub, V. Diaz-Sanchez, A. F. Estrada, S. Al-Babili, and J. Avalos, "Deviation of the neurosporaxanthin pathway towards beta-carotene biosynthesis in *Fusarium fujikuroi* by a point mutation in the phytoene desaturase gene," *FEBS J,* vol. 276, no. 16, pp. 4582-97, Aug, 2009.

[147] J. Avalos, and E. Cerdà-Olmedo, "Carotenoid mutants of *Gibberella fujikuroi*," *Current genetics,* vol. 11, no. 6-7, pp. 505-511, 1987.

[148] V. Diaz-Sanchez, A. F. Estrada, D. Trautmann, S. Al-Babili, and J. Avalos, "The gene carD encodes the aldehyde dehydrogenase responsible for neurosporaxanthin biosynthesis in *Fusarium fujikuroi*," *FEBS J,* vol. 278, no. 17, pp. 3164-76, Sep, 2011.

[149] A. M. Kot, S. Błażejak, I. Gientka, M. Kieliszek, and J. Bryś, "Torulene and torularhodin: "new" fungal carotenoids for industry?," *Microbial Cell Factories,* vol. 17, no. 1, pp. 49, 2018.

[150] C. Li, N. Zhang, B. Li, Q. Xu, J. Song, N. Wei, W. Wang, and H. Zou, "Increased torulene accumulation in red yeast *Sporidiobolus pararoseus* NGR as stress response to high salt conditions," *Food chemistry,* vol. 237, pp. 1041-1047, 2017.

[151] National Center for Biotechnology Information. "Torulene," 12 September 2018, 2018; https://www.ncbi.nlm.nih.gov/pubmed/.

[152] Royal Society of Chemistry. "Torulene," 2 September 2018, 2018; http://www.chemspider.com/Chemical-Structure.4444665.html?rid=28fe93b0-090b-48cf-ba81-28141d575d21.

[153] L. Saelices, L. Youssar, I. Holdermann, S. Al-Babili, and J. Avalos, "Identification of the gene responsible for torulene cleavage in the *Neurospora* carotenoid pathway," *Mol Genet Genomics,* vol. 278, no. 5, pp. 527-37, Nov, 2007.

[154] Q. Shi, H. Wang, C. Du, W. Zhang, and H. Qian, "Tentative identification of torulene cis/trans geometrical isomers isolated from *Sporidiobolus pararoseus* by high-performance liquid chromatography-diode array detection-mass spectrometry and preparation by column chromatography," *Anal Sci,* vol. 29, no. 10, pp. 997-1002, 2013.

[155] L. Zoz, J. C. Carvalho, V. T. Soccol, T. C. Casagrande, and L. Cardoso, "Torularhodin and Torulene: Bioproduction, Properties and Prospective Applications in Food and Cosmetics - a Review," *Brazilian Archives of Biology and Technology,* vol. 58, pp. 278-288, 2015.

[156] I. R. Maldonade, D. B. Rodriguez-Amaya, and A. R. P. Scamparini, "Carotenoids of yeasts isolated from the Brazilian ecosystem," *Food Chemistry,* vol. 107, no. 1, pp. 145-150, 2008/03/01/, 2008.

[157] J.-F. Martín, C. García-Estrada, and S. Zeilinger, *Biosynthesis and molecular genetics of fungal secondary metabolites*: Springer, 2014.

[158] National Center for Biotechnology Information. "Neurosporaxanthin," 11 September 2018, 2018; https://pubchem.ncbi.nlm.nih.gov/compound/637039.

[159] A. Prado-Cabrero, D. Scherzinger, J. Avalos, and S. Al-Babili, "Retinal biosynthesis in fungi: characterization of the carotenoid oxygenase CarX from *Fusarium fujikuroi*," *Eukaryot Cell,* vol. 6, no. 4, pp. 650-7, Apr, 2007.

[160] M. Streicher, "Biopure certificate of analysis: deoxynivalenol in acetonitrile," R. Labs, ed., Romer Labs Division Holding GmbH, 2016.

[161] H. S. Hussein, and J. M. Brasel, "Toxicity, metabolism, and impact of mycotoxins on humans and animals," *Toxicology,* vol. 167, no. 2, pp. 101-34, Oct 15, 2001.

[162] J. J. Pestka, "Deoxynivalenol: Toxicity, mechanisms and animal health risks," *Animal Feed Science and Technology,* vol. 137, no. 3–4, pp. 283-298, 10/1/, 2007.

[163] J. Berger, H. Le Meur, D. Dutykh, D. M. Nguyen, and A.-C. Grillet, "Analysis and improvement of the VTT mold growth model: Application to bamboo fiberboard," *Building and Environment*, 2018/03/28/, 2018.

[164] E. B. Møller, B. Andersen, C. Rode, and R. Peuhkuri, "Conditions for mould growth on typical interior surfaces," *Energy Procedia,* vol. 132, pp. 171-176, 2017/10/01/, 2017.

[165] Z. Sadovský, and O. Koronthályová, "Exploration of probabilistic mould growth assessment," *Applied Mathematical Modelling,* vol. 42, pp. 566-575, 2017/02/01/, 2017.

[166] R. L. Buchanan, R. C. Whiting, and W. C. Damert, "When is simple good enough: A comparison of the Gompertz, Baranyi, and three-phase linear models for fitting bacterial growth curves," *Food Microbiology,* vol. 14, no. 4, pp. 313-326, Aug, 1997.

[167] Y. Sugiura, Y. Watanabe, T. Tanaka, S. Yamamoto, and Y. Ueno, "Occurrence of *Gibberella zeae* strains that produce both nivalenol and deoxynivalenol," *Applied and Environmental Microbiology,* vol. 56, no. 10, pp. 3047-3051, 1990.

[168] C. Neagu, and D. Borda, "Modelling the growth of *Fusarium graminearum* on barley and wheat media extract," *Romanian Biotechnological Letters,* vol. 18, no. 4, pp. 8489, 2013.

[169] M. T. Madigan, J. M. Martinko, and J. Parker, *Brock biology of microorganisms*: Pearson, 2017.

[170] S. Marin, D. Cuevas, A. J. Ramos, and V. Sanchis, "Fitting of colony diameter and ergosterol as indicators of food borne mould growth to known growth models in solid medium," *Int J Food Microbiol,* vol. 121, no. 2, pp. 139-49, Jan 31, 2008.

[171] K. I. Suhr, I. Haasum, L. D. Steenstrup, and T. O. Larsen, "Factors Affecting Growth and Pigmentation of *Penicillium caseifulvum*," *Journal of Dairy Science,* vol. 85, no. 11, pp. 2786-2794, 2002/11/01/, 2002.

[172] H. C. Wong, and P. E. Koehler, "Production and isolation of an antibiotic from *Monascus purpureus* and its relationship to pigment production," *Journal of Food Science,* vol. 46, no. 2, pp. 589-592, 1981.

[173] S. Nasuno, and T. Asai, "Red pigments formation by interaction of molds," *The Journal of General and Applied Microbiology,* vol. 7, no. 1, pp. 78-87, 1961.

[174] E. Schneider, V. Curtui, C. Seidler, R. Dietrich, E. Usleber, and E. Märtlbauer, "Rapid methods for deoxynivalenol and other trichothecenes," *Toxicology Letters,* vol. 153, no. 1, pp. 113-121, 2004/10/10/, 2004.

[175] H. Takenaka, S. Kawamura, A. Sumino, and Y. Yano, "New combination use of gravity separator and optical sorter for decontamination deoxynivalenol of wheat." pp. 978-3.

[176] Romer Labs. "Mycotoxin Regulations for Food and Feed in Japan," 10 July 2018, 2018; https://www.romerlabs.com/fileadmin/user_upload/romerlabs/Documents/PDF_Files/Regulierungsposter_Mycotoxins_Japan_0916.pdf.

[177] M. K. Amistadi, J. K. Hall, E. R. Bogus, and R. O. Mumma, "Comparison of gas chromatography and immunoassay methods for the detection of atrazine in water and soil," *J Environ Sci Health B,* vol. 32, no. 6, pp. 845-60, Nov, 1997.

[178] N. W. Turner, S. Subrahmanyam, and S. A. Piletsky, "Analytical methods for determination of mycotoxins: a review," *Anal Chim Acta,* vol. 632, no. 2, pp. 168-80, Jan 26, 2009.

[179] L. Dufossé, P. Galaup, A. Yaron, S. M. Arad, P. Blanc, K. N. C. Murthy, and G. A. Ravishankar, "Microorganisms and microalgae as sources of pigments

for food use: a scientific oddity or an industrial reality?," *Trends in Food Science & Technology,* vol. 16, no. 9, 2005.

[180] L. Alpsoy, and M. E. Yalvac, "Chapter twelve - Key Roles of Vitamins A, C, and E in Aflatoxin B1-Induced Oxidative Stress," *Vitamins & Hormones*, G. Litwack, ed., pp. 287-305: Academic Press, 2011.

[181] H. Tanaka, Y. Ohne, N. Ogawa, and T. Tamura, "The Chemical Constitution of Rubrofusarin: Part II. Alkaline Degradation Studies," *Agricultural and Biological Chemistry,* vol. 27, no. 1, pp. 48-55, 1963.

[182] J. Avalos, A. Prado-Cabrero, and A. F. Estrada, "Neurosporaxanthin production by *Neurospora* and *Fusarium*," *Methods Mol Biol,* vol. 898, pp. 263-74, 2012.

[183] Y. Minomo, Y. Kakehi, M. Iida, and T. Naemura, "Transforming your shadow into colorful visual media: multiprojection of complementary colors," *Comput. Entertain.,* vol. 4, no. 3, pp. 10, 2006.

[184] R. W. Pridmore, "Complementary colors: Composition and efficiency in producing various whites*," *Journal of the Optical Society of America,* vol. 68, no. 11, pp. 1490-1496, 1978/11/01, 1978.

[185] D. Hagiwara, K. Sakai, S. Suzuki, M. Umemura, T. Nogawa, N. Kato, H. Osada, A. Watanabe, S. Kawamoto, T. Gonoi, and K. Kamei, "Temperature during conidiation affects stress tolerance, pigmentation, and trypacidin accumulation in the conidia of the airborne pathogen *Aspergillus fumigatus*," *PLoS One,* vol. 12, no. 5, pp. e0177050, 2017.

[186] A. Méndez, C. Pérez, J. C. Montañéz, G. Martínez, and C. N. Aguilar, "Red pigment production by *Penicillium purpurogenum* GH2 is influenced by pH

and temperature," *Journal of Zhejiang University. Science. B,* vol. 12, no. 12, pp. 961-968, 02/09/received

04/25/accepted, 2011.

[187] H. Chijiiwa, *Color Harmony: a Guide to Creative Color Combinations*: Page One-Designer's Bookshop, 1987.

[188] J. A. Ferwerda, and D. L. Long, "Fundamentals of color science," in ACM SIGGRAPH 2018 Courses, Vancouver, British Columbia, Canada, 2018, pp. 1-88.

[189] National Center for Biotechnology Information, "Deoxynivalenol," *PubChem Compound Database*, National Center for Biotechnology Information, U.S. National Library of Medicine, 2005.

[190] P. Sobrova, V. Adam, A. Vasatkova, M. Beklova, L. Zeman, and R. Kizek, "Deoxynivalenol and its toxicity," *Interdisciplinary toxicology,* vol. 3, no. 3, pp. 94-99, Sep, 2010.

[191] B. A. Rotter, D. B. Prelusky, and J. J. Pestka, "Toxicology of deoxynivalenol (vomitoxin)," *J Toxicol Environ Health,* vol. 48, no. 1, pp. 1-34, May, 1996.

[192] W. Wilson, B. Dahl, and W. Nganje, "Economic costs of *Fusarium* Head Blight, scab and deoxynivalenol," *World Mycotoxin Journal,* vol. 11, no. 2, pp. 291-302, 2018.

[193] D. G. Schmale III, and G. P. Munkvold. "Mycotoxins in Crops: A Threat to Human and Domestic Animal Health," 30 November 2018, 2018; https://www.apsnet.org/edcenter/intropp/topics/mycotoxins/pages/economicimpact.aspx.

[194] A. Velluti, V. Sanchis, A. J. Ramos, C. Turon, and S. Marín, "Impact of essential oils on growth rate, zearalenone and deoxynivalenol production by

Fusarium graminearum under different temperature and water activity conditions in maize grain," *Journal of Applied Microbiology,* vol. 96, no. 4, pp. 716-724, 2004.

[195] M. L. Ramirez, S. Chulze, and N. Magan, "Temperature and water activity effects on growth and temporal deoxynivalenol production by two Argentinean strains of *Fusarium graminearum* on irradiated wheat grain," *Int J Food Microbiol,* vol. 106, no. 3, pp. 291-6, Feb 15, 2006.

[196] R. Hope, D. Aldred, and N. Magan, "Comparison of environmental profiles for growth and deoxynivalenol production by Fusarium culmorum and F. graminearum on wheat grain," *Letters in Applied Microbiology,* vol. 40, no. 4, pp. 295-300, 2005.

[197] E. Cambaza, "Comprehensive Description of *Fusarium graminearum* Pigments and Related Compounds," *Foods,* vol. 7, no. 10, pp. 165, Oct 5, 2018.

[198] Sigma-Aldrich, "Supel™ Tox SPE Cartridges: Fast and Simple Cleanup for Mycotoxin Analysis," *Supelco: Solutions Within*, Sigma-Aldrich, ed., 2013.

[199] J. W. Bennett, and M. Klich, "Mycotoxins," *Clin Microbiol Rev,* vol. 16, no. 3, pp. 497-516, Jul, 2003.

[200] C. E. Windels, "Economic and social impacts of *Fusarium* head blight: changing farms and rural communities in the northern great plains," *Phytopathology,* vol. 90, no. 1, pp. 17-21, Jan, 2000.

[201] W. E. Nganje, D. A. Bangsund, F. L. Leistritz, W. W. Wilson, and N. M. Tiapo, "Estimating the economic impact of a crop disease: the case of *Fusarium* head blight in US wheat and barley." p. 275.

[202] E. Cambaza, S. Koseki, and S. Kawamura, "*Fusarium graminearum* colors and deoxynivalenol synthesis at different temperatures." p. 15.

[203] C. Gurrin, Z. Qiu, M. Hughes, N. Caprani, A. R. Doherty, S. E. Hodges, and A. F. Smeaton, "The Smartphone As a Platform for Wearable Cameras in Health Research," *American Journal of Preventive Medicine,* vol. 44, no. 3, pp. 308-313, 2013/03/01/, 2013.

[204] V. Oncescu, M. Mancuso, and D. Erickson, "Cholesterol testing on a smartphone," *Lab on a Chip,* vol. 14, no. 4, pp. 759-763, 2014.

[205] C. Boissin, J. Fleming, L. Wallis, M. Hasselberg, and L. Laflamme, "Can we trust the use of smartphone cameras in clinical practice? Laypeople assessment of their image quality," *TELEMEDICINE and e-HEALTH,* vol. 21, no. 11, pp. 887-892, 2015.

[206] E. Cambaza, S. Koseki, and S. Kawamura, "*Fusarium graminearum* Colors and Deoxynivalenol Synthesis at Different Water Activity," *Foods,* vol. 8, no. 1, 2018.

[207] D. R. Taylor, L. W. Aarssen, and C. Loehle, "On the relationship between r/K selection and environmental carrying capacity: a new habitat templet for plant life history strategies," *Oikos*, pp. 239-250, 1990.

[208] E. J. Zuza, "Effect of harvesting time and drying methods on aflatoxin contamination in groundnut in Mozambique," *Journal of Postharvest Technology,* vol. 6, no. 2, pp. In Press, 2018.

[209] J. Meletiadis, J. F. Meis, J. W. Mouton, and P. E. Verweij, "Analysis of growth characteristics of filamentous fungi in different nutrient media," *Journal of clinical microbiology,* vol. 39, no. 2, pp. 478-484, 2001.

[210] V. Muraliá-Madhav, "Assessment of growth of *Fusarium solani* by cyclic voltammetry and possible bioanalytical applications," *Analyst,* vol. 125, no. 12, pp. 2166-2168, 2000.

[211] S. Subrahmanyam, A. Balakrishnan, R. Viswanathan, H. P. Douglass, A. V. Raja, A. Barathan, A. Usmani, and K. Shanmugam, "Development of a Cytosensor for the Detection of *Fusarium Oxysporum* - A Functional Approach Towards Bioanalytical Applications," *European Scientific Journal, ESJ,* vol. 14, no. 21, pp. 42, 2018.

[212] M. Peleg, and M. G. Corradini, "Microbial Growth Curves: What the Models Tell Us and What They Cannot," *Critical Reviews in Food Science and Nutrition,* vol. 51, no. 10, pp. 917-945, 2011.

[213] T. Harrington, J. Steimel, F. Workneh, and X. Yang, "Molecular identification of fungi associated with vascular discoloration of soybean in the north central United States," *Plant Disease,* vol. 84, no. 1, pp. 83-89, 2000.

[214] H. S. Sherwin, and K. W. Kreitlow, "Discoloration of soybean seeds by the frogeye fungus, *Cercospora sojina*," *Phytopathology,* vol. 42, no. 10, 1952.

[215] M. A. Doster, and T. J. Michailides, "Relationship between shell discoloration of pistachio nuts and incidence of fungal decay and insect infestation," *Plant Disease,* vol. 83, no. 3, pp. 259-264, 1999.

[216] M. Bello, M. P. Tolaba, and C. Suarez, "Factors affecting water uptake of rice grain during soaking," *LWT-Food Science and Technology,* vol. 37, no. 8, pp. 811-816, 2004.

[217] H. O. Agu, and A. Michael-Agwuoke, "Optimization of Soaking Duration and Temperature for Two Nigerian Rice Cultivars," *Nigerian Food Journal,* vol. 30, no. 2, pp. 22-27, 2012/01/01/, 2012.

[218] S. Koseki, and J. Nonaka, "Alternative Approach To Modeling Bacterial Lag Time, Using Logistic Regression as a Function of Time, Temperature, pH, and Sodium Chloride Concentration," *Applied and Environmental Microbiology,* vol. 78, no. 17, pp. 6103-6112, 2012.

[219] C. Cortinovis, M. Battini, and F. Caloni, "Deoxynivalenol and T-2 Toxin in Raw Feeds for Horses," *Journal of Equine Veterinary Science,* vol. 32, no. 2, pp. 72-74, 2012/02/01/, 2012.

[220] M. E. Zain, "Impact of mycotoxins on humans and animals," *Journal of Saudi Chemical Society,* vol. 15, no. 2, pp. 129-144, 2011/04/01/, 2011.

[221] H. K. Abbas, C. J. Mirocha, R. J. Pawlosky, and D. J. Pusch, "Effect of cleaning, milling, and baking on deoxynivalenol in wheat," *Applied and environmental microbiology,* vol. 50, no. 2, pp. 482-486, 1985.

[222] M. Kushiro, "Effects of milling and cooking processes on the deoxynivalenol content in wheat," *International journal of molecular sciences,* vol. 9, no. 11, pp. 2127-2145, 2008.

[223] J. P. d. Oliveira, G. P. Bruni, K. O. Lima, S. L. M. E. Halal, G. S. d. Rosa, A. R. G. Dias, and E. d. R. Zavareze, "Cellulose fibers extracted from rice and oat husks and their application in hydrogel," *Food Chemistry,* vol. 221, pp. 153-160, 2017/04/15/, 2017.

[224] M. J. Carlile, S. C. Watkinson, and G. W. Gooday, *The Fungi*, 2nd ed., San Diego, Calif.: Academic Press, 2001.

[225] S. Choi, H. Jun, J. Bang, S. H. Chung, Y. Kim, B. S. Kim, H. Kim, L. R. Beuchat, and J. H. Ryu, "Behaviour of *Aspergillus flavus* and *Fusarium graminearum* on rice as affected by degree of milling, temperature, and

relative humidity during storage," *Food Microbiol,* vol. 46, pp. 307-313, Apr, 2015.

Summary

Fusarium graminearum Schwabe is a fungal plant parasite responsible for head blight (FHB) in cereals. This mold also synthesizes deoxynivalenol (DON), an emetic mycotoxin responsible for at least eight outbreaks since the beginning of the 20th century in Japan, including Hokkaido. The toxin is also a major problem in Austria, Italy, South Africa, Sweden, UK and US.

DON is highly stable and resistant to common processing methods such as milling, heating, drying and fermentation, often making into the food if synthesized. Thus, prevention is still the best alternative to control this chemical, and for that it is a key step to understand how environmental factors affect growth of *F. graminearum* and DON synthesis. Temperature and water activity (a_w) are already known to affect DON synthesis. The former factor seems to have an optimal range of minimal toxin production (25 °C), while the latter is likely to be directly proportional to DON quantity. In any case, DON production seems associated to stress caused by suboptimal growth conditions.

Size-based variables (e.g. radius, diameter) represent fungal growth in the currently used models, but they do not provide important growth information such as metabolic activity or state of maturity, especially during the stationary phase. Color is perhaps fitter for this purpose because it is a product of the mold's metabolism, changing even when the fungus is no longer expanding in the substrate. The current research aimed to analyze if *F. graminearum* surface colors are suitable as alternative to size in studies of growth and DON synthesis.

After a review on the principles underlying *F. graminearum* growth, toxin production and its color, the first step was to see if the mold's surface colors present a predictable pattern, fit for use as an estimator of metabolic changes and state of

maturity. Three specimens were incubated in yeast extract agar (YEA) at 25 °C for 20 days, photographed daily and the proportion of pixels with red, green and blue (RGB) components in the mold's surface were analyzed using ImageJ software. All RGB components cubic polynomial growth patterns, and all color components were highly correlated, especially red and green.

Some experiments aimed to analyze the relationship between RGB components and DON synthesis under different temperature and a_w. Specimens were incubated at 15 °C, 25 °C and 30 °C and a_w of 0.94, 0.97 and 0.99, and each 4 days, photos were taken and RGB was analyzed, and toxin concentration was determined. DON concentration was measured using HPLC (UV = 220 nm, 35 °C). All RGB components presented cubic relationship with DON, regardless of the temperature. However, water activity below 0.99 did promoted mycelium growth, masking the mold's surface and making it possible to visualize the color variation.

Reproduction of the same experiments in oat and rice grains showed similar trends: RGB variation was predictable and showed consistent relationship with DON concentration across temperatures. In this case, it was possible to verify that RGB correlated to DON variation at different a_w, especially in rice ($p < 0.001$). The latter observation was feasible in grains but not in YEA likely because grains presented much wider surface for mold growth and their cellulose wall slowing down the rate of degradation and production of white mycelia. These observations suggest that RGB components can effectively be used to predict the extent and severity of DON contamination when *F. graminearum* colonizes oat and rice grains at different temperatures and a_w.

The studies demonstrated that color measurement is fit to be an alternative for size variables in *F. graminearum* growth studies and prediction of DON quantity.